



NTP

National Toxicology Program

U.S. Department of Health and Human Services

NTP TECHNICAL REPORT ON THE TOXICITY STUDIES OF

Fullerene C₆₀
(1 μ m and 50 nm)
(CASRN 99685-96-8)
Administered by
Nose-only Inhalation to
Wistar Han [CrI:WI (Han)]
Rats and B6C3F1/N Mice

NTP TOX 87

JULY 2020

**NTP Technical Report on the
Toxicity Studies of Fullerene C₆₀
(1 µm and 50 nm) (CASRN 99685-96-8)
Administered by Nose-only Inhalation to Wistar
Han [Crl:WI (Han)] Rats and B6C3F1/N Mice**

Toxicity Report 87

July 2020

National Toxicology Program
Public Health Service
U.S. Department of Health and Human Services
ISSN: 2378-8992

Research Triangle Park, North Carolina, USA

Foreword

The National Toxicology Program (NTP), established in 1978, is an interagency program within the Public Health Service of the U.S. Department of Health and Human Services. Its activities are executed through a partnership of the National Institute for Occupational Safety and Health (part of the Centers for Disease Control and Prevention), the Food and Drug Administration (primarily at the National Center for Toxicological Research), and the National Institute of Environmental Health Sciences (part of the National Institutes of Health), where the program is administratively located. NTP offers a unique venue for the testing, research, and analysis of agents of concern to identify toxic and biological effects, provide information that strengthens the science base, and inform decisions by health regulatory and research agencies to safeguard public health. NTP also works to develop and apply new and improved methods and approaches that advance toxicology and better assess health effects from environmental exposures.

The Toxicity Report series began in 1991. The studies described in the NTP Toxicity Report series are designed and conducted to characterize and evaluate the toxicological potential of selected substances in laboratory animals (usually two species, rats and mice). Substances (e.g., chemicals, physical agents, and mixtures) selected for NTP toxicity studies are chosen primarily on the basis of human exposure, level of commercial production, and chemical structure. The interpretive conclusions presented in the Toxicity Reports are derived solely from the results of these NTP studies, and extrapolation of these results to other species, including characterization of hazards and risks to humans, requires analyses beyond the intent of these reports. Selection for study per se is not an indicator of a substance's toxic potential.

NTP conducts its studies in compliance with its laboratory health and safety guidelines and Food and Drug Administration [Good Laboratory Practice Regulations](#) and meets or exceeds all applicable federal, state, and local health and safety regulations. Animal care and use are in accordance with the [Public Health Service Policy on Humane Care and Use of Laboratory Animals](#). Studies are subjected to retrospective quality assurance audits before they are presented for public review. Draft reports undergo external peer review before they are finalized and published.

The NTP Toxicity Reports are available free of charge on the [NTP website](#) and cataloged in [PubMed](#), a free resource developed and maintained by the National Library of Medicine (part of the National Institutes of Health). Data for these studies are included in NTP's [Chemical Effects in Biological Systems](#) database.

For questions about the reports and studies, please email [NTP](#) or call 984-287-3211.

Table of Contents

Foreword.....	ii
Tables.....	v
Figures.....	v
About This Report.....	vii
Peer Review	x
Publication Details	xi
Acknowledgements.....	xi
Abstract.....	xii
Preface.....	xvi
Introduction.....	1
Chemical and Physical Properties.....	1
Production, Use, and Human Exposure	1
Regulatory Status	2
Absorption, Distribution, Metabolism, and Excretion	2
Experimental Animals	2
Humans	3
Toxicity	3
Experimental Animals	3
Humans	5
Reproductive and Developmental Toxicity	5
Experimental Animals	5
Humans	5
Carcinogenicity	5
Experimental Animals	5
Humans	5
Genetic Toxicity.....	6
Fullerenes.....	6
Modified Fullerenes	7
Study Rationale	7
Materials and Methods.....	8
Procurement and Characterization of Bulk Fullerene C ₆₀	8
Aerosol Generation and Exposure System for the Micro-C ₆₀ Studies.....	8
Aerosol Generation and Exposure System for the Nano-C ₆₀ Studies.....	11
Aerosol Concentration Monitoring for the Micro-C ₆₀ and Nano-C ₆₀ Studies	11
Carousel Atmosphere Characterization for the Micro-C ₆₀ and Nano-C ₆₀ Studies.....	13
Animal Source.....	15
Animal Welfare.....	15
Three-month Studies	15
Clinical Pathology.....	16
Reproductive Evaluations	17

Tissue Burden	17
Immunotoxicity	17
Necropsy	18
Statistical Methods	21
Calculation and Analysis of Lesion Incidences	21
Analysis of Continuous Variables	22
Quality Assurance Methods	22
Genetic Toxicology – Peripheral Blood Micronucleus Test.....	22
Results.....	24
Data Availability	24
Three-month Studies in Rats	24
Lung Burden	24
General Toxicity	26
Clinical Pathology.....	30
Reproductive Evaluations	30
Histopathology	30
Electron Microscopy.....	34
Immunotoxicity.....	34
Three-month Studies in Mice.....	37
Tissue Burden	37
General Toxicity	38
Hematology.....	43
Reproductive Evaluations	43
Histopathology.....	43
Immunotoxicity.....	46
Genetic Toxicology.....	47
Discussion.....	54
References.....	59
Appendix A. Reproductive Tissue Evaluations and Estrous Cycle Characterization	A-1
Appendix B. Tissue Burden Results	B-1
Appendix C. Immunotoxicity Results.....	C-1
Appendix D. Genetic Toxicology	D-1
Appendix E. Chemical Characterization and Generation of Carousel Concentrations	E-1
Appendix F. Ingredients, Nutrient Composition, and Contaminant Levels in NTP-2000 Rat and Mouse Ration.....	F-1
Appendix G. Sentinel Animal Program	G-1
Appendix H. Supplemental Data	H-1

Tables

Summary of Toxicologically Relevant Findings in Rats and Mice in the Three-month Nose-only Inhalation Study of Fullerene Micro-C ₆₀ (1 μm)	xiv
Summary of Toxicologically Relevant Findings Considered in Rats and Mice in the Three-month Nose-only Inhalation Study of Fullerene Nano-C ₆₀ (50 nm)	xv
Table 1. Experimental Design and Materials and Methods in the Three-month Nose-only Inhalation Studies of Fullerene Micro-C ₆₀ (1 μm) and Nano-C ₆₀ (50 nm)	19
Table 2. Lung Deposition and Clearance Parameter Estimates for Male Rats Exposed to Fullerene C ₆₀	25
Table 3. Survival and Body Weights of Rats in the Three-month Nose-only Inhalation Study of Fullerene Micro-C ₆₀ (1 μm).....	26
Table 4. Survival and Body Weights of Rats in the Three-month Nose-only Inhalation Study of Fullerene Nano-C ₆₀ (50 nm)	28
Table 5. Incidences of Selected Nonneoplastic Lesions in Rats in the Three-month Nose-only Inhalation Study of Fullerene Micro-C ₆₀ (1 μm).....	31
Table 6. Incidences of Selected Nonneoplastic Lesions in Rats in the Three-month Nose-only Inhalation Study of Fullerene Nano-C ₆₀ (50 nm)	32
Table 7. Bronchoalveolar Lavage Differential Results of Female Rats in the Three-month Nose-only Inhalation Study of Fullerene Micro-C ₆₀ (1 μm).....	34
Table 8. Bronchoalveolar Lavage Differential Results of Female Rats in the Three-month Nose-only Inhalation Study of Fullerene Nano-C ₆₀ (50 nm)	35
Table 9. Lung Deposition and Clearance Parameter Estimates for Male Mice Exposed to Fullerene C ₆₀	38
Table 10. Survival and Body Weights of Mice in the Three-month Nose-only Inhalation Study of Fullerene Micro-C ₆₀ (1 μm)	39
Table 11. Survival and Body Weights of Mice in the Three-month Nose-only Inhalation Study of Fullerene Nano-C ₆₀ (50 nm).....	41
Table 12. Incidences of Selected Nonneoplastic Lesions in Mice in the Three-month Nose-only Inhalation Study of Fullerene Micro-C ₆₀ (1 μm)	44
Table 13. Incidences of Selected Nonneoplastic Lesions in Mice in the Three-month Nose-only Inhalation Study of Fullerene Nano-C ₆₀ (50 nm).....	45
Table 14. Bronchoalveolar Lavage Differential Results of Female Mice in the Three- month Nose-only Inhalation Study of Fullerene Micro-C ₆₀ (1 μm)	46
Table 15. Bronchoalveolar Lavage Differential Results of Female Mice in the Three- month Nose-only Inhalation Study of Fullerene Nano-C ₆₀ (50 nm).....	46

Figures

Figure 1. Fullerene C ₆₀ (CASRN 99685-96-8; Chemical Formula: C ₆₀ ; Molecular Weight: 720.7).....	1
Figure 2. Schematic of the Aerosol Generation and Delivery System in the Three-month Nose-only Inhalation Studies of Fullerene Micro-C ₆₀ (1 μm)	10
Figure 3. Schematic of the Aerosol Generation and Delivery System in the Three-month Nose-only Inhalation Studies of Fullerene Nano-C ₆₀ (50 nm).....	12

Figure 4. Growth Curves for Rats Exposed to Fullerene Micro-C ₆₀ (1 μm) by Nose-only Inhalation for Three Months	27
Figure 5. Growth Curves for Rats Exposed to Fullerene Nano-C ₆₀ (50 nm) by Nose-only Inhalation for Three Months	29
Figure 6. Growth Curves for Mice Exposed to Fullerene Micro-C ₆₀ (1 μm) by Nose-only Inhalation for Three Months	40
Figure 7. Growth Curves for Mice Exposed to Fullerene Nano-C ₆₀ (50 nm) by Nose-only Inhalation for Three Months	42
Figure 8. Infiltration Cellular, Histiocyte and Pigmentation in the Lung of a Male Wistar Han Rat Exposed to 30 mg/m ³ Micro-C ₆₀ by Nose-only Inhalation for Three Months (H&E, 20×)	48
Figure 9. Infiltration Cellular, Histiocyte and Pigmentation in the Lung of a Male Wistar Han Rat Exposed to 2 mg/m ³ Nano-C ₆₀ by Nose-only Inhalation for Three Months (H&E, 40×)	48
Figure 10. Chronic Active Inflammation in the Lung of a Male Wistar Han Rat Exposed to 30 mg/m ³ micro-C ₆₀ by Nose-only Inhalation for Three Months (H&E, 40×)	49
Figure 11. Transmission Electron Micrograph of an Alveolar Macrophage in the Lung of a Male Wistar Han Rat Exposed by Nose-only Inhalation to 2 mg/m ³ Nano-C ₆₀ for Three Months (9900×)	49
Figure 12. Transmission Electron Micrograph of an Alveolar Macrophage in the Lung of a Male Wistar Han Rat Exposed by Nose-only Inhalation to 2 mg/m ³ Nano-C ₆₀ for Three Months (43,000×)	50
Figure 13. Transmission Electron Micrograph of a Macrophage in the Bronchial Lymph Node of a Male Wistar Han Rat Exposed to 30 mg/m ³ Micro-C ₆₀ by Nose-only Inhalation for Three Months	50
Figure 14. Transmission Electron Micrograph of a Macrophage in the Bronchial Lymph Node of a Male Wistar Han Rat Exposed by Nose-only Inhalation to 30 mg/m ³ Micro-C ₆₀ for Three Months	51
Figure 15. Cell Morphology of Bronchoalveolar Lavage Fluid in Rats	52
Figure 16. Cell Morphology of Bronchoalveolar Lavage Fluid in Mice	53

About This Report

National Toxicology Program¹

¹Division of the National Toxicology Program, National Institute of Environmental Health Sciences, Research Triangle Park, North Carolina, USA

Collaborators

D.L. Morgan, N.J. Walker, M.F. Cesta, G.L. Baker, C.R. Blystone, M.H. Boyle, A.E. Brix, J.A. Dill, P.M. Foster, D.R. Germolec, S.L. Grumbein, A. Gupta, B.T. Hamby, M.H. Hamlin, B.K. Hayden, R.A. Herbert, M.J. Hooth, A.P. King-Herbert, G.E. Kissling, W.G. Lieuallen, D.E. Malarkey, B.S. McIntyre, J.H. Roycroft, B.C. Sayers, K.A. Shipkowski, K.R. Shockley, C.S. Sloan, M.J. Smith, S.L. Smith-Roe, L.M. Staska, M.D. Stout, G.S. Travlos, R.W. Tyl, M.K. Vallant, S. Waidyanatha, , K.L. White, Jr., K.L. Witt

Division of the National Toxicology Program, National Institute of Environmental Health Sciences, Research Triangle Park, North Carolina, USA

Evaluated and interpreted results and reported findings

D.L. Morgan, Ph.D., Co-Study Scientist (retired)

N.J. Walker, Ph.D. Co-Study Scientist

M.F. Cesta, D.V.M., Ph.D., Study Pathologist

C.R. Blystone, M.S., Ph.D.

P.M. Foster, Ph.D. (retired)

D.R. Germolec, Ph.D.

R.A. Herbert, D.V.M., Ph.D.

M.J. Hooth, Ph.D.

A.P. King-Herbert, D.V.M.

G.E. Kissling, Ph.D. (retired)

B.S. McIntyre, Ph.D.

D.E. Malarkey, D.V.M., Ph.D.

J.H. Roycroft, Ph.D. (retired)

B.C. Sayers, Ph.D.

K.A. Shipkowski, Ph.D.

K.R. Shockley, Ph.D.

S.L. Smith-Roe, Ph.D.

M.D. Stout, Ph.D.

G.S. Travlos, D.V.M.

M.K. Vallant, B.S., MT (retired)

S. Waidyanatha, Ph.D.

K.L. Witt, M.S.

Battelle Columbus Operations, Columbus, Ohio, USA

Conducted studies and evaluated pathology findings

J.A. Dill, Ph.D., Principal Investigator

G.L. Baker, Ph.D.

A. Gupta, M.S.

B.K. Hayden
S.L. Grumbein, D.V.M., Ph.D.
L.M. Staska, D.V.M., Ph.D.

ILS, Inc., Research Triangle Park, North Carolina, USA

Evaluated and interpreted results and reported findings

M.H. Boyle, D.V.M.

Virginia Commonwealth University, Richmond, Virginia, USA

Conducted immunotoxicity studies

K.L. White, Jr., Ph.D., Principal Investigator

M.J. Smith, Ph.D.

Experimental Pathology Laboratories, Inc., Research Triangle Park, North Carolina, USA

Provided pathology review

M.H. Hamlin, II, D.V.M., Ph.D., Principal Investigator

A.E. Brix, D.V.M., Ph. D.

Pathology Associates, A Division of Charles River Laboratories, Inc., Research Triangle Park, North Carolina, USA

Coordinated NTP Pathology Peer Review of the 3-month rats and mice (November 16, 2009)

W.G. Lieuallen, D.V.M., Ph.D.

RTI International, Research Triangle Park, North Carolina, USA

Provided SMVCE analysis

R.W. Tyl, Ph.D., Principal Investigator

B.T. Hamby, B.S.

C.S. Sloan, M.S.

Contributors

NTP Pathology Peer Review, National Institute of Environmental Health Sciences, Research Triangle Park, North Carolina, USA

Participated in NTP Pathology Peer Review of the 3-month rats and mice (November 16, 2009)

A.E. Brix, D.V.M., Ph. D., Experimental Pathology Laboratories, Inc.

M.F. Cesta, D.V.M., Ph.D., National Toxicology Program

R.A. Herbert, D.V.M., Ph.D., National Toxicology Program

D.E. Malarkey, D.V.M., Ph.D., National Toxicology Program

Social and Scientific Systems, Inc., Research Triangle Park, North Carolina, USA

Provided statistical analyses

M.V. Smith, Ph.D., Principal Investigator

L.J. Betz, M.S.

S.F. Harris, M.S.

CSS, Inc., Research Triangle Park, North Carolina, USA

Prepared quality assessment audits

S. Brecher, Ph.D., Principal Investigator

S. Iyer, B.S.

V.S. Tharakan, D.V.M.

Biotechnical Services, Inc., Little Rock, Arkansas, USA

Prepared draft report

S.R. Gunnels, M.A., Principal Investigator

L.M. Harper, B.S.

J.I. Powers, M.A.P.

D.C. Serbus, Ph.D.

Division of the National Toxicology Program, National Institute of Environmental Health Sciences, Research Triangle Park, North Carolina, USA

Provided oversight of external peer review

E.A. Maull, Ph.D.

M.S. Wolfe, Ph.D.

ICF, Durham, North Carolina, USA

Provided contract oversight

D.F. Burch, M.E.M.

Conducted external peer review

L.M. Green, M.P.H.

A.L. Scheuer, B.A.

Prepared report

T.W. Cromer, M.P.S.

T. Hamilton, M.S.

M.E. McVey, Ph.D.

A.A.M. Murphy, B.S.

B.C. Riley, B.S.

Peer Review

The draft *NTP Technical Report on the Toxicity Studies of Fullerene C₆₀ (1 μm and 50 nm) (CASRN 99685-96-8) Administered by Nose-only Inhalation to Wistar Han [CrI:WI (Han)] Rats and B6C3F1/N Mice* was evaluated by the reviewers listed below. These reviewers served as independent scientists, not as representatives of any institution, company, or governmental agency. In this capacity, reviewers determined if the design and conditions of these NTP studies were appropriate and ensured that this Toxicity Study Report presents the experimental results and conclusions fully and clearly.

Alison Elder, Ph.D.

Department of Environmental Medicine, University of Rochester
Rochester, New York, USA

Clark Lantz, Ph.D.

Professor, Cellular and Molecular Medicine, University of Arizona
Tucson, Arizona, USA

Publication Details

Publisher: National Toxicology Program

Publishing Location: Research Triangle Park, NC

ISSN: 2378-8992

DOI: <https://doi.org/10.22427/NTP-TOX-87>

Report Series: NTP Toxicity Report Series

Report Series Number: 87

Official citation: National Toxicology Program (NTP). 2020. NTP technical report on the toxicity studies of fullerene C₆₀ (1 μm and 50 nm) (CASRN 99685-96-8) administered by nose-only inhalation to Wistar Han [CrI:WI (Han)] rats and B6C3F1/N mice. Research Triangle Park, NC: National Toxicology Program. Toxicity Report 87.

Acknowledgements

This work was supported by the Intramural Research Program (ES103316, ES103318, and ES103319) at the National Institute of Environmental Health Sciences, National Institutes of Health and performed for the National Toxicology Program, Public Health Service, U.S. Department of Health and Human Services under contracts HHSN273201800006C, HHSN273201600020C, GS00Q14OADU417 (Order no. HHSN273201600015U), HHSN273201600011C, HHSN273201500014C, HHSN273201500013C, HHSN273201500012C, HSN273201500006C, HHSN273201400015C, HHSN316201200054W, HHS273200900002C, N01-ES-55538, N01-ES-65557, N01-ES-45517, and N01-ES-55534.

Abstract

Fullerene C₆₀ (C₆₀), a primary allotrope of carbon, is used in a variety of consumer applications including microelectronics, photovoltaics, batteries and fuel cells, and water treatment methods. Human exposure to engineered C₆₀ due to industrial applications may occur via inhalation, oral, dermal, or parenteral routes. In these toxicity and tissue burden studies, male and female Wistar Han rats and B6C3F1/N mice were exposed to fullerene C₆₀ (at least 95% pure) via nose-only inhalation for 3 months. Two different C₆₀ fullerene aggregate sizes, 1 µm diameter (micro-C₆₀) and 50 nm diameter (nano-C₆₀) were studied to assess the potential for differential effects based on particle size.

Groups of 10 male and 10 female core study rats and mice were exposed to atmospheres of the two fullerene C₆₀ particle sizes via nose-only inhalation at concentrations of 0, 2, 15, or 30 mg/m³ (micro-C₆₀ studies) or 0, 0.5, or 2 mg/m³ (nano-C₆₀ studies), 3 hours per day, 5 days per week for 13 weeks. Additional groups of rats and mice were analyzed for tissue burden and studied for clearance studies and immunotoxicity.

Lung tissue weights were significantly increased at multiple timepoints in male rats and mice exposed to micro- or nano-C₆₀ particles. Lung tissue burden increased with exposure concentration following exposure to either micro- or nano-C₆₀ particles and was greater in rats and mice exposed to the same concentration (2 mg/m³) of nano-C₆₀ relative to micro-C₆₀ particles. The calculated lung clearance half-life (t_{1/2}) for both particle sizes was, in general, longer in male rats than in male mice. In male rats, the t_{1/2} of micro-C₆₀ was shorter than that of nano-C₆₀ particles at the same mass-based exposure concentration (2 mg/m³).

In the micro-C₆₀ study in rats no exposure-related effects on body weights or clinical pathology were found in male or female rats. Liver weights of 30 mg/m³ males were significantly greater than those of the control males. Histologically, exposure-related increases in the lung (chronic active inflammation and histiocyte infiltration) of both male and female rats occurred. Exposure-related increases in pigmentation (presumably test article) were seen in the lung and the bronchial (male) and mediastinal (females) lymph nodes. Micro-C₆₀ exposure exhibited the potential to be a reproductive toxicant in male rats on the basis of decreased sperm motility and low incidences of histopathological findings in the testes (germinal epithelium degeneration).

In the micro-C₆₀ study in mice, mean body weights of exposed groups of males and females were similar to those of the control groups. Lung weights of 30 mg/m³ exposed females were significantly higher than those of the control females. There were no exposure-related effects on hematology in male or female mice. Histologically, exposure-related lesions occurred in the lung (chronic active inflammation and histiocyte infiltration) and larynx (squamous metaplasia). Exposure-related increases in pigmentation were seen in the lung and bronchial lymph nodes (males). Micro-C₆₀ exposure also exhibited the potential to be a reproductive toxicant in female mice on the basis of increased probability of extended estrus and in male mice on the basis of decreased sperm motility.

In the nano-C₆₀ study in rats, no effects were observed on body weights, clinical pathology, or organ weights, and no exposure-related increases were found in chronic active inflammation and histiocyte infiltration in the lung. Exposure-related increases in pigmentation were seen in the lung (females) and bronchial lymph nodes. Low incidences of germinal epithelium degeneration in the testis and hypospermia were observed in male rats in the 2 mg/m³ group compared to none

in control males. Sperm motility was significantly reduced in all exposed groups. Nano-C₆₀ exposure exhibited the potential to be a reproductive toxicant in male rats, but not in male mice, on the basis of lower sperm motility and low incidences of histopathological findings in the testis (germinal epithelium degeneration) and epididymis (hypospermia).

In the nano-C₆₀ study in mice, there were no exposure-related effects on body weights, organ weights, and clinical pathology and no exposure-related increase in chronic active inflammation as seen with micro-C₆₀. Exposure-related increases in histiocyte infiltration were seen in the lungs of male mice. Exposure-related increases in pigmentation were seen in the lung and bronchial lymph nodes (males). Nano-C₆₀ exposure exhibited the potential to be a reproductive toxicant in female mice on the basis of increased probability of extended estrus compared to control females.

Micro- and nano-C₆₀ exposure had minimal effects on the components of the immune system examined, including innate, humoral, and cell-mediated immunity, in female rats and mice. Bronchoalveolar lavage fluid (BALF) macrophages from female rats and mice exposed to nano-C₆₀ and micro-C₆₀ contained intracytoplasmic, brown to black, granular to globular pigment. Mice exposed to micro-C₆₀ demonstrated a significant increase in MIP-1 α levels in the BALF, while those exposed to nano-C₆₀ demonstrated no such effect. Alterations in BALF cell phenotype were observed in female Wistar Han rats at all exposure levels. Levels of specific cytokines in the BALF were altered following exposure to micro- or nano-C₆₀ in both rats and mice. Shifts in spleen cell phenotype were noted in B6C3F1/N female mice exposed to either micro- (15 and 30 mg/m³) or nano- (0.5 and 2 mg/m³) C₆₀.

Neither micro- nor nano-C₆₀ increased the frequencies of micronucleated reticulocytes or erythrocytes in peripheral blood of male or female Wistar Han rats or B6C3F1/N mice. Neither size particle affected the percentage of reticulocytes in peripheral blood, suggesting no exposure-related bone marrow toxicity.

In conclusion, C₆₀ fullerene nose-only inhalation in both rats and mice for 13 weeks had little effect on systemic immune function. Locally, lung inflammatory responses were observed, primarily at the higher exposure concentrations. Inflammatory effects of nano-C₆₀ exposure were, in general, more severe than micro-C₆₀ exposure at the same mass-based atmospheric exposure concentrations.

Synonyms: Buckminsterfullerene; Buckminsterfullerene (C₆₀); Buckyball, C₆₀ fullerene carbon (C₆₀); carbon cluster (C₆₀); carbon C₆₀ fullerene; carbon (C₆₀) mol.; carbon, mol. (C₆₀); follene-60, footballene; footballene (C₆₀); [60]fullerene; [5,6]fullerene C₆₀; fullerene-60, fullerene-C₆₀; fullerene C₆₀ cluster; icosahedral C₆₀; soccerballene

Summary of Toxicologically Relevant Findings in Rats and Mice in the Three-month Nose-only Inhalation Study of Fullerene Micro-C₆₀ (1 µm)

	Male Wistar Han Rats	Female Wistar Han Rats	Male B6C3F1/N Mice	Female B6C3F1/N Mice
Concentrations in Air	0, 2, 15, or 30 mg/m ³	0, 2, 15, or 30 mg/m ³	0, 2, 15, or 30 mg/m ³	0, 2, 15, or 30 mg/m ³
Survival Rates	10/10, 10/10, 10/10, 10/10	10/10, 9/10, 10/10, 10/10	10/10, 9/10, 10/10, 10/10	10/10, 10/10, 10/10, 10/10
Body Weights	Exposed groups similar to the control group	Exposed groups similar to the control group	Exposed groups similar to the control group	Exposed groups similar to the control group
Lung Burden				
µg C ₆₀ /Total Lung ^a	439; 2,182; 5,749	234; 1,763; 4,658	38; 209; 595	36; 190; 560
t _{1/2} (days)	27, 69, 55	Not assessed	16, 18, 68	Not assessed
Organ Weights	↑ Liver (absolute and relative) ^b	None	None	↑ Lung (absolute and relative)
Clinical Pathology	None	None	None	None
Immunotoxicity	Not assessed	BALF: pigmented macrophages in all exposed groups; ↑ % neutrophils at 30 mg/m ³ ; ↑ % lymphocytes at 15 and 30 mg/m ³ ; ↑IL-1 at 15 and 30 mg/m ³ ; ↑MCP-1 at 30 mg/m ³	Not assessed	BALF: pigmented macrophages in exposed groups. ↑ % neutrophils and ↑ % lymphocytes at 15 and 30 mg/m ³ ; ↑MIP-1α at 15 and 30 mg/m ³
Reproductive Toxicity	↓ Sperm motility	Not assessed	↓ Sperm motility	↑ Probability of extended estrus
Nonneoplastic Effects	<u>Lymph node, bronchial:</u> pigmentation (0/7, 1/5, 3/6, 7/8) <u>Lung:</u> infiltration cellular, histiocyte (1/10, 1/10, 8/9, 10/10); inflammation, chronic active (1/10, 4/10, 8/9, 10/10); pigmentation (0/10, 1/10, 8/9, 10/10); <u>Testes:</u> germinal epithelium (0/10, 1/10, 3/10, 1/10)	<u>Lymph node, mediastinal:</u> pigmentation (3/8, 9/10, 7/8, 7/9) <u>Lung:</u> infiltration cellular, histiocyte (1/10, 1/10, 8/10, 10/10); inflammation, chronic active (0/10, 0/10, 1/10, 10/10); pigmentation (0/10, 0/10, 8/10, 10/10)	<u>Lymph node, bronchial:</u> pigmentation (2/6, 1/4, 2/5, 9/9) <u>Larynx:</u> metaplasia, squamous (1/10, 0/9, 5/10, 9/10) <u>Lung:</u> infiltration cellular, histiocyte (0/10, 0/10, 10/10, 10/10); inflammation, chronic active (0/10, 0/10, 10/10, 10/10); inflammation, chronic active (0/10, 0/10, 10/10, 10/10); pigmentation (0/10, 0/10, 10/10, 10/10)	<u>Larynx:</u> metaplasia, squamous (0/10, 1/8, 6/10, 9/10) <u>Lung:</u> infiltration cellular, histiocyte (0/10, 0/10, 10/10, 10/10); inflammation, chronic active (0/10, 0/10, 3/10, 10/10); pigmentation (0/10, 0/10, 10/10, 10/10)
Genetic Toxicology				
Micronucleated Erythrocytes				
Peripheral blood in vivo:				Negative in male and female rats and mice

t_{1/2} = half-life; BALF = Bronchoalveolar lavage fluid.

^aPostexposure day 0.

^bRelative to body weight.

Summary of Toxicologically Relevant Findings Considered in Rats and Mice in the Three-month Nose-only Inhalation Study of Fullerene Nano-C₆₀ (50 nm)

	Male Wistar Han Rats	Female Wistar Han Rats	Male B6C3F1/N Mice	Female B6C3F1/N Mice
Concentrations in Air	0, 0.5, or 2 mg/m ³	0, 0.5, or 2 mg/m ³	0, 0.5, or 2 mg/m ³	0, 0.5, or 2 mg/m ³
Survival Rates	10/10, 10/10, 10/10	10/10, 10/10, 10/10	10/10, 10/10, 10/10	10/10, 10/10, 10/10
Body Weights	Exposed groups similar to the control group	Exposed groups similar to the control group	Exposed groups similar to the control group	Exposed groups similar to the control group
Lung Burden				
μg C ₆₀ /Total Lung ^a	189, 581	128, 434	24, 115	26, 98
t _{1/2} (days)	38, 61	Not assessed	17, 15	Not assessed
Organ Weights	None	None	None	None
Clinical Pathology	None	None	None	None
Immunotoxicity	Not assessed	BALF: Pigmented macrophages in exposed groups	Not assessed	BALF: Pigmented macrophages in exposed groups
Reproductive Toxicity	↓ Sperm motility	Not assessed	None	↑ Probability of extended estrus
Nonneoplastic Effects	<u>Lymph node, bronchial:</u> pigmentation (0/10, 3/9, 4/10) <u>Lymph node, mediastinal:</u> pigmentation (1/10, 6/8, 2/10) <u>Testes:</u> germinal epithelium: degeneration (0/10, 0/10, 3/10)	<u>Lymph node, bronchial:</u> pigmentation (0/10, 1/10, 5/10) <u>Lymph node, mediastinal:</u> pigmentation (0/8, 7/8, <u>Lung:</u> infiltration cellular, histiocyte (2/10, 1/10, 8/10); pigmentation (0/10, 0/10, 8/10)	<u>Lymph node, bronchial:</u> pigmentation (0/9, 2/7, 5/7) <u>Lung:</u> infiltration cellular, histiocyte (1/10, 2/10, 7/10); pigmentation (0/10, 0/10, 7/10)	<u>Lymph node, bronchial:</u> pigmentation (2/10, 3/10, 4/10) <u>Lung:</u> infiltration cellular, histiocyte (2/10, 1/10, 5/10); pigmentation (0/10, 0/10, 5/10)
Genetic Toxicology				
Micronucleated Erythrocytes				
Peripheral blood in vivo:			Negative in male and female rats and mice	

t_{1/2} = half-life; BALF = Bronchoalveolar lavage fluid.

^aPostexposure day 0.

^bRelative to body weight.

Preface

The National Toxicology Program's (NTP's) Nanotechnology Safety Initiative was instituted in 2004 due to the widespread use of nanoscale materials and inadequate information on possible biological interactions and toxicity following exposure. This initiative is a broad-based research program with the goal of addressing potential human health hazards associated with the manufacture and use of nanoscale materials and is driven by the current and anticipated future research and development focus on nanotechnology. The research program was designed to comprehensively evaluate the toxicological properties of major nanoscale materials classes, which represent a cross-section of composition, size, surface coatings, and physiochemical properties. Nanoscale materials evaluated under this initiative include: (1) metal oxides (titanium dioxide and zinc oxide), (2) fluorescent crystalline semiconductors (quantum dots; cadmium selenide/zinc sulfite spheres), (3) carbon-based fullerenes, (4) carbon nanotubes, (5) nanoscale silver, and (6) nanoscale gold. Further information about the NTP Nanotechnology Safety Initiative is available at: <https://ntp.niehs.nih.gov/results/nano/index.html>.

Introduction

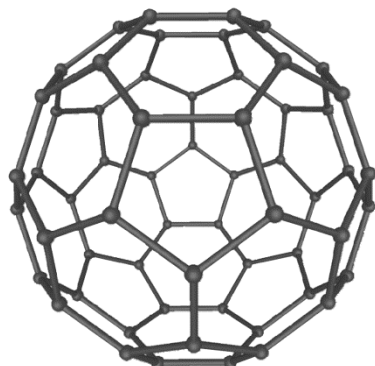


Figure 1. Fullerene C₆₀ (CASRN 99685-96-8; Chemical Formula: C₆₀; Molecular Weight: 720.7)

Synonyms: Buckminsterfullerene; Buckminsterfullerene (C₆₀); Buckyball, C₆₀ fullerenecarbon (C₆₀); carbon cluster (C₆₀); carbon C₆₀ fullerene; carbon (C₆₀) mol.; carbon, mol. (C₆₀); follene-60, footballene; footballene (C₆₀); [60]fullerene; [5,6]fullerene C₆₀; fullerene-60, fullerene-C₆₀; fullerene C₆₀ cluster; icosahedral C₆₀; soccerballene.

Chemical and Physical Properties

Fullerene C₆₀ (C₆₀) is one of the primary allotropes of carbon; the others are graphite and diamond.¹ C₆₀ is a stable aggregate of 60 carbon atoms in the form of a truncated icosahedron with 60 vertices and 32 faces.^{2;3} C₆₀ has a molecular weight of 720.66 g/mol, a melting point greater than 280 C, a relative density of 1.600 g/cm³ (at 20°C), and a log K_{ow} of 6.67.^{4;5}

The diameter of single C₆₀ particles is approximately 1 nanometer (nm), thereby classifying them as nanoscale materials.⁶ The European Union defines nanoscale materials as materials having at least one dimension between 1 and 100 nm.^{7;8} Like many other nanoscale materials, C₆₀ molecules can aggregate into nanoscale or microscale particles.^{7;9} C₆₀ can form a stable, colloidal nanocrystalline structure (nano-C₆₀) in water at concentrations up to 100 µg/mL, in which the nano-C₆₀ particles consist of faceted crystals varying in size from 50 to 300 nm.⁹

C₆₀ is commercially available in a dry state in a highly aggregated crystalline form, and this crystal state can vary based on the degree of purity.⁵ At 98% purity, C₆₀ exists as faceted, spherical particles ranging from 20 to 150 µm in diameter, with most particles falling in the range of 50 to 100 µm. At 99.5% purity, C₆₀ exists as elongated particles ranging from 50 to 200 µm in length. These particles can be faceted or smooth and consist of 1 µm particles packed tightly together. At 99.9% purity, C₆₀ exists as needle-like particles ranging from approximately 10 µm to approximately 1.5 mm in length and appearing as smaller, tightly bundled particles.^{10;5} C₆₀ is hydrophobic, although water-soluble C₆₀ suspensions have been created using solvents such as tetrahydrofuran, toluene, and dichlorobenzene.¹¹⁻¹³

Production, Use, and Human Exposure

Various methods are used to prepare C₆₀, the most common being the pyrolysis of toluene, which produces a fullerene mixture that comprises C₆₀ (60% to 70%), C₇₀ (20% to 30%), and other higher order fullerenes. This mixture is then further purified into specific purities of C₆₀ and C₇₀.¹⁴

Industrial manufacturing in the United States produces an estimated 80 tons per year of engineered C₆₀.¹⁵ Natural generation of C₆₀ occurs following volcanic eruptions, forest fires, and the combustion of carbon-based materials, although the amount of C₆₀ produced from natural or anthropogenic sources is currently unknown.^{11; 16; 17} The incidences of C₆₀ in both ice-core samples and the fossil record suggest that C₆₀ has existed in the environment throughout human history.^{16; 17}

Nanomaterials have many unique properties that make them ideal for use in a variety of products. Due to their small size, they often have chemical, biological, or physical properties that differ relative to the same material of a larger size; examples include higher strength, durability, and conductivity.¹⁸⁻²⁰ These materials also have an increased surface-area-to-mass ratio, which, although ideal in some consumer applications, also means nanomaterials are more reactive; this increased reactivity makes nanomaterials more biologically active.^{21; 19} Due to their small size, nanomaterials, including C₆₀, have been investigated as drug delivery agents; however, there is concern for the materials accumulating in non-target tissues due to their ability to enter systemic circulation and pass through biological barriers such as the blood-brain barrier.²²

C₆₀ has been engineered for many uses and was once widely used in a variety of consumer applications including microelectronics, photovoltaics, batteries and fuel cells, and water treatment methods and as a drug delivery agent.^{23; 15; 24} Use of C₆₀ in cosmetics products is steadily increasing as free radical scavenging properties of C₆₀ are purported to be anti-aging.^{25;}²⁶ In 2014, the Food and Drug Administration (FDA) published guidance on the use of nanomaterials in cosmetic products, citing concerns that the size of nanomaterials allows for differential biological activity relative to the same material in larger size.¹⁸ Exposure to C₆₀ in aerosolized cosmetics is of particular concern, as pulmonary exposure to C₆₀ has been shown to induce respiratory toxicity.^{11; 27; 28}

Human exposure to engineered C₆₀ due to industrial applications could occur via inhalation, oral, dermal, or parenteral routes.⁶ C₆₀ has been determined to be present in urban air samples, and human exposure to airborne C₆₀ released from combustion sources and industrial processes occurs primarily via inhalation.²⁹ Nano-C₆₀ is stable in water, allowing for the possibility of this form of C₆₀ to exist in aqueous environmental samples.⁹

Regulatory Status

There are no workplace exposure limits for C₆₀.

Absorption, Distribution, Metabolism, and Excretion

Experimental Animals

General factors known to affect the absorption and distribution of nanoparticles include particle size, shape, aggregation size, and dispersion pattern. Following inhalation exposure, well dispersed nanoparticles tend to deposit at the alveolar duct bifurcations and epithelial surfaces in the distal regions of the lung in rodents.^{30; 31} Particle size is an important factor, as smaller particles tend to travel farther into the pulmonary interstitium.³² Once particles are in the lung, retention depends on dose and particle size, as smaller nanoparticles are retained longer, especially at higher doses.³³

Clearance of nanoparticles from the lung can occur following phagocytosis of particles by alveolar macrophages and by removal from the respiratory tract via the mucociliary escalator. In addition, alveolar macrophages can remove particles from the lung via the tracheobronchial and pleural lymphatic systems.^{34; 35} Particles can also be trapped in the mucous layer of the airways and subsequently be cleared from the lung via translocation, without the involvement of macrophages.

The deposition rate and half-life of micro- and nano-C₆₀ particles were evaluated in male F344 rats exposed by nose-only inhalation for 10 days.¹¹ Exposure to C₆₀ nanoparticles (55 nm diameter) 3 hours per day at a concentration of 2.22 mg/m³ resulted in a 41% higher deposition rate and a 50% higher deposition fraction than exposure to C₆₀ microparticles (0.93 μm diameter) 3 hours per day at a concentration of 2.35 mg/m³. The half-life of the C₆₀ nanoparticles (26 days) was similar to that of the C₆₀ microparticles (29 days).

The National Toxicology Program (NTP) investigated the disposition of C₆₀ (suspended in toluene) following intratracheal (IT) instillation and intravenous (IV) administration of 1 or 5 mg C₆₀ per kg body weight (mg/kg).³⁶ Particle size distribution analysis indicated that the average size of the fullerene C₆₀ aggregates in suspension was approximately 1 μm. Following IT instillation, C₆₀ in the lung showed minimal clearance over the 168-hour observation period and showed a greater than dose-proportional increase over the dose range tested. C₆₀ was not detected in extrapulmonary tissues. Following IV administration, C₆₀ was rapidly eliminated from the blood and was undetectable after 0.5 hours. The highest tissue concentrations occurred in the liver, followed by the spleen, lung, and kidney. C₆₀ was cleared slowly from the kidney and the lung with estimated half-lives of 24 and 139 hours, respectively. The liver concentration decreased minimally over time; more than 90% of the C₆₀ present at 0.5 hours remained at 168 hours. C₆₀ also was not detected in urine or feces. The maternal transfer of C₆₀ was evaluated in pregnant Sprague Dawley rats injected intravenously via the tail vein on gestational day 15 or postnatal day 8 with radiolabeled solubilized C₆₀.^{37; 38} Radioactivity (as a percentage of the total injected) was measured in the liver (43%), spleen (4%), reproductive tract (3%), placenta (2%), and fetuses (0.87%) 24 hours postinjection. In lactating dams, radioactivity was measured 24 hours postexposure in the liver (35%), spleen (4%), reproductive tract (0.10% to 0.42%), mammary tissue (0.48% to 0.94%), and milk. Distribution to the gastrointestinal tract of pups increased between 24 (0.28%) and 48 (0.43%) hours postinjection.

Humans

Studies on the absorption, distribution, metabolism, or excretion of C₆₀ in humans were not identified in the available literature.

Toxicity

Experimental Animals

Limited studies have assessed C₆₀ toxicity following inhalation exposure in animals. A comparative study to analyze the toxicity of nano- or microscale C₆₀ particles exposed male F344 rats (Taconic) to C₆₀ fullerene nanoparticles (2.22 mg/m³, 55 nm diameter) and microparticles (2.35 mg/m³, 0.93 μm diameter) for 3 hours/day for 10 consecutive days using a nose-only exposure system. This study indicated that exposure to C₆₀ nanoparticles increased total

bronchoalveolar fluid (BALF) protein concentrations relative to control rats without altering cytokine concentrations.¹¹ Rats exposed to C₆₀ microparticles had lower concentrations of the cytokines GRO/KC and IL-18 and higher concentrations of TNF α and IL-1 β in the BALF than did the control groups.

DNA microarray analysis has been used to assess gene expression profiles in the lungs of male Wistar rats exposed to C₆₀ nanoparticles (0.12 mg/m³, 96 nm diameter) via nose-only inhalation for 4 weeks (6 hours/day, 5 days/week).²⁷ Upregulation of genes involved in apoptosis, oxidative stress, inflammation, and metalloendopeptidase activity occurred 3 days and 1 month after C₆₀ exposure.

Intratracheal instillation of a water-soluble suspension of C₆₀ (47 nm average particle size), at doses of 0.5–2 mg/kg, caused increased neutrophilia and upregulated levels of pro-inflammatory cytokines in the lungs of ICR male mice.^{6; 39} However, a single intratracheal instillation of C₆₀ aggregates (160 nm diameter) to male Crl:CD[®](SD)IGS BR rats at doses ranging from 0.2 to 3 mg/kg induced limited pulmonary toxicity; the only effects observed were increased neutrophilia in the BALF 24 hours postexposure and increased lipid peroxidation 24 hours and 3 months postinstillation.⁴⁰ No histopathological effects were observed in the lungs.

To study interactions between hydroxylated fullerene and crystalline α -quartz, 0.2, 2 and 20 μ g fullerenol (C₆₀[OH]_{20 \pm 2}) was administered as an intratracheal bolus prior to intratracheal instillation of 50 μ g quartz to female BALB/cJ mice. These data showed decreased levels of neutrophils and induced an anti-inflammatory response in the lungs of exposed animals, suggesting that surface modification of C₆₀ particles can alter potential in vivo toxicity.⁴¹

Intraperitoneal exposure to C₆₀ has been associated with renal and hepatotoxicity.⁶ Exposure to C₆₀ (60 mg/kg per day) via intraperitoneal injection for 12 days caused increased absolute and relative weight of the spleen in female Japan Charles River Sprague Dawley rats.⁴² Swiss mice exposed to 100 mg/mL micro-C₆₀ (up to 10 g/kg) via intraperitoneal injection had increased liver and spleen weights 14 days postexposure.⁴³ Histopathological examination of livers and spleens from the exposed mice demonstrated accumulation of C₆₀ in the liver, predominantly in the Kupffer and perisinusoidal cells. Mice exposed to 2.5 g/kg C₆₀ had increased relative liver and spleen weights 8 weeks postexposure, increased hypertrophy and hyperplasia of hepatic stellate cells, and increased hyperplasia of the spleen.

Intraperitoneal injection of aqueous C₆₀ suspensions (developed without an organic solvent) to male Wistar rats at up to 2 g/kg caused no observable signs of acute or subacute toxicity and protected against hepatic oxidative stress.¹³ Toxicity has not been demonstrated for oral exposure to C₆₀.⁶ Male and female Sprague–Dawley rats orally administered 2 g/kg fullerene, a mixture of C₆₀ and C₇₀, showed no signs of toxicity after 14 days of exposure.⁴⁴ Chen et al.⁴² reported that oral administration of a single 50 mg/kg dose of polyalkylsulfonated C₆₀ (water-soluble) to female Sprague-Dawley CD(Crl:CDR (SD)BR) rats was not toxic; rats administered the same dose for 12 days also showed no signs of toxicity. Male Wistar rats orally administered C₆₀ in olive oil (0.8 mg/mL; 1.7 mg/kg) for 7 months survived approximately twice as long as control animals.⁴⁵

Concern for nanomaterial-induced immunotoxicity derives from phagocytes (i.e., neutrophils, monocytes, macrophages, and dendritic cells) ability to take up nanomaterials, although few in vivo studies have analyzed the effects of exposure to C₆₀ on the immune system.^{46; 47} Female

C57BL/6 mice exposed to 1.1 µg colloidal C₆₀ aggregates (165 nm mean diameter) via intravenous injection had repressed delayed-type hypersensitivity responses to methyl bovine serum albumin.⁴⁸ Intraperitoneal exposure (daily injection with 5 µg of nano-C₆₀) of C57BL/6 mice to a range of H₂O-soluble C₆₀ aggregates (50 to 250 nm size) caused a decrease in splenocyte proliferation and an increase in nitric oxide production by splenocytes.⁴⁹ BALB/c mice produced anti-C₆₀ antibodies when immunized (three intraperitoneal doses) with C₆₀ particles conjugated to bovine thyroglobulin and administered in Freund's complete and incomplete adjuvants.⁵⁰

Humans

Studies on the effects of C₆₀ exposure in humans were not identified in the available literature.

Reproductive and Developmental Toxicity

Experimental Animals

Intraperitoneal injection of pregnant Slc mice on gestation day 10 with C₆₀ (25, 50, or 137 mg/kg) solubilized in poly(vinylpyrrolidone) (PVP) resulted in the death of all embryos at 137 mg/kg.^{37; 51} C₆₀ was present in the yolk sac of mice exposed to 50 mg/kg, and the heads and tails of 50% of the embryos from these mice were abnormal in shape.

Zebrafish (*Danio rerio*) embryos exposed to nano-C₆₀ (a core of C₆₀ coated with hydroxylated C₆₀) (1.5 mg/L) for up to 96 hours delayed zebrafish embryo and larval development, decreased survival and hatching rates, and caused pericardial edema.⁵² There are no studies on zebrafish with pure C₆₀.

Humans

Studies on the developmental or reproductive toxicity of C₆₀ in humans were not identified in the available literature.

Carcinogenicity

Experimental Animals

No 2-year carcinogenicity studies of C₆₀ were identified in the available literature. Dimethylbenz[*a*]anthracene-initiated CD-1 mice dermally exposed to C₆₀/C₇₀ (1 mg/mL in benzene) for 24 weeks had no skin tumors, demonstrating that C₆₀/C₇₀ is not a skin tumor promoter.⁵³ Intraperitoneal exposure to H₂O-soluble C₆₀ aggregates (50 to 250 nm size) caused an increase in tumor proliferation in C57BL/6 mice also inoculated with B61F10 melanoma cells.⁴⁹

Humans

Epidemiological studies of C₆₀ in humans were not identified in the available literature.

Genetic Toxicity

The genotoxicity of nanomaterials, including carbon black and fullerenes, has been reviewed by Roller.⁵⁴ Most nanomaterials have shown genotoxic potential *in vitro* for some endpoints, particularly DNA damage measured by the comet assay. Results are not consistent across all studies, however, and attempts to correlate responses with the physical properties of the various nanomaterials have not revealed any clear association.

Fullerenes

Positive results have been reported with an aqueous C₆₀ suspension over a concentration range of 0.048 to 0.43 µg/mL in the absence of an exogenous metabolic activation system (S9 mix) in the *Bacillus subtilis* Rec-assay, which measures differential toxicity between repair competent and repair deficient strains of the bacterium.⁵⁵ The average diameter of fullerene particles was 117 nm in aqueous solution, but in bacterial culture broth, particle size increased to an average of 320 nm, which may have limited the ability of bacteria to take up the particles. Therefore, the results reported in this assay could have represented minimal responses. In a second DNA damage/repair assay in bacteria, the *umu* test in *Salmonella typhimurium* strain TA1535/pSK1002, positive results were seen with an aqueous suspension of C₆₀ (320 nm) at 0.43 µg/mL in the presence and absence of S9 mix.⁵⁵ In standard bacterial gene mutation assays with fullerenes (concentration ranges extending to 5,000 µg/plate), no mutagenicity was observed in any of several strains of *S. typhimurium* or *Escherichia coli* WP2uvrA/pKM101, with or without S9 mix.^{44; 56} The dispersants used in these bacterial mutagenicity assays and particle sizes were 0.1% carboxymethylcellulose sodium (CMC-Na) with a C₆₀ average diameter of 53 nm⁵⁶ and dimethylsulfoxide with a mixture of C₆₀ and C₇₀ fullerite particles, not further characterized.⁴⁴

Mixed results were also reported in chromosome damage assays *in vitro* with C₆₀, with negative results reported in Chinese hamster CHL/IU cells for chromosomal aberrations, with and without S9,^{44; 56} and positive results reported for micronucleus induction (a biomarker of chromosomal damage) in human A549 cells.⁵⁷ In the micronucleus test, A549 cells were exposed to fullerenes (0.7 nm; suspended in physiological saline with 0.05% Tween 80) in the absence of S9 only, and a clear, dose-related increase in the frequency of micronucleated cells was seen over a concentration range of 0.02 to 200 µg/mL (0.003 to 34 µg/cm²). In the chromosomal damage assay reported by Shinohara et al.,⁵⁶ particle size was approximately 57 nm and a 0.1% CMC-Na dispersant was used; the highest concentration tested, 100 µg/mL with or without S9, was limited by precipitation of the nanoparticle suspension.

In contrast to the positive *in vitro* micronucleus test results reported by Totsuka et al.,⁵⁷ results of an *in vivo* bone marrow micronucleus test in male ICR mice treated with 88 mg/kg fullerenes (34 nm diameter, dispersed in 0.1% Tween 80) by gavage twice at 24-hour intervals were negative.⁵⁶

Results of an *in vitro* comet assay for assessing DNA damage conducted in primary BALB/c mouse embryonic fibroblasts (FE1 MutaMouse™) treated with 100 µg/mL fullerenes (average particle size in media of 311 nm) for 3 hours were positive for oxidized purines and negative for DNA strand breaks.⁵⁸ Results reported from *in vivo* DNA damage studies with fullerenes are mixed. Totsuka et al.⁵⁷ reported increased levels of DNA damage, measured by the comet assay,

in lung cells of male C57BL/6J mice treated with 0.2 mg fullerenes (0.7 nm diameter; suspended in saline/0.05% Tween 80) by intratracheal instillation and evaluated 3 hours after treatment, although some of the protocol details reported by these authors were inconsistent. Results of a second comet assay in lung cells of male Crl:CD9SD rats, dosed by intratracheal instillation with up to 2.5 mg/kg fullerenes (mean diameter 33 nm; suspended in 0.1% Tween 80 aqueous solution) one time or 0.5 mg/kg once weekly for 5 weeks, and killed 3 or 24 hours after final treatment, were negative.⁵⁹ Consistent with these results, negative results were also reported in a comet assay that assessed DNA damage in bronchoalveolar lavage cells of ApoE^{-/-} mice given a single treatment of fullerenes average diameter of 122 to 164 nm; 54 µg/mouse) by intratracheal instillation and examined 3 hours later.⁶⁰ In F344 rats, high-performance liquid chromatography (HPLC) revealed DNA damage in the form of 8-oxo-7-8-dihydro-2'-deoxyguanosine (8-oxodG) adducts in lung and liver cells of males 24 hours after administration of fullerenes (0.7 nm; 0.064 or 0.64 mg/kg) by single gavage; no increases in DNA adducts were seen in colon cells of these rats.⁶¹ Consistent with the increases in DNA adducts observed in lung tissue in the F344 rats, *gpt* mutant frequencies were reported to be significantly increased in lung tissues of C57BL/6J mice treated with 1 or 4 intratracheal instillations of fullerenes (0.7 nm; 0.2 mg/mouse) and sampled 8 to 12 weeks following treatment.⁵⁷

Modified Fullerenes

One laboratory investigated the genetic toxicity of water soluble polymer-enwrapped fullerenes (PVP/fullerenes), using the bacterial gene mutation and in vitro mammalian cell chromosomal aberrations assays, both with and without exogenous metabolic activation.⁶² No increases in mutations or cytotoxicity were seen in any of several strains of bacteria treated with up to 5,000 µg/plate of PVP/fullerenes. No increases in chromosomal aberrations were observed in Chinese hamster lung cells exposed for 6 or 24 hours to concentrations of PVP/fullerenes ranging from 1,000 to 5,000 µg/mL.

Study Rationale

Nanometer-scale (nanoscale) and micrometer-scale (microscale) fullerene C₆₀ were evaluated as part of an extensive assessment of nanomaterials under the National Toxicology Program's Nanotechnology Safety Initiative. Nanomaterials were initially nominated by the Rice University Center for Biological and Environmental Nanotechnology due to their widespread use in a variety of commercial applications and inadequate information on possible biological interactions and toxicity following exposure. To evaluate the potential for differential effects based on particle size, two C₆₀ fullerene aggregate sizes, 50 nm diameter (nano-C₆₀) and 1 µm diameter (micro-C₆₀), were selected for toxicity and tissue burden studies. Because inhalation is a primary route of exposure and inhalation toxicity data are limited, 3-month inhalation studies were conducted to assess the effects of nano-C₆₀ and micro-C₆₀ on pulmonary toxicity, tissue burden, and immunotoxicity, as well as general toxicity effects, in male and female Wistar Han rats and B6C3F1/N mice.

The work presented here is a complete assessment of the toxicity of micro- (1 µm) and nano- (50 nm) fullerene C₆₀ particles. Some of the tissue burden, respiratory toxicity, and immunotoxicity data from this work been published previously.^{63; 64}

Materials and Methods

Procurement and Characterization of Bulk Fullerene C₆₀

Fullerene C₆₀ was obtained from SES Research (Houston, TX) in one lot (BT-6947). The study laboratory milled the test chemical in a ball mill to reduce particle size. After milling, initial purity and exposure testing revealed an insoluble impurity that was not present in the original unmilled material. The milled fullerene C₆₀ was sent back to the manufacturer for repurification. The reprocessed fullerene C₆₀ with the impurity removed (99.5% pure) was received from SES Research in one lot (BT-6947-Reprocess) that was used during the 3-month studies. Identity, purity, and moisture analyses were performed by the study laboratory at Battelle Toxicology Northwest [Richland, WA; high-performance liquid chromatography (HPLC) and gas chromatography (GC)] and by the analytical chemistry laboratories at Cyanta Analytical Services [Maryland Heights, MO; Fourier transform infrared (FTIR) spectroscopy, elemental analyses, and Karl Fisher titration], H & M Analytical Services, Inc. [Allentown, NJ; X-ray diffraction (XRD)], and Pacific Northwest National Laboratory (Richland, WA; laser Raman analysis) as described in Appendix E. Reports on analyses performed in support of the fullerene C₆₀ studies are on file at the National Institute of Environmental Health Sciences.

The FTIR and laser Raman spectra of the test chemical were consistent with literature spectra (FTIR; Nakamoto and McKinney⁶⁵), and the structure and composition of fullerene C₆₀ XRD with Rietveld analysis showed only the face-centered cubic polymorph of fullerene C₆₀.

The purity of the bulk chemical was determined by elemental analysis, GC, and HPLC. Elemental analyses showed a composition of 99.7% carbon, 0.24% nitrogen, less than 0.1% hydrogen, and less than 300 ppm sulfur. GC with flame ionization detection indicated one residual solvent, 1,2,4-trimethylbenzene (TMB), at approximately 0.8% (predrying) and 0.6% (postdrying). HPLC indicated an area percent purity of 98.5%. The overall purity of lot BT-6947-Reprocess was determined to be 98.5%. Karl Fischer titration indicated a water content of less than 0.09%.

To ensure stability, the bulk chemical was stored at room temperature in amber glass containers. Periodic reanalyses of the bulk chemical were performed during the 3-month studies by the study laboratory using HPLC, and no degradation of the bulk chemical was detected.

Aerosol Generation and Exposure System for the Micro-C₆₀ Studies

The aerosol generation and delivery system used a linear feed powder-metering device, particle attrition chamber, dispersion jet, and cyclone separator all located within a glove box in the exposure room (Figure 2). The air-driven shuttle bar in the powder-metering device dispersed the bulk material at timed intervals into a nitrogen gas stream; nitrogen gas was used to minimize oxidation of the test chemical during vaporization. The material suspended in the gas stream was further reduced in size by passing through the particle attrition chamber, which used a pressurized nitrogen stream to promote particle-to-particle impaction, breaking apart the particles. A high-pressure dispersion jet at the output of the particle attrition chamber added dispersion energy to drive the aerosol into the cyclone separator, which removed unwanted large

particles from the aerosol stream. The aerosol stream from the glove box was directed to a residence chamber to allow for additional separation of larger particles by gravitational settling. The residence chamber was monitored to maintain generator output consistency using a real-time aerosol monitor (RAM), and material in excess of that required to maintain the exposure units at target concentrations was withdrawn through high-efficiency particulate air (HEPA) filters prior to delivery to the residence chamber. Aerosol was delivered from the residence chamber to each exposure carousel through a metering element that fixed the flow to each carousel. Humidified air was added to the aerosol-laden air downstream from the metering element to provide dilution and to humidify the airstream. Concentration was controlled by siphoning excess delivery flow from a point following the metering element but before the introduction of dilution air. Past the dilution air input, aerosol-laden air was directed to a computer-controlled pneumatic slide valve that served as the on-off control valve for the flow through a dedicated distribution system branch line to each exposure carousel.

The rodent exposure carousel was developed by the study laboratory and consisted of stackable tiers with 16 nose-only exposure ports per tier. Each carousel consisted of five tiers, thus providing 80 ports for animal exposure. One end of the tube that served to restrain the individual animal was tapered to approximately fit the shape of the its head, and the diameter of the remaining cylindrical portion of the tube made it difficult for the animal to turn in the tube. The back portion of the tube was covered with a plastic cap, and tubes containing animals were fastened to the inhalation carousel by means of a bracket that ensured the nose portion of the tube protruded through a gasket and into the carousel.

The test aerosol entered the carousel through the top and then flowed radially to each of the 16 evenly spaced exposure ports per tier. Each port received approximately 500 mL/minute of exposure atmosphere, which equated to a total exposure unit inlet flow of 40 L/minute. Ports not used for animal exposure or sampling were closed off. This design provided uniform concentration and fresh test chemical to each animal connected to the exposure system and minimized any effect of the animals on the atmosphere because no exhaled air from one animal was able to reach the breathing zone of another. Each exposure carousel was surrounded by a temperature-controlled ventilated enclosure that minimized the release of aerosol from the carousel to the room and provided a means of cooling the animals confined to the nose tubes.

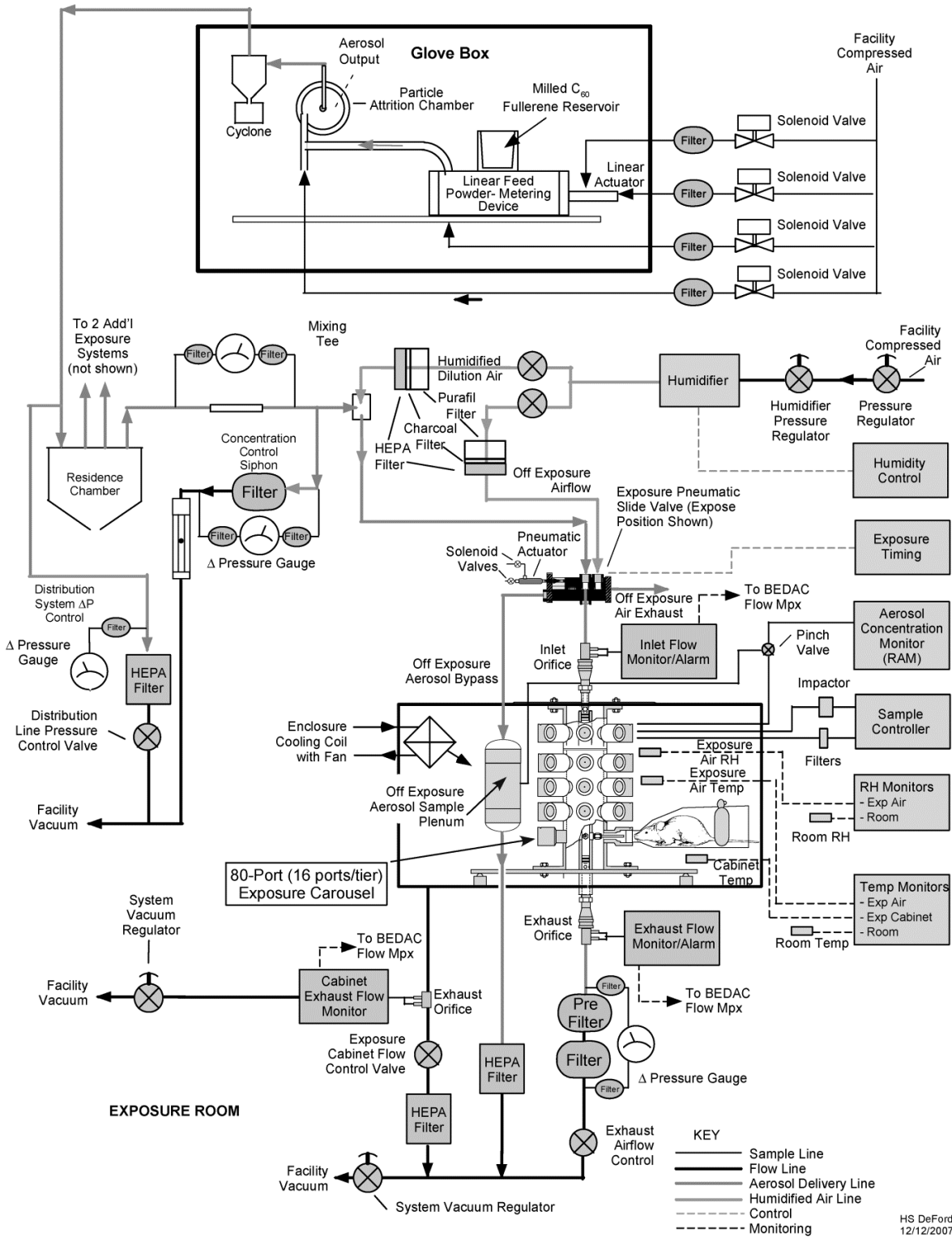


Figure 2. Schematic of the Aerosol Generation and Delivery System in the Three-month Nose-only Inhalation Studies of Fullerene Micro-C₆₀ (1 μm)

Aerosol Generation and Exposure System for the Nano-C₆₀ Studies

The aerosol generation and delivery system used the same glove box and residence chamber components as described for the micro-C₆₀ studies (Figure 2). For the nano-C₆₀ studies, however, the aerosol-laden airstream from the residence chamber was directed into four identically configured delta tubes designed to provide a metered flow in relation to the pressure drop maintained in the residence chamber (Figure 3). Downstream from each delta tube, a flowmeter-controlled siphon allowed for regulation of the flow into quartz tube furnaces present at a target of approximately 520°C for flash vaporization of the test article. Near the exit of each furnace tube, additional nitrogen gas was introduced into the flow to rapidly cool the vaporized test material, condensing it into nanometer-sized particles. The additional nitrogen also increased the velocity of the carrier stream, diluted the concentration of the particles, and reduced the opportunity for particle agglomeration. Humidified air was added to the aerosol-laden nitrogen gas stream that exited each furnace tube to provide additional dilution, cooling, humidification, and oxygenation to the exposure atmosphere.

Subsequent aerosol flow through the computer-controlled pneumatic slide valves and exposure carousels was as described for the 1- μ m studies, except that a second siphon and dilution air assembly was located just prior to the slide valves to reduce aerosol concentrations in the test atmosphere further. Exposure carousels for the nano-C₆₀ studies provided 40 ports for animal exposure via 8 ports on each of the 5 tiers.

Aerosol Concentration Monitoring for the Micro-C₆₀ and Nano-C₆₀ Studies

Summaries of the carousel aerosol concentrations are presented in Table E-1 and Table E-2. For the micro-C₆₀ studies, micrometer-sized fullerene C₆₀ aerosol was monitored for concentration using an online RAM. For the nano-C₆₀ studies, nanometer-sized fullerene C₆₀ was similarly monitored using a RAM-1 instrument. The analog output voltage from each RAM was recorded by the Battelle Exposure Data Acquisition and Control (BEDAC) software system and converted to mg/m³ exposure concentration by the application of a calibration curve. During the studies, if a measured concentration exceeded its allowed limits, the BEDAC program triggered an audible alarm or, in extreme cases, terminated the exposure.

RAM calibrations were performed by constructing response curves using RAM voltage recorded each day at the same time that duplicate atmosphere samples were collected from each exposure carousel on 25 mm Teflon[®]-coated glass-fiber filters; RAM voltages were corrected for zero-offset voltage measured in a HEPA-filtered airstream. Fullerene C₆₀ collected on the filters from each exposure carousel was dissolved in a 50:50 mixture of TMB:toluene containing a known amount of internal standard and quantified using HPLC on an off-line chromatograph.

The off-line chromatograph was calibrated using gravimetrically prepared standard solutions of the test article and the internal standard in 50:50 TMB:toluene. These methods were demonstrated by the study laboratory to have adequate precision, accuracy, linear working range, day-to-day repeatability, and detection limits for measuring 1 μ m and 50 nm fullerene C₆₀ concentrations in the exposure carousels.

Fullerene C₆₀, TOX 87

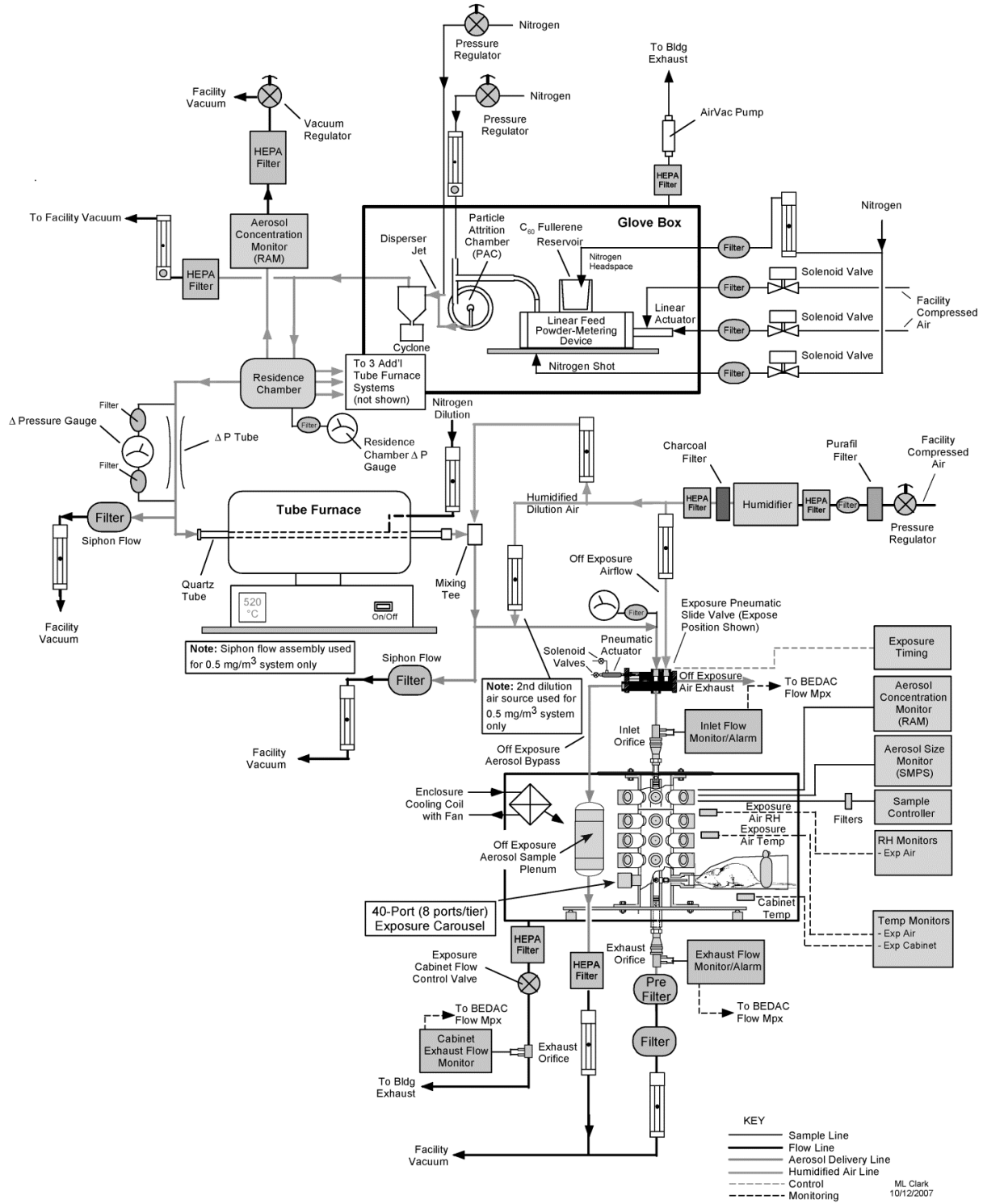


Figure 3. Schematic of the Aerosol Generation and Delivery System in the Three-month Nose-only Inhalation Studies of Fullerene Nano-C₆₀ (50 nm)

Carousel Atmosphere Characterization for the Micro-C₆₀ and Nano-C₆₀ Studies

More comprehensive details and results of carousel atmosphere characterizations for both nano and micro-C₆₀ are found in Appendix E.

Aerosol particle size distribution was determined once prior to, and approximately monthly during, the micro-C₆₀ studies by collecting aerosol samples from each exposure carousel (except the 0 mg/m³ carousels) using a Mercer style cascade impactor. Fullerene C₆₀ was collected on stages one through seven within the impactor on 22 mm diameter stainless steel slides coated with silicone spray. The final, stage-eight sample was collected on a 25 mm diameter Pallflex[®] Emfab[™] glass-fiber filter. Collected aerosol was dissolved in a 50:50 mixture of TMB:toluene and assayed for mass of test material using HPLC. The relative mass collected on each stage was analyzed by the probit-based CASPACT impactor analysis program developed at the study laboratory⁶⁶ to yield estimates of the mass median aerodynamic diameter (MMAD) of the particles.

The surface-area-to-mass ratio of micrometer-sized particles was estimated using data derived from the Mercer cascade impactor data and carousel mass concentrations. Mass median diameter (MMD) was calculated from MMAD using the Hatch-Choate relationships for log-normal distributions. Count median diameter (CMD) was calculated from MMD. The average surface area particle diameter (d_s) and the average mass particle diameter (d_m) were calculated from CMD, assuming a spherical particle shape. The surface area per particle was calculated from d_s . The total number of particles per volume of air was calculated from d_m and the aerosol concentration determined from the RAM data. Once the total number of particles per volume of air was determined, the surface area per particle was multiplied by this value to obtain total surface area per volume of air. Total surface area per volume of air was divided by total mass per volume of air to obtain the ratio of total surface area to total mass. Estimates of particle sizes and surface-area-to-mass ratios during the micro-C₆₀ studies are presented in Table E-3; MMAD values fell well below the 3.0 μm upper limit criterion required by the design of the studies.

For the nano-C₆₀ studies, aerosol particle size distribution was initially measured without animals in the exposure carousels during prestart studies using a Model 125B NanoMOUDI[™] Low Pressure Cascade Impactor. The NanoMOUDI[™] classified particles according to aerodynamic size by inertial impaction in several multinozzle stages stacked in series. The chemically analyzed relative mass collected on each impactor stage was analyzed from a validated spreadsheet using the manufacturer's values for impactor stage effective cutoff diameter. Data from this impactor resulted in a true measurement of MMAD for the aerosolized test article in each exposure carousel, but the device could not be used with animals in the exposure carousels because diversion of approximately half the aerosol flow to each carousel was required for proper functioning of the impactor. Accordingly, size distribution of the 50 nm particles was also measured using a Scanning Mobility Particle Sizer (SMPS[™]) that combined particle sizing by electrical mobility with condensation particle counting. The primary measurement output of the SMPS[™] was particle CMD. MMD was calculated from measured CMD, and the associated geometric standard deviation (GSD) using Hatch-Choate relationships assuming log-normal aerosol size distribution, and then converted to MMAD assuming a particle density of 1.72 g/mL. By these means, a correlation was established between the results of NanoMOUDI[™]

impactor and SMPSTM analyses enabling the use of the SMPSTM during the animal exposures to provide estimates of particle size distribution.

Measurements of particle size during animal exposures were conducted daily during the nano-C₆₀ studies using the SMPSTM. Monthly averaged results for these measurements in each exposure carousel during the 3-month nano-C₆₀ studies are presented in Table E-4 and demonstrate the particles delivered to each exposure unit were nanometer sized.

The surface-area-to-mass ratios of nanometer-sized particles in the nano-C₆₀ studies were estimated using data derived from the SMPSTM CMD and carousel exposure concentration using the same calculations as described for the micrometer-sized particles; the results are presented in Table E-5.

Buildup and decay rates for carousel aerosol concentrations were not determined. For nose-only carousels, the time for the concentration to reach 90% of its stable final concentration after start of exposure is less than the resolving ability of the measurement instrumentation and is calculated to be less than 2 seconds.

Uniformity of the aerosol concentration in the inhalation exposure carousels without animals present was evaluated before the 3-month micro- and nano-C₆₀ studies began. The aerosol concentration was measured using the online monitor with continuous monitoring from the input line. Measurements were taken from carousel exposure ports located on the top, middle, and bottom tiers of the carousel. For the micro-C₆₀ studies, total port variability (TPV) for the three carousels ranged from 4.0% to 4.7% relative standard deviation (RSD), and for the nano-C₆₀ studies, TPV for the four carousels ranged from 4.3% to 4.8% RSD.

Fullerene C₆₀ was determined to be stable under the generation and exposure conditions used during the 3-month studies by analyses conducted before and during the 3-month studies by the study laboratory and the analytical chemistry laboratories. Samples were collected and analyzed from all exposure carousels and from the generator reservoir. During the 3-month studies, bulk fullerene C₆₀ in the generator reservoir was refilled as needed, and the analysis sample was collected from the reservoir at the end of the day after it was placed in service. Analyses included HPLC for area percent purity, GC with mass spectrometry (MS) detection for determination of residual TMB (not performed on reservoir samples before the 3-month studies), inductively coupled plasma/atomic emission spectroscopy (ICP/AES) for elemental analysis, and XRD and laser Raman spectroscopy for characterization of the form of the test material.

Exposure atmosphere samples were collected from all rat and mouse carousels on 25 mm glass-fiber Teflon[®]-coated filters for HPLC and ICP/AES analyses, and on A/E glass-fiber filters for XRD and laser Raman analyses. Atmosphere samples for GC/MS analyses were collected on activated coconut charcoal sorbent tubes.

For area percent purity assessments, filters and generator reservoir samples were extracted with TMB:toluene (50:50). For determination of TMB as a residue of repurification of the bulk test material, the sorbent tubes and generator reservoir samples were extracted with carbon disulfide. For elemental analyses, samples were microwave-digested in concentrated HCl:HNO₃ (2:1) containing indium as an internal standard, filtered through Teflon[®]-coated syringe filters, and analyzed for the concentration of 15 elements.

XRD with Rietveld analysis indicated that the principal crystalline phase in samples from the generator reservoir and exposure atmosphere samples from all carousels both before and during the 3-month micro- and nano-C₆₀ studies in rats and mice was the disordered face-centered cubic form of fullerene C₆₀. The XRD-determined purity of all generator reservoir and atmosphere samples exceeded 99.7% and 98%, respectively. Laser Raman assays concluded that all the elemental carbon in the samples was in the form of C₆₀ fullerene. Using HPLC, average area percent purity for the generator reservoir samples exceeded 98% prior to and during all studies. Area percent purity for the atmosphere samples collected from all carousels prior to and during the micro-C₆₀ studies exceeded 98%; similar measurements prior to and during the nano-C₆₀ studies indicated an exposure atmosphere purity of 99% or greater. GC/MS detected 0.6% TMB in all reservoir samples collected during the 3-month studies. TMB concentrations in atmosphere samples ranged from 0.4% to 0.6% prior to and during the micro-C₆₀ studies and from 0.6% to 2.5% prior to and during the nano-C₆₀ studies. ICP/AES analyses showed no elemental contamination in either the generator reservoir or exposure atmosphere samples collected before or during each study.

Animal Source

Male and female Wistar Han [CrI:WI(Han)] rats were obtained from Charles River Laboratory (Raleigh, NC), and male and female B6C3F1/N mice were obtained from the National Toxicology Program (NTP) colonies maintained at Taconic Biosciences (formerly Taconic Farms, Inc.) Germantown, NY.

Animal Welfare

All NTP animal toxicity studies are conducted in accordance with Public Health Service Policy on Humane Care and Use of Animals. All animal studies were conducted in an animal facility accredited by AAALAC International. Studies were approved by the Battelle Toxicology Northwest Animal Care and Use Committee and conducted in accordance with all relevant NIH and NTP animal care and use policies and applicable federal, state, and local regulations and guidelines.

Three-month Studies

On receipt, rats were 4 weeks old and mice were 4 to 5 weeks old. Animals were quarantined for 13 (rats) or 12 (mice) days and were 6 (rats) or 6 to 7 (mice) weeks old on the first day of the studies. Before the studies began, five male and five female rats and mice were randomly selected for parasite evaluation and gross observation for evidence of disease. The health of the animals was monitored during the studies according to the protocols of the NTP Sentinel Animal Program (Appendix G). All test results were negative.

Groups of 10 male and 10 female core study rats and mice were exposed to fullerene C₆₀ via nose-only inhalation at concentrations of 0, 2, 15, or 30 mg/m³ (micro-C₆₀ studies) or 0, 0.5, or 2 mg/m³ (nano-C₆₀ studies), 3 hours per day, 5 days per week, for 13 weeks. Additional groups of 24 male rats and mice and 8 female rats and mice designated for tissue burden studies and groups of 16 female rats and mice designated for immunotoxicity studies were exposed to the same concentrations for 12 to 13 weeks. Prior to the initiation of the study, animals were placed

in the nose-only restraint tubes for up to 2 hours per day for at least 3 days to acclimate to handling and the exposure system.

NTP historically has used only female rodents for immunotoxicology studies, as they tend to be more immunologically responsive than their male counterparts, which allows for the detection of subtle immunological effects. In addition, resource and operational constraints limited the number of animals that could be studied in the nose-only system, so pragmatic decisions were made to study both male and female mice for the core toxicity study but use only female mice for the immunotoxicity study arm and use male mice for the post-exposure clearance studies.

NTP-2000 feed and water were available ad libitum except during exposure periods. Rats and mice were housed individually. Core study animals were weighed initially, and body weights and clinical findings were recorded on day 3 (micro-C₆₀ rats and mice) or 4 (nano-C₆₀ rats and mice), weekly thereafter, and at the end of the studies. Details of the study design and animal maintenance are summarized in Table 1. Information on feed composition and contaminants is provided in Appendix F.

The 3-month rat and mouse inhalation studies were designed on the basis of published data from preliminary 10-day nose-only inhalation studies,¹¹ which were the first reported inhalation studies of fullerene C₆₀. A high exposure concentration of 2 mg/m³ was selected for the nano-C₆₀ studies because minimal toxicity was observed at that concentration in the Baker et al.¹¹ studies and because generation of higher concentrations was not technically feasible. The subsequent exposure concentrations for the nano- and micro-C₆₀ studies were selected to adequately compare across equivalent mass and equivalent surface area. The surface area (m²/g) of the 15 to 30 mg/m³ micro-C₆₀ particles was approximately equivalent to the surface area of the 2 mg/m³ nano-C₆₀ particles, allowing for comparison of equivalent surface area with different size particles. The lowest exposure concentration for the micro-C₆₀ particles was 2 mg/m³ to allow comparison of equivalent masses of different size particles.

Clinical Pathology

Animals were anesthetized with carbon dioxide, and blood was collected from the retroorbital plexus (rats) or supraorbital sinus (mice) of core study animals at the end of the studies for hematology and clinical chemistry (rats only) analyses. Blood samples for hematological analyses were placed in tubes containing potassium EDTA. Packed cell volume; hemoglobin concentration; erythrocyte, platelet, and leukocyte counts; mean cell volume; mean cell hemoglobin; and mean cell hemoglobin concentration were determined using an Abbott Cell-Dyn 3700 Analyzer (Abbott Diagnostics Systems, Abbott Park, IL). Manual hematocrit values were determined using a microcentrifuge (Heraeus haemofuge; Heraeus Holding, GmbH, Hanau, Germany) and a Damon/IEC capillary reader (International Equipment Co., Needham Heights, MA) for comparison to Cell-Dyn values for packed cell volume. Blood smears were stained with Romanowsky-type aqueous stain in a Wescor 1720 aerospray slide stainer (Wescor, Inc., Logan, UT). Reticulocytes were stained with New Methylene Blue and enumerated as a reticulocyte:erythrocyte ratio using the Miller disc method.⁶⁷ Blood samples for clinical chemistry analyses were placed in tubes containing a separator gel, allowed to clot, and centrifuged. Parameters were determined using a Roche Hitachi 912 System (Roche Diagnostic Corporation, Indianapolis, IN). Table 1 lists the parameters measured.

Reproductive Evaluations

At the end of the 3-month studies, samples were collected for sperm motility and vaginal cytology evaluations on core study rats and mice according to NTP specifications.⁶⁸ The parameters evaluated are listed in Table 1. For 16 consecutive days prior to scheduled terminal sacrifice, the vaginal vaults of the female mice were moistened with saline, if necessary, and samples of vaginal fluid and cells were stained. Relative numbers of leukocytes, nucleated epithelial cells, and large squamous epithelial cells were determined and used to ascertain estrous cycle stage (i.e., diestrus, proestrus, estrus, and metestrus). Male animals were evaluated for sperm count and motility. The left testis and left epididymis were isolated and weighed. The tail of the epididymis (cauda epididymis) was then removed from the epididymal body (corpus epididymis) and weighed. Test Yolk buffer (rats) or modified Tyrode's buffer (mice) was applied to slides and a small incision was made at the distal border of the cauda epididymis.⁶⁸ The sperm effluxing from the incision were dispersed in the buffer on the slides, and the numbers of motile and nonmotile spermatozoa were counted for five fields per slide by two observers. Following completion of sperm motility estimates, each left cauda epididymis was placed in buffered saline solution. Caudae were finely minced, and the tissue was incubated in the saline solution and then heat fixed at 65°C. Sperm density was then determined microscopically with the aid of a hemacytometer. To quantify spermatogenesis, the testicular spermatid head count was determined by removing the tunica albuginea and homogenizing the left testis in phosphate-buffered saline containing 10% dimethyl sulfoxide. Homogenization-resistant spermatid nuclei were counted using a hemacytometer.

Tissue Burden

The liver, lungs, bronchial lymph nodes, and spleen were collected from six male and eight female tissue burden animals per exposure group immediately postexposure on the last exposure day, and lungs were collected from six male tissue burden animals per exposure group at 14, 28, and 56 days postexposure. Tissues were weighed and stored at -70°C until analysis. Tissues were placed in centrifuge tubes, magnesium perchlorate (0.1 M) was added, an internal standard (C₇₀) was added, and the contents were mixed. The solution was centrifuged to separate the aqueous and organic layers, and an aliquot of the organic layer was removed, filtered, and analyzed for fullerene C₆₀ concentration using HPLC with ultraviolet-visible detection.

Immunotoxicity

Immunotoxicity study animals were divided into two cohorts of eight female rats and mice per exposure group. On day 74 (mice) or 81 (rats), cohort 1 animals were immunized by tail-vein injection with a T-dependent antigen [sheep erythrocytes (sRBC)]. On day 78 (mice) or 85 (rats), blood and spleens were collected from cohort 1 animals for evaluation of antigen specific antibody responses to sRBC by evaluating the antibody-forming cell (AFC) response (rats and mice) and serum anti-sRBC IgM antibody levels (mice). Cohort 2 animals were not immunized and were used in evaluating responses to the following immunotoxicological assays: splenocyte phenotyping, anti-CD3 mediated proliferation, natural killer (NK) cell activity, bronchoalveolar lavage fluid (BALF) cell differentials (rats), and BALF cytokine levels; mice were also assayed for mixed leukocyte response. On day 79 (mice) or 86 (rats), cohort 2 animals were euthanized and the lungs were lavaged twice with 1 (mice), 5 (50 nm rats), or 10 (micro-C₆₀ rats) mL aliquots of Hank's Balanced Salt Solution (HBSS) with 50 µg/mL gentamicin, a bacteriostatic

antibiotic. The lavage fluid was centrifuged, and the cell pellet was separated from the fluid. The cell pellet was washed with 10 mL HBSS and centrifuged, the supernatant was discarded, and the cell pellet was resuspended in 1 mL HBSS. The spleen of each cohort 2 animal was removed and placed in individual collecting tubes containing Earl's Balanced Salt Solution (EBSS) with 15 mM 4-(2-hydroxyethyl)-1-piperazineethanesulfonic acid (HEPES), supplemented with gentamicin. A wet weight was obtained for each individual spleen. The spleens and BALF cells were shipped in tubes on crushed ice to Virginia Commonwealth University (VCU) (Richmond, VA) for immunoassay evaluations on the following day. The collected serum and BALF samples were frozen and shipped separately on dry ice to VCU where they were maintained at -70°C until evaluated. Upon arrival at the VCU testing facility, single-cell spleen suspensions were prepared. Spleen cell suspensions for cohort 1 were centrifuged and resuspended in 6 mL (rats) or 3 mL (mice) of EBSS with 15 mM HEPES. Cell suspensions for cohort 2 were centrifuged and resuspended in Roswell Park Memorial Institute (RPMI) 1640 media supplemented with 10% fetal bovine serum. For cohort 2, spleen cells were resuspended in 6 mL (rats) or 3 mL (mice) of RPMI, and BALF cells were resuspended in 1 mL of RPMI. The parameters evaluated are listed in Table 1.

Necropsy

Necropsies were performed on all core study animals. The heart, right kidney, liver, lung, right testis, and thymus were weighed. Tissues for microscopic examination were fixed and preserved in 10% neutral buffered formalin (except eyes were first fixed in Davidson's solution, and testes, epididymides, and vaginal tunics were first fixed in modified Davidson's solution), processed and trimmed, embedded in paraffin, sectioned to a thickness of 4 to 6 μm , and stained with hematoxylin and eosin. The lungs and trachea were infused with 10% neutral buffered formalin up to a normal inspiratory volume prior to fixation and processing. Complete histopathological examinations were performed by the study laboratory pathologist on all control, 30 mg/m^3 (micro-C₆₀ study) and 2 mg/m^3 (nano-C₆₀ study) animals. Histopathological evaluation of the lung and mainstem bronchi, bronchial and mediastinal lymph nodes, and testis with epididymis was performed in all exposure groups. Table 1 lists the tissues and organs routinely examined.

After a review of the laboratory reports and selected histopathological slides by a quality assessment (QA) pathologist, the findings and reviewed slides were submitted to an NTP Pathology Peer Review (PPR) coordinator for a second independent review. Any inconsistencies in the diagnoses made by the study laboratory and QA pathologists were resolved by the NTP PPR process. Final diagnoses for reviewed lesions represent a consensus of the PPR or a consensus among the study laboratory pathologist, NTP pathologist, QA pathologist(s), and the PPR coordinator. Details of these review procedures have been described, in part, by Maronpot and Boorman⁶⁹ and Boorman et al.⁷⁰

Table 1. Experimental Design and Materials and Methods in the Three-month Nose-only Inhalation Studies of Fullerene Micro-C₆₀ (1 µm) and Nano-C₆₀ (50 nm)

Study Design
Study Laboratory
Battelle Toxicology Northwest (Richland, WA)
Strain and Species
Wistar Han [CrI:WI(Han)] rats
B6C3F1/N mice
Animal Source
Rats: Charles River Laboratory (Raleigh, NC)
Mice: Taconic Farms, Inc. (Germantown, NY)
Time Held Before Studies
Rats: 13 days
Mice: 12 days
Average Age When Studies Began
Rats: 6 weeks
Mice: 6 to 7 weeks
Date of First Exposure
November 5, 2007
Duration of Exposure
3 hours per day, 5 days per week, for 13 weeks
Date of Last Exposure
1 µm rats and mice: January 31, 2008
50 nm rats and mice: February 1, 2008
Necropsy Dates
1 µm rats and mice: February 1, 2008
50 nm rats and mice: February 2, 2008
Average Age at Necropsy
Rats: 18 weeks
Mice: 19–20 weeks
Size of Study Groups
10 males and 10 females (core studies), 24 males and 8 females (tissue burden studies), or 16 females (immunotoxicity studies)
Method of Distribution
Animals were distributed randomly into groups of approximately equal initial mean body weights.
Animals per Cage
1

Study Design

Method of Animal Identification

Tail tattoo

Diet

NTP-2000 irradiated wafers (Zeigler Brothers, Inc., Gardners, PA), available ad libitum (except during exposure periods); changed weekly

Water

Tap water (Richland, WA, municipal supply) via automatic watering system (Edstrom Industries, Waterford, WI); available ad libitum except during exposure periods

Cages

Polycarbonate solid bottom (Lab Products, Inc., Seaford, DE); changed and rotated weekly

Bedding

Heat-treated, irradiated, hardwood bedding (Sani-Chip[®], PJ Murphy Forest Products, Montville, NJ); changed weekly

Room Air Supply Filters

Single HEPA; changed as needed (indicator light), new at study start

Racks

Stainless steel housing racks holding hanging cages (Lab Products, Inc., Seaford, DE); changed weekly

Room Environment

Temperature: 72° ± 3°F

Relative humidity: 50% ± 15%

Room fluorescent light: 12 hours/day

Chamber air changes: 10/hour

Exposure Tube Environment

Temperature: 75° ± 3°F

Relative humidity: 55% ± 15%

Inlet air flow: 18–22 liters/minute

Exposure Concentrations

0, 2, 15, and 30 mg/m³ (1 μm studies)

0, 0.5, and 2 mg/m³ (50 nm studies)

Type and Frequency of Observation

Observed twice daily. Animals were weighed initially, on day 3 (1 μm studies) or 4 (50 nm studies), weekly thereafter, and at the end of the studies; clinical findings were recorded on day 3 (1 μm studies) or 4 (50 nm studies), weekly thereafter, and at the end of the studies.

Method of Euthanasia

100% carbon dioxide

Necropsy

Necropsies were performed on all core study animals. Organs weighed were heart, right kidney, liver, lung, right testis, and thymus.

Study Design

Clinical Pathology

Blood was collected from the retroorbital sinus (rats) or supraorbital sinus (mice) from core study animals at the end of the studies for hematology and clinical chemistry (rats).

Hematology: hematocrit; packed cell volume; hemoglobin; hemolysis; erythrocyte, nucleated erythrocyte, reticulocyte, and platelet counts; Howell-Jolly bodies (mice); mean cell volume; mean cell hemoglobin; mean cell hemoglobin concentration; and leukocyte count and differentials

Clinical chemistry: urea nitrogen, creatinine, glucose, total protein, albumin, globulin, cholesterol, triglyceride, alanine aminotransferase, alkaline phosphatase, creatine kinase, sorbitol dehydrogenase, and bile salts

Histopathology

Complete histopathology was performed on 0, 30 (micro-C₆₀ studies), and 2 (nano-C₆₀ studies) mg/m³ core study rats and mice and on those that died early. In addition to gross lesions and tissue masses, the following tissues were examined: adrenal gland, bone with marrow, brain, clitoral gland, esophagus, eyes, gallbladder (mice), Harderian gland, heart and aorta, large intestine (cecum, colon, rectum), small intestine (duodenum, jejunum, ileum), kidney, larynx, liver, lung and mainstem bronchi, lymph nodes (mandibular, mesenteric, bronchial, mediastinal), mammary gland, ovary, pancreas, parathyroid gland, pituitary gland, preputial gland, prostate gland, salivary gland, seminal vesicle, skin, spleen, stomach (forestomach and glandular), testis with epididymis, thymus, thyroid gland, trachea, urinary bladder, and uterus. In addition, the lung, bronchial and mediastinal lymph nodes, and testis with epididymis in the remaining exposure groups, the kidney and larynx in the micro-C₆₀ study mice, and the kidney in the nano-C₆₀ study rats were examined.

Sperm Motility and Vaginal Cytology

At the end of the studies, sperm samples were collected from male core study rats and mice for sperm motility evaluations. The following parameters were evaluated: spermatid heads per testis and per gram testis, motility, and sperm per cauda epididymis and per gram epididymis. The left cauda, left epididymis, and left testis were weighed. Vaginal samples were collected for up to 16 consecutive days prior to the end of the studies from core study female mice for vaginal cytology evaluations.

Tissue Burden

Liver, lungs, bronchial lymph nodes, and spleen were collected and analyzed for fullerene C₆₀ concentrations from six male and eight female tissue burden animals per exposure group on the last exposure day, immediately postexposure. Lungs were collected from six male tissue burden animals per exposure group per time point and analyzed for fullerene C₆₀ concentrations at 14, 28, and 56 days postexposure.

Immunotoxicity

At study termination, blood and spleens of cohort 1 animals (8 females per exposure concentration) and bronchoalveolar lavage fluid (BALF) and spleens of cohort 2 animals (8 females per exposure concentration) were collected for immunotoxicity evaluation. Cohort 1 animals were evaluated for antigen-specific antibody responses. Cohort 2 animals were assayed for splenocyte phenotyping, anti-CD3 mediated proliferation, natural killer cell activity, BALF cell differentials (rats), BALF cytokine levels, and mixed leukocyte response (mice).

Statistical Methods

Calculation and Analysis of Lesion Incidences

The incidences of lesions are presented as the numbers of animals bearing such lesions at a specific anatomic site and the numbers of animals with that site examined microscopically. The Fisher exact test,⁷¹ a procedure based on the overall proportion of affected animals, was used to determine significance.

Analysis of Continuous Variables

Two approaches were employed to assess the significance of pairwise comparisons between exposed and control groups in the analysis of continuous variables. Organ and body weight data, which historically have approximately normal distributions, were analyzed with the parametric multiple comparison procedures of Dunnett⁷² and Williams.^{73; 74} Hematology, clinical chemistry, spermatid concentrations, epididymal spermatozoal measures, tissue burden, and immunotoxicity data, which have typically skewed distributions, were analyzed using the nonparametric multiple comparison methods of Shirley⁷⁵ (as modified by Williams⁷⁶) and Dunn.⁷⁷ Jonckheere's test⁷⁸ was used to assess the significance of the dose-related trends and to determine whether a trend-sensitive test (Williams' or Shirley's test) was more appropriate for pairwise comparisons than a test that does not assume a monotonic dose-related trend (Dunnett's or Dunn's test). Prior to statistical analysis, extreme values identified by the outlier test of Dixon and Massey⁷⁹ were examined by NTP personnel, and implausible values were eliminated from the analysis. Tests for extended periods of estrus, diestrus, metestrus, and proestrus, and skipped estrus and skipped diestrus, were constructed based on a Markov chain model proposed by Girard and Sager.⁸⁰ For each exposure group, a transition probability matrix was estimated for transitions among the proestrus, estrus, metestrus, and diestrus stages, with provision for extended stays within each stage and for skipping estrus or diestrus within a cycle. Equality of transition matrices among exposure groups and between the control group and each exposed group was tested using chi-square statistics.

Quality Assurance Methods

The 3-month studies were conducted in compliance with Food and Drug Administration Good Laboratory Practice Regulations.⁸¹ In addition, the 3-month study reports were audited retrospectively by an independent QA contractor against study records submitted to the NTP Archives. Separate audits covered completeness and accuracy of the pathology data, pathology specimens, final pathology tables, and a draft of this NTP Toxicity Study Report. Audit procedures and findings are presented in the audit reports and are on file at NIEHS. The audit findings were reviewed and assessed by NTP staff, and all comments were resolved or otherwise addressed during the preparation of this Toxicity Study Report.

Genetic Toxicology – Peripheral Blood Micronucleus Test

Peripheral blood samples from male and female rats and mice were collected in tubes containing EDTA at the end of the 3-month studies and processed for flow cytometric evaluation of micronucleated reticulocytes (polychromatic erythrocytes; PCEs) and erythrocytes (normochromic erythrocytes; NCEs) as described by Witt et al.⁸² Briefly, cells were fixed and labeled using a MicroFlow^{PLUS} Kit (Litron Laboratories, Rochester, NY) according to the manufacturer's instructions. For each blood sample, 20,000 immature CD71⁺ reticulocytes and approximately 1 million mature erythrocytes were analyzed using a flow cytometer to determine the frequency of micronucleated cells of each type; in addition, the percentage of reticulocytes among the total erythrocytes was calculated as a measure of bone marrow toxicity.

Prior experience with the large number of cells scored using flow cytometric scoring techniques⁸³ suggests assuming the proportion of micronucleated reticulocytes is approximately normally distributed is reasonable. The statistical tests selected for trend and for pairwise

comparisons with the control group depend on whether the variances among the groups are equal. Levene's test at $\alpha = 0.05$ is used to test for equal variances. In the case of equal variances, linear regression is used to test for a linear trend with dose, and Williams' test^{73:74} is used to test for pairwise differences between each treated group and the control group. In the case of unequal variances, Jonckheere's test⁷⁸ is used to test for linear trend, and Dunn's test⁷⁷ is used for pairwise comparisons of each treated group with the control group. Trend tests and pairwise comparisons with the controls are considered statistically significant if $p \leq 0.025$. Ultimately, the scientific staff determined the final call after considering the results of statistical analyses, reproducibility of any effects observed, and the magnitude of effects.

Results

Data Availability

The National Toxicology Program (NTP) evaluated all study data. Data relevant for evaluating toxicological findings are presented here. All study data are available in the NTP Chemical Effects in Biological Systems (CEBS) database: <https://doi.org/10.22427/NTP-DATA-TOX-87>.⁸⁴

Three-month Studies in Rats

Lung Burden

Tissue burden data for rats are presented in Appendix B. In the current studies, lung weights (g) and lung C₆₀ concentrations (µg C₆₀/g lung) were determined in male and female rats following the last exposure. In addition, lung burdens were assessed in male rats only 14, 28, and 56 days after exposure to assess lung clearance rates. Total C₆₀ lung burden (µg C₆₀/lung) and exposure-concentration-normalized lung burden (µg C₆₀/lung per mg C₆₀/m³) were calculated. Due to the increased lung weights in exposed rats, lung burdens, instead of lung tissue concentrations, were used to calculate lung clearance rates.

In the micro-C₆₀ study, lung weights were significantly increased 14 and 56 days postexposure in males exposed to 30 mg/m³ relative to control animals (Table B-1). Lung weights were significantly increased in males 56 days postexposure to 15 mg/m³, relative to control animals. There were no significant differences in lung weights of females. In the nano-C₆₀ study, males exposed to 0.5 mg/m³ had significantly increased lung weights 28 days postexposure (Table B-3). There were no significant differences in lung weights of females.

Lung burden rapidly decreased 14 days postexposure in male rats exposed to all concentrations of micro-C₆₀, with the exception of the groups exposed to 30 mg/m³ (Table B-1). Clearance decreased between postexposure days 14 and 28 in males exposed to all concentrations, with the exception of the group exposed to 30 mg/m³. Lung burden rapidly decreased between postexposure days 14 and 28 in males exposed to 30 mg/m³. Clearance decreased rapidly between postexposure days 28 and 56 in males in all exposure concentration groups. In the nano-C₆₀ study, lung burden rapidly decreased 14 days postexposure in males exposed to all concentrations (Table B-3). Clearance decreased between postexposure days 14 and 28 in males exposed to all concentrations. Clearance decreased rapidly between postexposure days 28 and 56 in males at all concentrations.

In the micro-C₆₀ study, normalized retained lung burdens were higher with increasing exposure concentration at postexposure days 28 and 56 in males (Table B-1). There were no exposure concentration-related effects on normalized lung burden in females.

In the nano-C₆₀ study, normalized lung burdens (µg C₆₀/lung per mg C₆₀/m³) at postexposure day 0 were higher in both males and females exposed to 0.5 mg/m³ relative to groups exposed to 2 mg/m³. In the clearance study (males only), burdens were marginally higher at postexposure days 14 and 28 (Table B-3).

Lung deposition and clearance parameters for male rats were calculated from C₆₀ burden data (Table 2). In the micro-C₆₀ study, the clearance rate constant (k) was determined to be approximately twofold greater in male rats exposed to 2 mg/m³ than in rats exposed to 15 and 30 mg/m³, which had comparable k values. In the nano-C₆₀ study, the clearance rate constant was determined to be greater in male rats exposed to 0.5 mg/m³ than in those exposed to 2 mg/m³, and the clearance rate constant of the 2 mg/m³ exposure group was comparable to those of the 15 and 30 mg/m³ groups in the micro-C₆₀ study. At the same mass-based exposure concentration, 2 mg/m³, clearance rate constant of the 1 µm particles was more than twofold greater than the clearance rate constant of the 50 nm particles.

In male rats exposed to micro-C₆₀, clearance half-life (t_{1/2}) increased between exposure concentrations of 2 and 15 mg/m³ (27 and 69 days, respectively), and then decreased to 55 days in rats exposed to 30 mg/m³ (Table 2). In male rats exposed to nano-C₆₀, the calculated clearance half-life increased between exposure concentrations of 0.5 mg/m³ and 2 mg/m³ (38 and 61 days, respectively). In the nano-C₆₀ study, the t_{1/2} of 2 mg/m³ was longer than that in animals exposed to the same concentration in the micro-C₆₀ study (61 versus 27 days, respectively).

Assuming clearance is a first-order process over time, steady-state lung burdens would be reached in approximately five half-lives. In the micro-C₆₀ study, immediately following exposure to 2 mg/m³, lung burden in males was measured at 439 µg C₆₀/total lung (Table B-1) and represented 94% of the calculated steady-state lung burden (465 µg C₆₀/lung) (Table 2). Steady-state lung burdens were likely not reached in males exposed to 15 or 30 mg/m³ micro-C₆₀. In the nano-C₆₀ study, immediately following exposure to 2 mg/m³, lung burden in males was 581 µg C₆₀/total lung (Table B-3) and represented 61% of the calculated steady-state lung burden (946 µg C₆₀/lung) (Table 2). Steady-state lung burdens were likely not reached in males exposed to 2 mg/m³ nano-C₆₀.

Table 2. Lung Deposition and Clearance Parameter Estimates for Male Rats Exposed to Fullerene C₆₀^a

Parameter	0.5 mg/m ³	2 mg/m ³	15 mg/m ³	30 mg/m ³
Micro-C ₆₀ (1 µm)				
A ₀ (µg fullerene C ₆₀ /total lung)		416	2,037	6,032
k (days ⁻¹)		0.026	0.010	0.013
t _{1/2} (days)		27	69	55
α (µg fullerene C ₆₀ /total lung per day)		12	35	113
A _e (µg fullerene C ₆₀ /total lung)		465	3,472	9,010
Nano-C ₆₀ (50 nm)				
A ₀ (µg fullerene C ₆₀ /total lung)	185	604		
k (days ⁻¹)	0.018	0.011		
t _{1/2} (days)	38	61		
α (µg fullerene C ₆₀ /total lung per day)	4.2	10.8		
A _e (µg fullerene C ₆₀ /total lung)	229	946		

A₀ = lung burden at t = 0 days postexposure; k = first-order lung clearance rate constant; t_{1/2} = lung clearance half-life; α = lung deposition rate; A_e = steady-state lung burden.

^aData presented as mean values.

General Toxicity

In the micro-C₆₀ study, all males survived to the end of the study (Table 3). One 2 mg/m³ female was euthanized moribund on day 88 of the study, which was not considered related to exposure. Final mean body weights and mean body-weight gains of exposed groups of males and females were similar to those of the control groups (Table 3 and Figure 4). There were no clinical findings in males or females considered to be exposure related. In the nano-C₆₀ study, all males and females survived to the end of the study (Table 4 and Figure 5). Final mean body weights and mean body weight gains of exposed groups of males and females were similar to those of the control groups (Table 4 and Figure 4). No clinical findings in males or females were deemed related to exposure.

Following exposure to micro-C₆₀, absolute and relative liver weights of 30 mg/m³ males were significantly greater than those of the control animals (Appendix H). There were no exposure-related changes in organ weights in females. There were no exposure-related changes in organ weights in males or females exposed to nano-C₆₀ (Appendix H).

Table 3. Survival and Body Weights of Rats in the Three-month Nose-only Inhalation Study of Fullerene Micro-C₆₀ (1 μm)^a

Concentration (mg/m ³)	Survival ^b	Initial Body Weight (g)	Final Body Weight (g)	Change in Body Weight (g)	Final Weight Relative to Controls (%)
Male					
0	10/10	143 ± 4	353 ± 12	210 ± 10	
2	10/10	139 ± 2	350 ± 10	210 ± 11	99
15	10/10	144 ± 4	373 ± 16	229 ± 14	106
30	10/10	143 ± 4	368 ± 9	224 ± 8	104
Female					
0	10/10	124 ± 3	222 ± 8	98 ± 6	
2	9/10 ^c	127 ± 3	222 ± 7	96 ± 5	100
15	10/10	123 ± 3	211 ± 6	88 ± 4	95
30	10/10	121 ± 2	224 ± 7	103 ± 6	101

^aWeights and weight changes are presented as mean ± standard error. Subsequent calculations are based on animals surviving to the end of the study. Differences from the control group are not significant by Dunnett's test.

^bNumber of animals surviving at 13 weeks/number initially in group.

^cWeek of death: 13.

Fullerene C₆₀, TOX 87

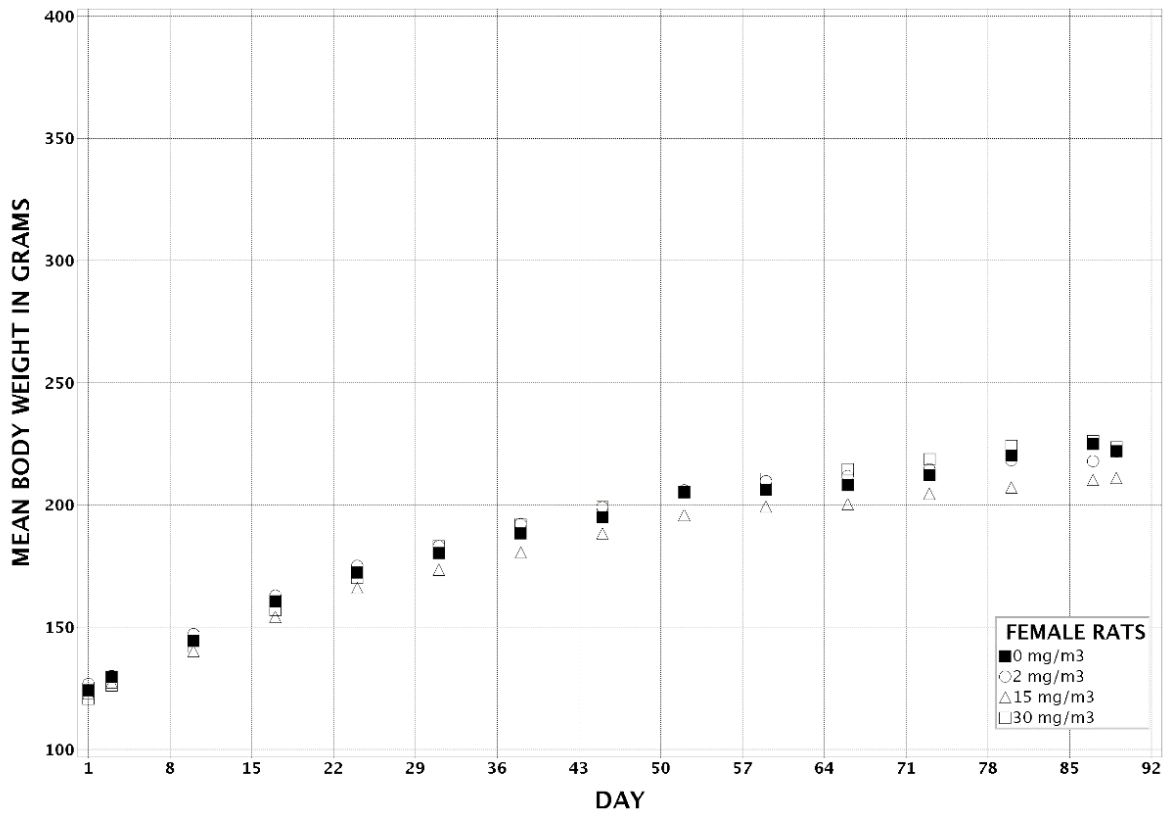
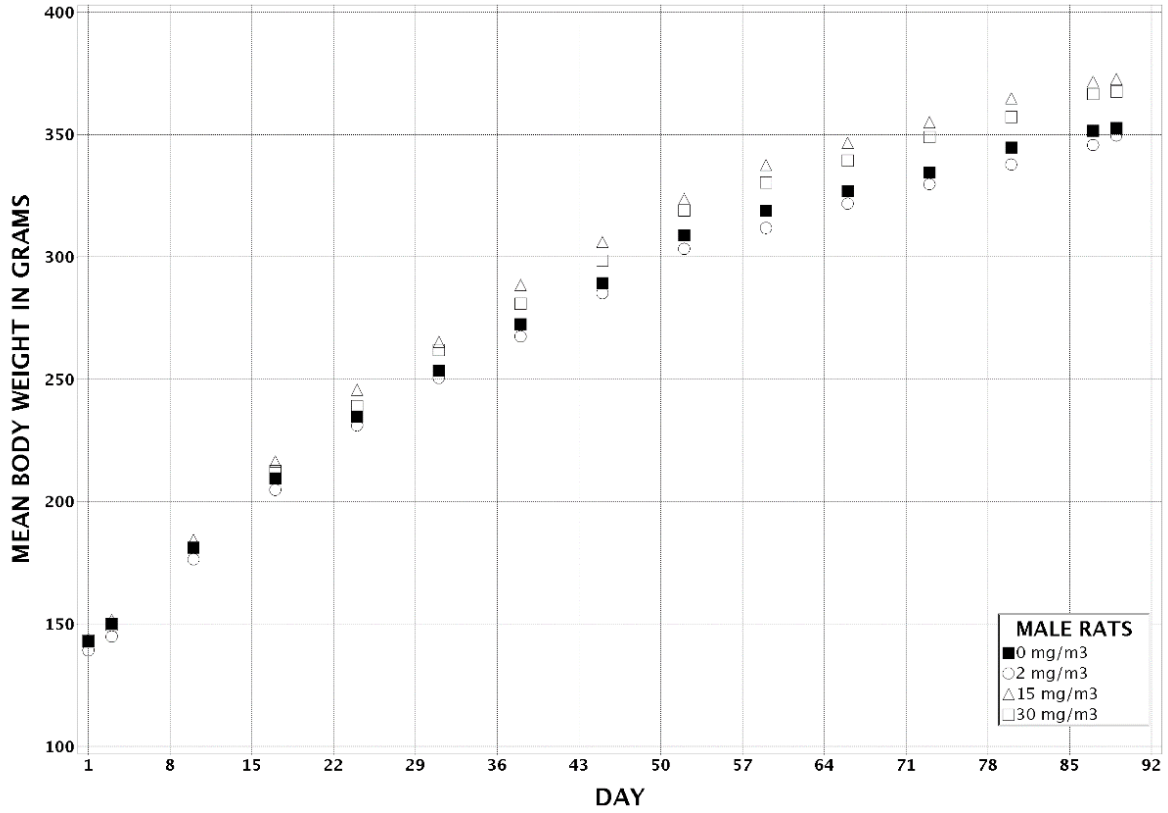


Figure 4. Growth Curves for Rats Exposed to Fullerene Micro-C₆₀ (1 μm) by Nose-only Inhalation for Three Months

Table 4. Survival and Body Weights of Rats in the Three-month Nose-only Inhalation Study of Fullerene Nano-C₆₀ (50 nm)^a

Concentration (mg/m ³)	Survival ^b	Initial Body Weight(g)	Final Body Weight (g)	Change in Body Weight (g)	Final Weight Relative to Controls (%)
Male					
0	10/10	152 ± 3	362 ± 10	210 ± 9	
0.5	10/10	146 ± 3	360 ± 12	215 ± 9	100
2	10/10	150 ± 4	356 ± 9	207 ± 8	99
Female					
0	10/10	118 ± 3	207 ± 6	89 ± 4	
0.5	10/10	117 ± 2	207 ± 7	89 ± 6	100
2	10/10	115 ± 2	201 ± 3	86 ± 3	97

^aWeights and weight changes are presented as mean ± standard error. Differences from the control group are not significant by Dunnett's test.

^bNumber of animals surviving at 13 weeks/number initially in group.

Fullerene C₆₀, TOX 87

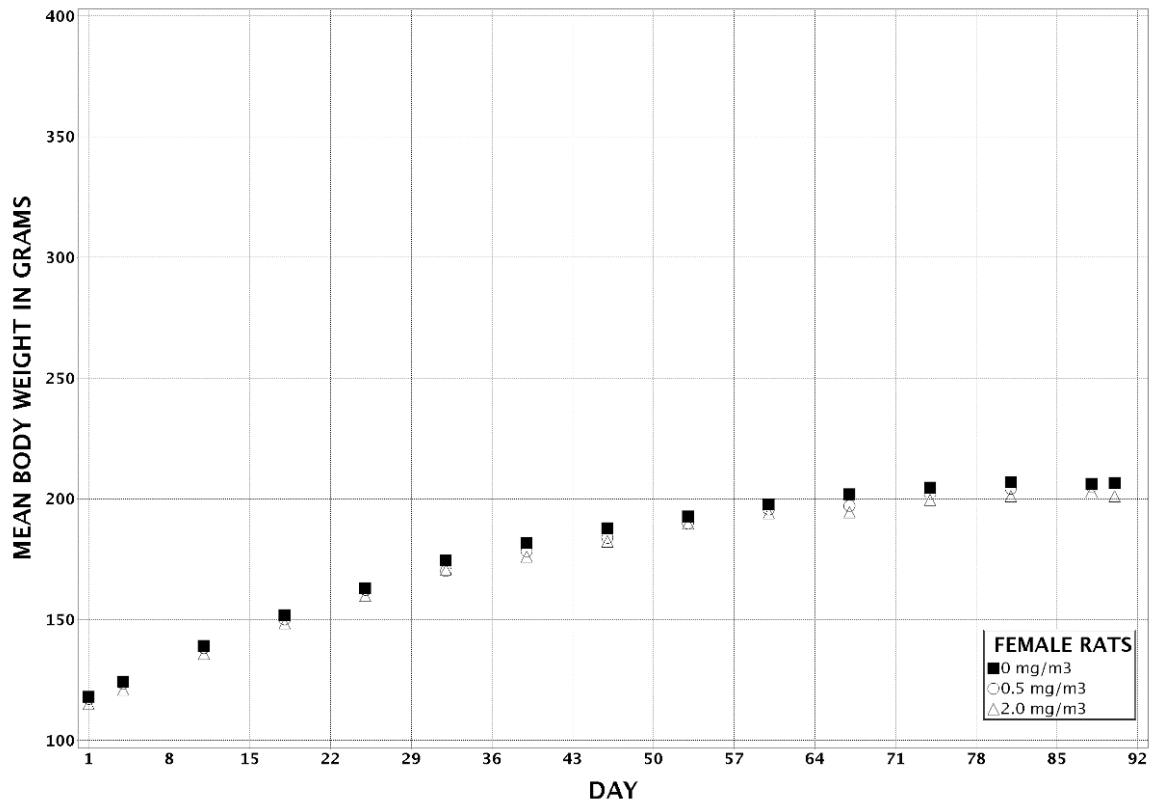
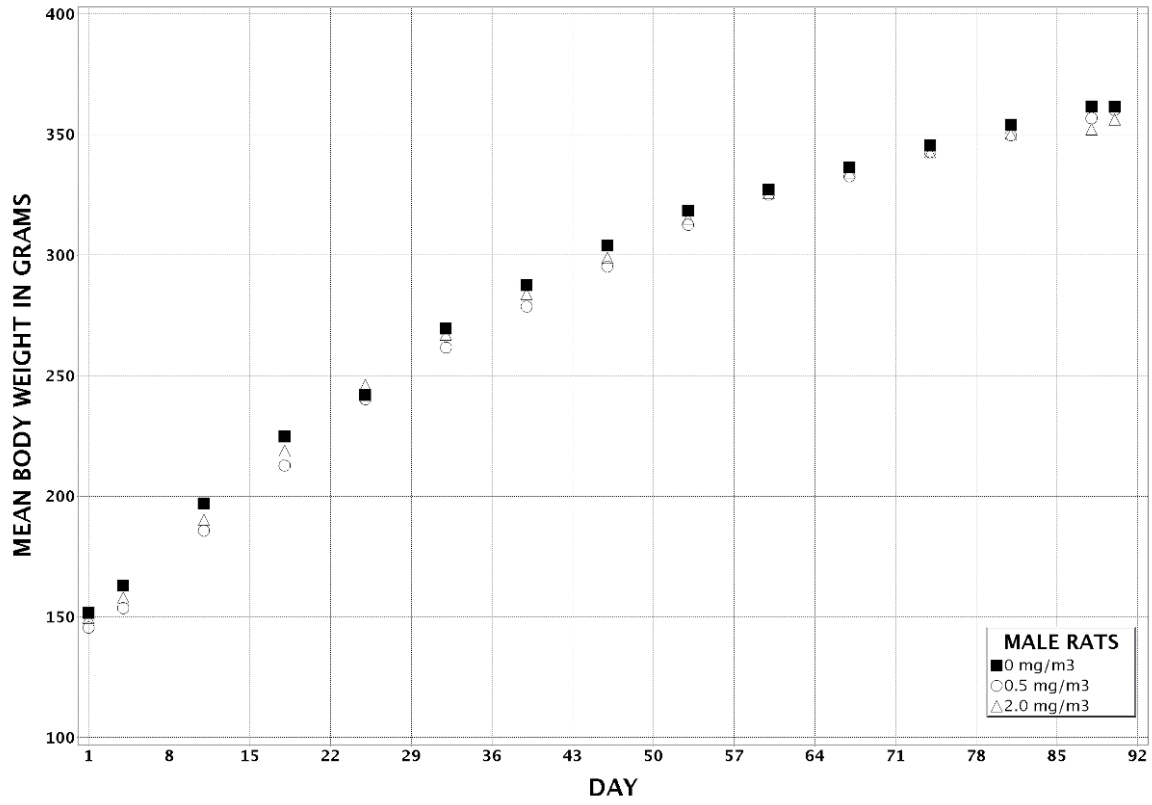


Figure 5. Growth Curves for Rats Exposed to Fullerene Nano-C₆₀ (50 nm) by Nose-only Inhalation for Three Months

Clinical Pathology

The summary clinical pathology data for rats exposed to micro-C₆₀ can be found in Appendix H. No changes in the hematological parameters were attributable to inhalation exposure. A few statistically significant results were found in the serum chemistry data, including minimal increase in glucose in the 15 mg/m³ males and minimal decrease in alanine aminotransferase in the 30 mg/m³ males; none of these changes were considered toxicologically significant.

The summary clinical pathology data for rats exposed to nano-C₆₀ can be found in Appendix H. No treatment-related changes in the hematological parameters occurred in male or female rats. A few statistically significant results were found in the serum chemistry data, including minimal decreases in albumin and in the albumin-to-globulin ratio (A:G) in the 2 mg/m³ males and decreased bile acids in the 2 mg/m³ females; none of these changes were considered toxicologically significant.

Reproductive Evaluations

Male rats exposed to micro-C₆₀ displayed no changes in reproductive organ weights or sperm counts. Sperm motility was slightly lower in all exposed groups (74% to 80% in exposed groups compared to 84% in controls) (Table A-1). Histopathological findings were observed at low incidences in the testes (germinal epithelium, degeneration) in all exposed groups (Table 5). Males exposed to nano-C₆₀ displayed no changes in reproductive organ weights or sperm counts. Sperm motility was slightly lower in rats exposed to 2 mg/m³ nano-C₆₀ (71% compared to 85% in controls) (Table A-2). Histopathological findings in the testes (germinal epithelium, degeneration) and epididymis (hypospermia) also were observed at this exposure level (Table 6).

Histopathology

Micro-C₆₀ Study

Exposure-related gross lesions were limited to brown discoloration (presumably the test article) of the lungs of all male and female rats in the 15 and 30 mg/m³ groups and many rats in the 2 mg/m³ groups. Histologically, exposure-related lesions were present in the lung and bronchial and mediastinal lymph nodes. A complete summary of histopathological findings can be found in Appendix H.

Lung: Exposure-related findings in the lung of rats were limited to infiltration cellular, histiocyte (increased numbers of alveolar macrophages in the alveoli), chronic active inflammation, and pigmentation (presumed to be the test article) (Table 5). The incidence of infiltration cellular, histiocyte was statistically significant compared to controls in the 15 and 30 mg/m³ groups in both sexes. In males, the average severity was increased in the 15 and 30 mg/m³ groups (1.4 and 3.8, respectively) compared to the controls (in which the average severity was minimal, 1.0). In females, the average severity was minimal (1.0) in the controls and in the 2, and 15 mg/m³ groups, but was marked in all animals in the 30 mg/m³ group. The incidence of chronic inflammation in the males was increased in all exposed groups compared to the control group, but the increase was statistically significant only in the 15 and 30 mg/m³ groups. In the females, the incidences of chronic inflammation were increased in the 15 and 30 mg/m³ groups, and the increase was statistically significant in the 30 mg/m³ group. The severity generally increased with increasing exposure concentration. In males, pigment was seen in all exposed groups and

the severity increased with increasing exposure concentration. In females, pigment was seen in the 15 and 30 mg/m³ groups only, and the severity increased with increasing exposure.

Table 5. Incidences of Selected Nonneoplastic Lesions in Rats in the Three-month Nose-only Inhalation Study of Fullerene Micro-C₆₀ (1 µm)

	0 mg/m ³	2 mg/m ³	15 mg/m ³	30 mg/m ³
Male				
Lymph Node, Bronchial ^a	7	5	6	8
Pigmentation ^b	0	1 (1.0) ^c	3 (1.0)	7** (1.9)
Lymph Node, Mediastinal	8	9	8	9
Pigmentation	4 (1.0)	4 (1.0)	3 (1.7)	5 (1.6)
Lung	10	10	9	10
Infiltration cellular, histiocyte	1 (1.0)	1 (1.0)	8** (1.4)	10** (3.8)
Inflammation, chronic active	1 (1.0)	4 (1.0)	8** (1.8)	10** (2.0)
Pigmentation	0	1 (1.0)	8** (2.1)	10** (3.2)
Testes	10	10	10	10
Germinal epithelium, degeneration	0	1 (1.0)	3 (2.0)	1 (1.0)
Female				
Lymph Node, Bronchial	6	5	7	5
Pigmentation	1 (1.0)	1 (1.0)	3 (1.3)	4 (1.5)
Lymph Node, Mediastinal	8	10	8	9
Pigmentation	3 (1.0)	9* (1.1)	7 (1.3)	7 (1.6)
Lung	10	10	10	10
Infiltration cellular, histiocyte	1 (1.0)	1 (1.0)	8** (1.0)	10** (4.0)
Inflammation, chronic active	0	0	1 (1.0)	10** (2.0)
Pigmentation	0	0	8** (2.3)	10** (3.2)

*Significantly different ($p \leq 0.05$) from the control group by the Fisher exact test; ** $p \leq 0.01$.

^aNumber of animals with tissue examined microscopically.

^bNumber of animals with lesion.

^cAverage severity grade of lesions in affected animals: 1 = minimal, 2 = mild, 3 = moderate, 4 = marked.

Infiltration cellular, histiocyte was characterized by the accumulation of alveolar macrophages within the lungs. The alveolar macrophages were enlarged, had foamy cytoplasm, and often contained pigment (Figure 8 and Figure 9). The pigment was golden brown to dark brown and mostly small granules; larger granules were darker brown and refractile. The pigment was presumed to be the test article because it was not seen in the control animals. Chronic active inflammation was characterized by thickened alveolar septa, a mixed population of inflammatory cells, primarily macrophages and lymphocytes with fewer plasma cells and occasional neutrophils, and increased numbers of type II pneumocytes (Figure 10). These foci of inflammation were typically associated with areas of histiocyte infiltration. One control rat was diagnosed with chronic active inflammation; however, the distribution of inflammation in this animal differed from that of the exposed animals in that it was found at the periphery of the lung.

Inflammation in the control animal was considered to be the background form of chronic active inflammation often seen in rodents, whereas inflammation in the exposed animals was associated with the pigment-containing macrophages and was considered exposure-related.

Bronchial and mediastinal lymph nodes: In both sexes, pigment was observed in the bronchial and mediastinal lymph nodes (Table 5). A few control rats had pigment in the lymph nodes, but there was a statistically significant increase in incidence in the bronchial lymph node of 30 mg/m³ males and the mediastinal lymph node of 2 mg/m³ females. In most cases, however, the average severity was higher in the exposed groups than in controls. The pigment was present within macrophages in the subcapsular sinus or cortex. In some cases, pigment was present in control animals or was present in areas of hemorrhage. The pigment was morphologically indistinguishable from that seen in the lung (presumed test article). The lesions were morphologically identical to the lymph node lesions seen in rats exposed to nano-C₆₀ particles.

Other lesions: In the testes, one animal in the 2 mg/m³ group, three in the 15 mg/m³ group, and one in the 30 mg/m³ group had degeneration of the germinal epithelium compared to none in the control group (Table 5). The incidences were not statistically significant, and as this is a common background lesion in rats, the significance of this finding is unclear.

Nano-C₆₀ Study

Exposure-related gross lesions were limited to slight brown discoloration of the lungs of several rats in both exposure groups (whereas in the micro-C₆₀ studies, the lungs of many rats in the 2 mg/m³ and all rats in the 15 and 30 mg/m³ groups were brown at necropsy). Histologically, exposure-related lesions were found in the lung and bronchial and mediastinal lymph nodes. A complete summary of histopathological findings can be found in Appendix H.

Lung: Exposure-related findings in the lung of male and female rats were limited to infiltration cellular, histiocyte (increased numbers of alveolar macrophages in the alveoli) and pigmentation (presumed to be the test article). In contrast to micro-C₆₀ no evidence of chronic active inflammation in the lung was found in nano-C₆₀-exposed rats. The incidences of these lesions were statistically significant in high exposure females only (Table 6). In the males, infiltration cellular, histiocyte was seen in one control, in one 0.5 mg/m³ animal, and in three 2 mg/m³ animals. Severity was minimal in the control and 0.5 mg/m³ groups and was minimal to mild in the 2 mg/m³ group. In the females, infiltration cellular, histiocyte was seen in two control animals, in one 0.5 mg/m³ animal, and in eight of the 2 mg/m³ animals. The severity was minimal in all animals. Pigmentation was seen in eight females in the 2 mg/m³ group only, and the severity was mild. The lesions in both sexes were morphologically identical to the lung lesions seen in the rats exposed to micro-C₆₀ particles.

Table 6. Incidences of Selected Nonneoplastic Lesions in Rats in the Three-month Nose-only Inhalation Study of Fullerene Nano-C₆₀ (50 nm)

	0 mg/m ³	0.5 mg/m ³	2 mg/m ³
Male			
Lymph Node, Bronchial ^a	10	9	10
Pigmentation ^b	0	3 (1.0) ^c	4* (1.0)
Lymph Node, Mediastinal	10	8	10

	0 mg/m ³	0.5 mg/m ³	2 mg/m ³
Pigmentation	1 (1.0)	6* (1.0)	2 (1.0)
Lung	10	10	10
Infiltration cellular, histiocyte	1 (1.0)	1 (1.0)	3 (1.3)
Pigmentation	0	0	3 (1.0)
Kidney	10	10	10
Nephropathy	1 (1.0)	1 (1.0)	6* (1.0)
Epididymis	10	10	10
Hypospermia	0	0	2 (3.0)
Testes	10	10	10
Germinal epithelium, degeneration	0	0	3 (2.0)
Female			
Lymph Node, Bronchial	10	10	10
Pigmentation	0	1 (1.0)	5* (1.2)
Lymph Node, Mediastinal	8	8	10
Pigmentation	0	7** (1.0)	9** (1.3)
Lung	10	10	10
Infiltration cellular, histiocyte	2 (1.0)	1 (1.0)	8* (1.0)
Pigmentation	0	0	8** (2.0)

Significantly different ($p \leq 0.05$) from the control group by the Fisher exact test; ** $p \leq 0.01$.

^aNumber of animals with tissue examined microscopically.

^bNumber of animals with lesion.

^cAverage severity grade of lesions in affected animals: 1 = minimal, 2 = mild, 3 = moderate, 4 = marked.

Bronchial and mediastinal lymph nodes: Pigmentation was the only exposure-related finding in the bronchial and mediastinal lymph nodes (Table 6) and was seen in males and females. Pigmentation incidence in the bronchial lymph node was significantly increased in the 2 mg/m³ groups of males and females. In the mediastinal lymph node in males, the incidence of pigmentation was significantly increased only in the 0.5 mg/m³ group compared to the control group. In females, the incidences of pigmentation were statistically significant in the 0.5 and 2 mg/m³ groups. All instances of this lesion were of minimal severity. The lesions were morphologically identical to the lymph node lesions seen in the rats exposed to micro-C₆₀ particles.

Other lesions: In the testes, three animals in the 2 mg/m³ group had degeneration of the germinal epithelium compared to none in the control and 0.5 mg/m³ groups (Table 6). Two of these animals also had hypospermia in the epididymis. The incidence was not statistically significant, and as a common background lesion in rats, the significance of this finding is unclear. The incidence of chronic progressive nephropathy was significantly increased in the 2 mg/m³ group compared to controls. The severity in all cases was minimal. Because this is a common background lesion in rats, especially males, the significance of this finding is unclear.

Electron Microscopy

Micro-C₆₀ Study

Transmission electron microscopy (TEM) was performed on formalin-fixed tissues from three male rats from the 30 mg/m³ group. The lung from two animals and the bronchial lymph node and liver from one animal each were examined. Electron-dense material consisting of agglomerations of rounded profiles consistent with C₆₀ nanoparticles as described by Yamawaki and Iwai⁸⁵ and Shinohara et al.⁸⁶ were observed within macrophages in the lung (Figure 11 and Figure 12) and bronchial lymph node (Figure 13 and Figure 14). Similar material was not observed in other structures within the lung or bronchial lymph node or in the liver.

Nano-C₆₀ Study

TEM was performed on formalin-fixed lung tissue from one male rat exposed to 2 mg/m³ nano-C₆₀ particles. The findings were identical to those described above for the lungs of the rats exposed to 30 mg/m³ micro-C₆₀ particles.

Immunotoxicity

BALF Cell Differentials

Changes were observed in the differential cell counts of BALF collected from female rats as part of the immunotoxicological evaluations. In general, cellularity of the BALF in the micro-C₆₀ exposure groups was increased, particularly in the 15 and 30 mg/m³ groups. Changes in BALF in the nano-C₆₀ exposed female rats was restricted to a small but statistically significant increase in lymphocytes in the 0.5 mg/m³ exposure group. The increased cellularity in the micro-C₆₀ exposure groups was accompanied by an alteration in the cell types observed in the BALF (Table 7 and Table 8). For example, whereas the BALF of controls consisted almost exclusively (>99%) of macrophages (Figure 15A), the BALF differential of the 30 mg/m³ group included 81%, 16.5%, 2.2%, 0.3%, and 0.0% of macrophages, neutrophils, lymphocytes, eosinophils, and basophils, respectively, and would be consistent with the inflammatory process observed in the lung histopathological findings. Further, similar to the bronchoalveolar macrophages observed in the lung histopathology, macrophages of the BALF contained intracytoplasmic, brown to black, granular to globular pigment (presumptive test article) in the 2, 15, and 30 mg/m³ micro-C₆₀ groups (Figure 15C).

Table 7. Bronchoalveolar Lavage Differential Results of Female Rats in the Three-month Nose-only Inhalation Study of Fullerene Micro-C₆₀ (1 μm)^a

	0 mg/m ³	2 mg/m ³	15 mg/m ³	30 mg/m ³
Macrophages (%)	99.7 ± 0.4	99.6 ± 0.2	98.5 ± 0.6	81.0 ± 3.7*** ^c
Neutrophils (%)	0.2 ± 0.2	0.2 ± 0.1	0.9 ± 0.4	16.5 ± 3.3**
Lymphocytes (%)	0.2 ± 0.2	0.2 ± 0.1	0.6 ± 0.2*	2.2 ± 0.8**
Eosinophils (%)	0.0 ± 0.0	0.0 ± 0.0	0.0 ± 0.0	0.3 ± 0.2
Basophils (%)	0.0 ± 0.0	0.0 ± 0.0	0.0 ± 0.0	0.0 ± 0.0

*Significantly different ($p \leq 0.05$) from the control group by Shirley's test; ** $p \leq 0.01$.

^aData presented as mean ± standard error.

Table 8. Bronchoalveolar Lavage Differential Results of Female Rats in the Three-month Nose-only Inhalation Study of Fullerene Nano-C₆₀ (50 nm)^a

	0 mg/m ³	0.5 mg/m ³	2 mg/m ³
Macrophages (%)	99.5 ± 0.1	98.1 ± 0.8	99.3 ± 0.06
Neutrophils (%)	0.3 ± 0.01	1.4 ± 0.07	0.04 ± 0.01
Lymphocytes (%)	0.0 ± 0.0	0.5 ± 0.2**	0.2 ± 0.1
Eosinophils (%)	0.1 ± 0.1	0.0 ± 0.0	0.1 ± 0.0
Basophils (%)	0.0 ± 0.0	0.0 ± 0.0	0.0 ± 0.0

*Significantly different ($p \leq 0.05$) from the control group by Shirley's test; ** $p \leq 0.01$.

^aData presented as mean ± standard error.

Phenotyping also was performed on BALF cells from the additional immunotoxicity study female rats, and the data are presented in Table C-6. Rat BALF cells were dually stained with antibodies against ED2-like antigen CD163 and against CD11b. Quadrant analysis was conducted to calculate both the absolute number and percentage of BALF cells expressing one, both, or neither of the markers. Exposure to either particle size did not affect the total number of cells recovered from the BALF that ranged from 10–15 × 10⁵ cells.

In the micro-C₆₀ study, a significant increase occurred in the absolute number (30 mg/m³, approximately 71%) and percentages (2 and 15 mg/m³, approximately 22%) of double-negative cells. These double-negative (i.e., CD163⁻CD11b⁻) rat BALF cells in the present study consisted primarily of alveolar macrophages, in addition to a smaller population of other cell types, including T and B lymphocytes, NK cells, eosinophils, and mast cells. Compared to the control group, significantly lower absolute numbers (2 and 15 mg/m³, 98%) and percentages (all exposed groups, 95% to 98%) of double-positive cells were observed. The cells staining positive for both CD163 and CD11b were most likely a combination of resident airway macrophages. Rats exposed to 30 mg/m³ C₆₀ had significant increases in both the absolute number (568%) and percentage (498%) of single-positive CD163⁻CD11b⁺ cells accompanied by significant positive trends. The cells staining positive for CD11b only (i.e., CD163⁻CD11b⁺) were neutrophils and other myeloid cells. The significant increases in the percentage and absolute numbers of CD163⁻CD11b⁺ neutrophils observed in rats exposed to 30 mg/m³ micro-C₆₀, correlated with the significant increase in neutrophils in rats in the same exposure group identified by BAL fluid differential cell counting (Table 7).

In the nano-C₆₀ study, absolute numbers (86% and 91%, respectively) and percentages (86% and 89%, respectively) of double-positive cells (resident airway macrophages) were significantly lower following exposure to 0.5 or 2 mg/m³ compared to the control group; significant negative trends in both absolute number and percentage also occurred (Table C-6).

Spleen Cell Phenotype

Results of the spleen cell phenotype analysis in female rats exposed to micro-C₆₀ are presented in Table C-1. Surface markers used for spleen cell phenotyping were CD45⁺ B-cells, CD5⁺ T-cells, CD4⁺CD5⁺ helper T cells (T_H), CD8⁺CD5⁺ cytotoxic T-cells, NK⁺CD8⁺ natural killer cells, and HIS6⁺ splenic macrophages. In the micro-C₆₀ study, there was a slight, but significant, increase in HIS6⁺ splenic macrophages (absolute number and percentage) in rats exposed to 15 mg/m³

C₆₀. In the nano-C₆₀ study, there was a significantly decreasing trend in the number of CD4⁺CD5⁺ T_H cells (absolute number and percentage).

The functional humoral immune response was evaluated by analyzing the spleen IgM AFC response to sRBC (Table C-2). In the nano-C₆₀ study, there was a significant increase in the total number of spleen cells in rats exposed to 2 mg/m³. A significant positive trend in spleen weight was also observed.

Cytokine levels in the BALF of rats are presented in Table C-7. In the micro-C₆₀ study, exposure to 15 or 30 mg/m³ C₆₀ induced significant increases in concentrated IL-1 levels; a significant increasing trend also was observed. The level of concentrated MCP-1 was increased in rats exposed to 30 mg/m³, and a significant positive trend was observed. A significant negative trend in levels of neat TNF- α was observed in rats, with significant decreases occurring following exposure to 15 or 30 mg/m³. In the nano-C₆₀ study, a significant negative trend in the levels of concentrated TNF- α occurred, with exposure to 2 mg/m³ resulting in a significant decrease.

Three-month Studies in Mice

Tissue Burden

Tissue burden data for mice are presented in Appendix B. In the current studies, lung weights (g) and lung C₆₀ concentrations (µg C₆₀/g lung) were determined in male and female mice following the final exposure (day 89). In addition, lung burdens were assessed in male mice only 14, 28, and 56 days after exposure to assess lung clearance rates. Total C₆₀ lung burden (µg C₆₀/total lung) and exposure concentration-normalized lung burden (µg C₆₀/lung per mg C₆₀/m³) were calculated. Due to the increased lung weights in exposed mice, lung burdens, instead of concentrations in lung tissues, were used to calculate lung clearance rates.

In the micro-C₆₀ studies, lung tissue weights were significantly increased at 0 days postexposure in females exposed to 30 mg/m³ C₆₀ and at 0, 28 and 56 days postexposure in males exposed to 30 mg/m³ C₆₀, relative to control animals (Table B-5). At lower concentrations, lung weights were significantly increased in males 56 days postexposure (15 mg/m³). In the nano-C₆₀ studies, males exposed to 0.5 mg/m³ had significantly increased lung weights at all postexposure time points except day 0 (Table B-7). Males exposed to 2 mg/m³ had significantly increased lung weights 56 days postexposure.

Lung burden rapidly decreased at all postexposure time points in males exposed to all concentrations of the micro-C₆₀ particles, with the exception of the groups exposed to 30 mg/m³ at 14 days (Table B-5). Clearance between postexposure days 0 and 14 was marginal in males exposed to 30 mg/m³, but following exposure day 14, lung burdens in this group decreased rapidly as well. Lung burdens rapidly decreased at all postexposure time points in males exposed to all concentrations of the nano-C₆₀ particles (Table B-7).

There were no exposure concentration-related effects on normalized lung burdens in males or females exposed to the micro-C₆₀ particles, although normalized lung burdens were slightly higher in males exposed to 30 mg/m³ at days 14, 28, and 56 postexposure compared to the 2 mg/m³ group (Table B-5). In the nano-C₆₀ studies, normalized lung burdens were slightly higher at postexposure days 0 and 14 in males exposed 2 mg/m³, relative to those in the 0.5 mg/m³ group; the opposite effect occurred at postexposure days 28 and 56 (Table B-7).

Lung deposition and clearance parameters for males were calculated from C₆₀ lung burden data (Table 9). The clearance rate constants (k) were comparable for both particle sizes at every exposure concentration except 30 mg/m³ (micro-C₆₀), at which the clearance rate constant was approximately fourfold less. The calculated clearance half-life (t_{1/2}) of both particles was generally unaffected by exposure concentration or particle size.

Assuming first-order removal process, steady-state lung burdens are reached in approximately five half-lives. In the micro-C₆₀ studies, the measured lung burdens in the 2 mg/m³ (38 µg C₆₀/total lung; Table B-5) group were identical to the calculated steady-state lung burden for exposure to the same concentration (Table 9). Steady-state lung burdens were likely reached in males exposed to 2 or 15 mg/m³, but not 30 mg/m³. In the nano-C₆₀ studies, the measured lung burden for exposure to 2 mg/m³ (115 µg C₆₀/total lung; Table B-7) was almost identical to the calculated steady-state lung burden for exposure to the same concentration (118 µg C₆₀/lung) (Table 9). Steady-state lung burdens were likely reached in males exposed to 2 mg/m³.

Table 9. Lung Deposition and Clearance Parameter Estimates for Male Mice Exposed to Fullerene C₆₀^a

Parameter	0.5 mg/m ³	2 mg/m ³	15 mg/m ³	30 mg/m ³
Micro-C ₆₀ (1 µm)				
A ₀ (µg fullerene C ₆₀ /total lung)		37	204	615
k (days ⁻¹)		0.044	0.039	0.010
t _{1/2} (days)		16	18	68
α (µg fullerene C ₆₀ /total lung per day)		2	8	11
A _e (µg fullerene C ₆₀ /total lung)		38	211	1,038
Nano-C ₆₀ (50 nm)				
A ₀ (µg fullerene C ₆₀ /total lung)	23	116		
k (days ⁻¹)	0.040	0.047		
t _{1/2} (days)	17	15		
α (µg fullerene C ₆₀ /total lung per day)	0.9	5.5		
A _e (µg fullerene C ₆₀ /total lung)	24	118		

A₀ = lung burden at t = 0 days postexposure; k = first-order lung clearance rate constant; t_{1/2} = lung clearance half-life; α = lung deposition rate; A_e = steady-state lung burden.

^aData are presented as mean values.

General Toxicity

In the micro-C₆₀ studies, all females survived to the end of the study (Table 10). One 2 mg/m³ male was euthanized moribund on day 63 of the study, however this was not considered to be related to exposure. Final mean body weights and mean body-weight gains of exposed groups of males and females were similar to those of the control groups (Table 10 and Figure 6). There were no exposure-related clinical findings in females throughout the study. The 2 mg/m³ male found moribund was lethargic with abnormal breathing, however these observations were not considered to be exposure-related. In the nano-C₆₀ studies, all males and females survived to the end of the study (Table 11). Final mean body weights and mean body-weight gains of exposed groups of males and females were similar to those of the control groups (Table 11 and Figure 7). There were no exposure-related clinical findings in males or females.

Following exposure to micro-C₆₀, absolute and relative lung weights of 30 mg/m³ females were significantly higher than those of the control group (Appendix H). There were no exposure-related changes in organ weights in males or females exposed to nano-C₆₀ (Appendix H).

Table 10. Survival and Body Weights of Mice in the Three-month Nose-only Inhalation Study of Fullerene Micro-C₆₀ (1 µm)^a

Concentration (mg/m ³)	Survival ^b	Initial Body Weight (g)	Final Body Weight (g)	Change in Body Weight (g)	Final Weight Relative to Controls (%)
Male					
0	10/10	20.6 ± 0.4	31.6 ± 0.7	11.0 ± 0.7	
2	9/10 ^c	20.9 ± 0.7	32.1 ± 0.9	11.6 ± 0.6	102
15	10/10	21.4 ± 0.4	30.9 ± 0.5	9.5 ± 0.7	98
30	10/10	21.2 ± 0.5	31.3 ± 0.7	10.1 ± 0.6	99
Female					
0	10/10	17.5 ± 0.4	28.1 ± 0.6	10.6 ± 0.5	
2	10/10	17.8 ± 0.2	28.4 ± 0.7	10.5 ± 0.7	101
15	10/10	17.7 ± 0.2	27.9 ± 0.5	10.2 ± 0.6	99
30	10/10	17.6 ± 0.2	28.6 ± 0.8	11.0 ± 0.9	102

^aWeights and weight changes are presented as mean ± standard error. Subsequent calculations are based on animals surviving to the end of the study. Differences from the control group are not significant by Dunnett's test.

^bNumber of animals surviving at 13 weeks/number initially in group.

^cWeek of death: 9.

Fullerene C₆₀, TOX 87

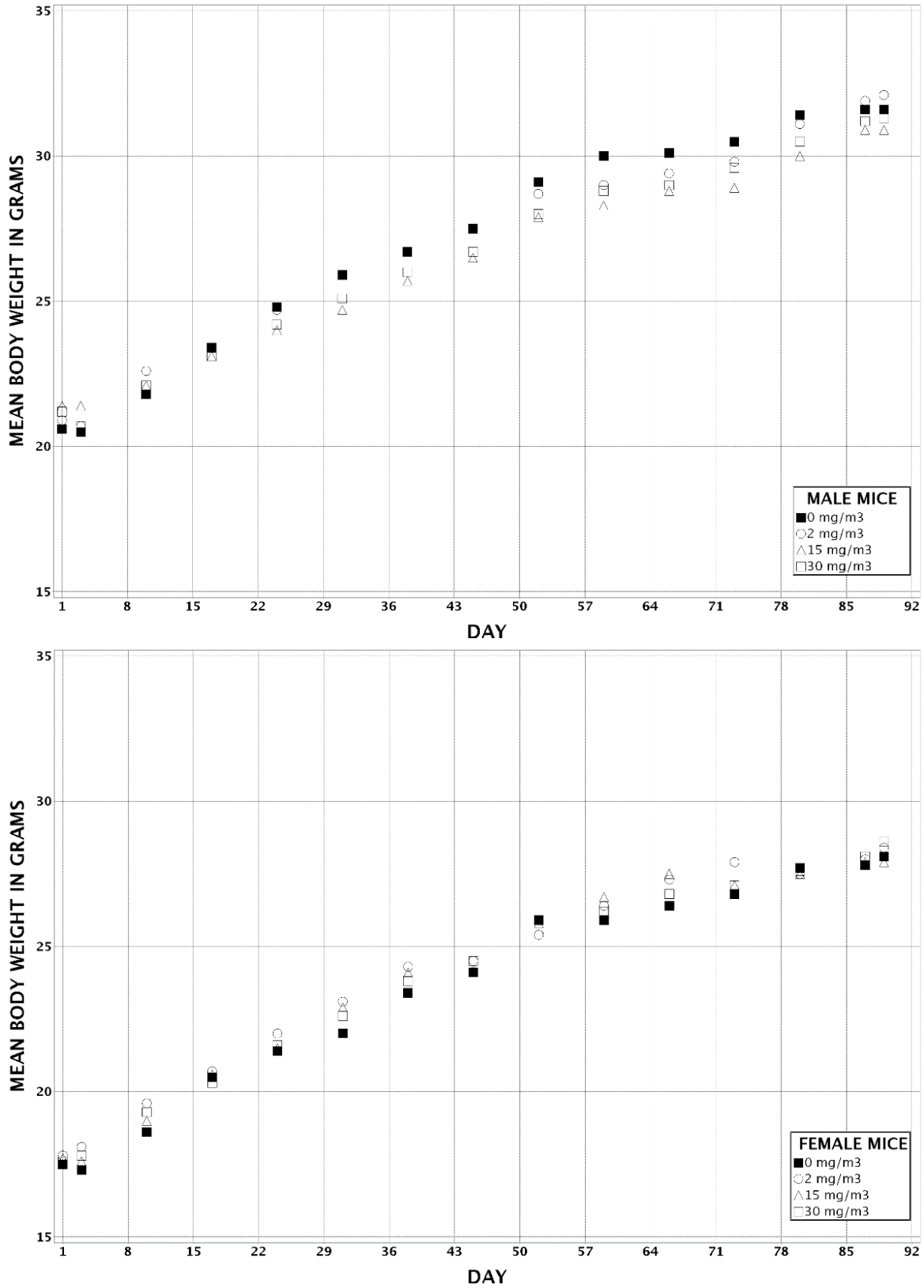


Figure 6. Growth Curves for Mice Exposed to Fullerene Micro-C₆₀ (1 µm) by Nose-only Inhalation for Three Months

Table 11. Survival and Body Weights of Mice in the Three-month Nose-only Inhalation Study of Fullerene Nano-C₆₀ (50 nm)^a

Concentration (mg/m ³)	Survival ^b	Initial Body Weight (g)	Final Body Weight (g)	Change in Body Weight (g)	Final Weight Relative to Controls (%)
Male					
0	10/10	21.3 ± 0.5	31.5 ± 0.8	10.2 ± 0.5	
0.5	10/10	21.1 ± 0.8	31.7 ± 1.1	10.6 ± 0.7	101
2	10/10	21.0 ± 0.5	31.3 ± 0.6	10.3 ± 0.6	99
Female					
0	10/10	17.6 ± 0.2	26.5 ± 0.5	8.9 ± 0.4	
0.5	10/10	17.9 ± 0.3	27.9 ± 0.7	10.1 ± 0.6	105
2	10/10	18.3 ± 0.2	26.6 ± 0.4	8.3 ± 0.4	100

^aWeights and weight changes are presented as mean ± standard error. Differences from the control group are not significant by Dunnett's test.

^bNumber of animals surviving at 13 weeks/number initially in group.

Fullerene C₆₀, TOX 87

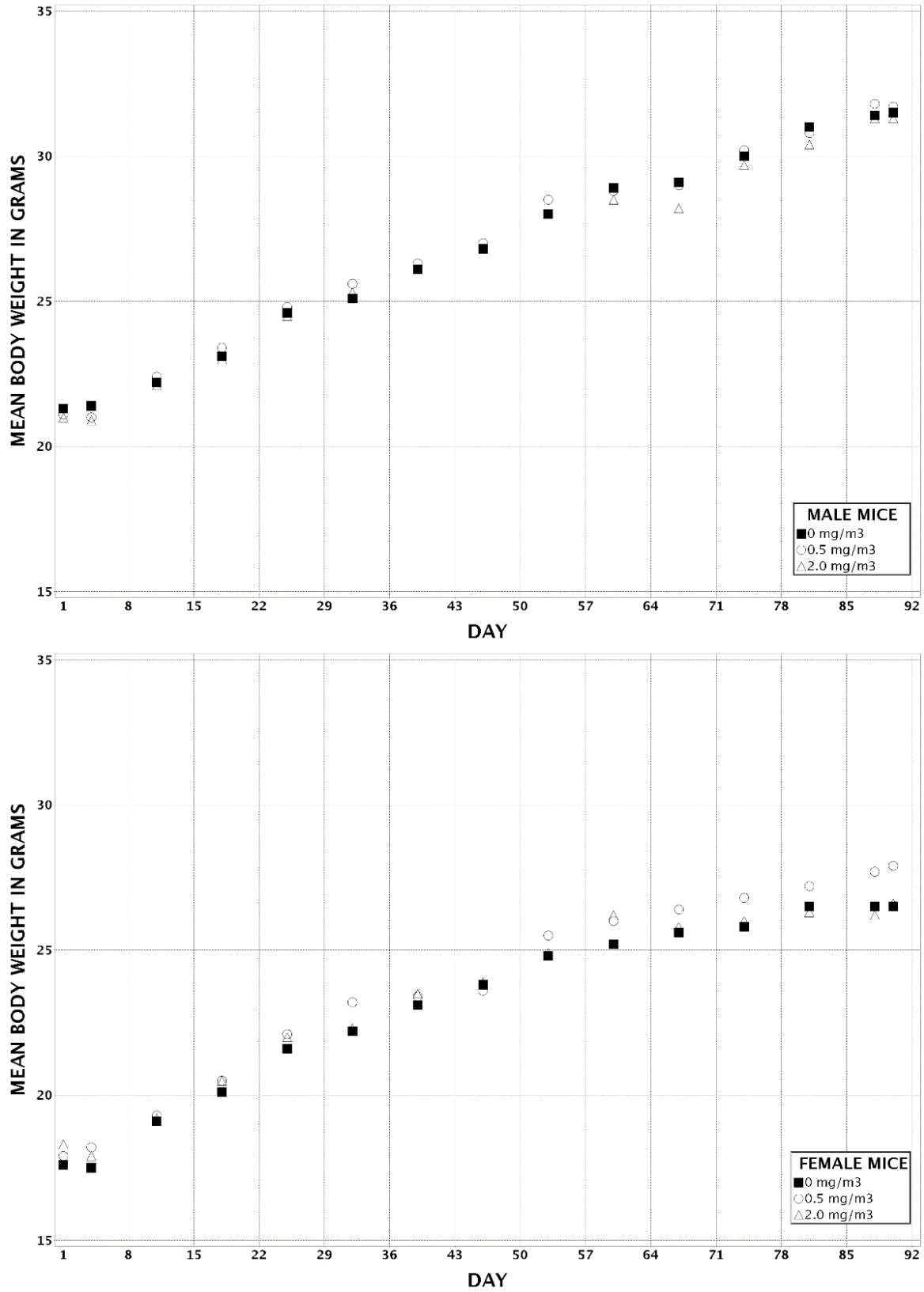


Figure 7. Growth Curves for Mice Exposed to Fullerene Nano-C₆₀ (50 nm) by Nose-only Inhalation for Three Months

Hematology

The summary hematology data for mice exposed to micro-C₆₀ can be found in Appendix H. An apparent decrease in the erythron, evidenced by a minimally ($\leq 3\%$) decreased red blood cell count, hemoglobin concentration, and automated instrument-derived hematocrit values, occurred in the 15 and 30 mg/m³ females, suggesting potential toxicological relevance. The manual spun hematocrit, however, did not corroborate the automated hematocrit. Additionally, no erythron effect occurred in the males (or in either males or females in the rat study.) Because the erythron changes were considered minimal (with results considered within biological limits), were inconsistent with the manual hematocrit values, and were not observed in male mice or in male or female rats, the toxicological relevance of this erythron finding is questionable.

The summary hematological data for mice exposed to nano-C₆₀ can be found in Appendix H. The only finding of statistical significance was a minimal decrease in reticulocyte counts in males exposed to 0.5 or 2 mg/m³; this finding was not considered toxicologically significant.

Reproductive Evaluations

Male mice exposed to micro-C₆₀ displayed no changes in reproductive organ weights or sperm counts (Table A-3). Sperm motility was slightly lower in all exposed groups (72% to 78% compared to 83% in the controls). Males exposed to nano-C₆₀ displayed no exposure-related changes in reproductive organ weights, sperm counts, or motility (Table A-6).

In the micro-C₆₀ study, females exposed to 15 mg/m³ displayed an increased probability of extended estrus compared to controls (Table A-5). The time spent in any particular stage, however, was unaffected (Table A-4). In the nano-C₆₀ study, females exposed to 0.5 or 2 mg/m³ displayed an increased probability of extended estrus, compared to controls (Table A-8). The time spent in any particular stage, however, was unaffected (Table A-7).

Histopathology

Micro-C₆₀ study

Exposure-related gross lesions were limited to brown discoloration of the lungs of all mice in the 30 mg/m³ groups, most mice in the 15 mg/m³ groups, and one male in the 2 mg/m³ group. Histologically, exposure-related lesions occurred in the lung, larynx, and bronchial lymph node. A complete summary of histopathological findings can be found in Appendix H.

Lung: Exposure-related findings in the lungs were limited to infiltration cellular, histiocyte (increased numbers of alveolar macrophages in the alveoli), chronic inflammation, and pigmentation (presumed to be the test article) (Table 12). The incidences of infiltration cellular, histiocyte, were statistically significant compared to controls in the 15 and 30 mg/m³ groups of males and females. The average severity increased with increasing exposure concentration.

Table 12. Incidences of Selected Nonneoplastic Lesions in Mice in the Three-month Nose-only Inhalation Study of Fullerene Micro-C₆₀ (1 µm)

	0 mg/m ³	2 mg/m ³	15 mg/m ³	30 mg/m ³
Male				
Lymph Node, Bronchial ^a	6	4	5	9
Pigmentation ^b	2 (1.0) ^c	1 (1.0)	2 (1.0)	9* (2.9)
Larynx	10	9	10	10
Metaplasia, squamous	1 (1.0)	0	5 (1.0)	9** (1.1)
Lung	10	10	10	10
Infiltration cellular, histiocyte	0	0	10** (2.9)	10** (3.9)
Inflammation, chronic active	0	0	10** (1.0)	10** (1.9)
Pigmentation	0	0	10** (3.2)	10** (3.8)
Female				
Lymph Node, Bronchial	5	6	5	6
Pigmentation	2 (1.0)	3 (1.0)	1 (1.0)	6 (2.7)
Larynx	10	8	10	10
Metaplasia, squamous	0	1 (1.0)	6** (1.0)	9** (1.2)
Lung	10	10	10	10
Infiltration cellular, histiocyte	0	0	10** (2.4)	10** (4.0)
Inflammation, chronic active	0	0	3 (1.0)	10** (2.0)
Pigmentation	0	0	10** (2.9)	10** (4.0)

*Significantly different ($p \leq 0.05$) from the control group by the Fisher exact test; ** $p \leq 0.01$.

^aNumber of animals with tissue examined microscopically.

^bNumber of animals with lesion.

^cAverage severity grade of lesions in affected animals: 1 = minimal, 2 = mild, 3 = moderate, 4 = marked.

The incidences of chronic active inflammation were significantly increased in 15 and 30 mg/m³ males and in 30 mg/m³ females compared to the control groups. Chronic active inflammation was not present in lungs of male or female mice in control or 2 mg/m³ groups. The severity of inflammation increased with increasing exposure concentration. The incidences of pigmentation were significantly increased in 15 and 30 mg/m³ males and females; pigment was not seen in the control or 2 mg/m³ groups. The severity of the pigment increased with increasing exposure concentration. Lung lesions in mice were morphologically identical to lung lesions observed in rats exposed to micro-C₆₀.

Larynx: Incidences of squamous metaplasia of the laryngeal epithelium were increased in the 15 and 30 mg/m³ males, compared to the control group, and the increase was significant in the 30 mg/m³ males (Table 12). Incidences of squamous metaplasia of the laryngeal epithelium were increased compared to controls, and the increases were significant in the 15 and 30 mg/m³ groups. Average severity was comparable in all groups. Squamous metaplasia of the laryngeal epithelium is characterized by a change from the normally single-layer cuboidal, ciliated epithelium to a flattened, multilayered, nonciliated epithelium. This lesion was observed at the base of the epiglottis.

Bronchial lymph node: The incidences of pigmentation were increased in the 30 mg/m³ males and females, and the increase in males was significant compared to controls; the severity of pigmentation was also increased. The lesions in mice were morphologically identical to the lymph node lesions in rats exposed to micro-C₆₀ particles.

Nano-C₆₀ Study

There were no exposure-related gross lesions in mice exposed to nano-C₆₀ particles. Histologically, exposure-related lesions occurred in the lung and bronchial lymph nodes. A complete summary of histopathological findings can be found in Appendix H.

Lung: Incidences of infiltration cellular, histiocyte (increased numbers of alveolar macrophages in the alveoli), were significantly increased in the 2 mg/m³ males and slightly increased in 2 mg/m³ females compared to controls (Table 13). Incidences of pigmentation were significantly increased in the 2 mg/m³ males and females. One 2 mg/m³ male had chronic active inflammation, likely related to exposure to nano-C₆₀ particles (no exposure-related inflammation occurred in the females). The lesions in mice were morphologically identical to the lung lesions observed in rats exposed to micro-C₆₀ particles.

Bronchial lymph node: Incidences of pigmentation were increased in the 0.5 and 2 mg/m³ groups of males and females, compared to controls (Table 13), and the increase was significant in the 2 mg/m³ males. The severity was minimal in all groups. The lesions were morphologically identical to the lymph node lesions observed in rats exposed to micro-C₆₀ particles.

Table 13. Incidences of Selected Nonneoplastic Lesions in Mice in the Three-month Nose-only Inhalation Study of Fullerene Nano-C₆₀ (50 nm)

	0 mg/m ³	0.5 mg/m ³	2 mg/m ³
Male			
Lymph Node, Bronchial ^a	9	7	7
Pigmentation ^b	0	2 (1.0) ^c	5** (1.0)
Lung	10	10	10
Infiltration cellular, histiocyte	1 (1.0)	2 (1.0)	7** (2.3)
Inflammation, chronic active	0	0	1 (1.0)
Pigmentation	0	0	7** (2.9)
Female			
Lymph Node, Bronchial	10	7	10
Pigmentation	2 (1.0)	3 (1.0)	4 (1.0)
Lung	10	10	10
Infiltration cellular, histiocyte	2 (1.5)	1 (1.0)	5 (1.0)
Pigmentation	0	0	5* (2.4)

*Significantly different ($p \leq 0.05$) from the control group by the Fisher exact test; ** $p \leq 0.01$.

^aNumber of animals with tissue examined microscopically.

^bNumber of animals with lesion.

^cAverage severity grade of lesions in affected animals: 1 = minimal, 2 = mild, 3 = moderate, 4 = marked.

Immunotoxicity

BALF Cell Differentials

In general, cellularity of the BALF in the micro-C₆₀ fullerene exposure groups was increased, particularly in the 15 and 30 mg/m³ animals. The increased cellularity was accompanied by an alteration in the cell types observed in the BALF (Table 14). For example, whereas the BALF of controls consisted almost exclusively (>99%) of macrophages (Figure 16A), the BALF differential of the 30 mg/m³ group changed to include 71.9%, 25.6%, 2.5%, 0.0%, and 0.0% of macrophages, neutrophils, lymphocytes, eosinophils, and basophils, respectively, which is consistent with the inflammatory process observed in the lung histopathological findings. Further, similar to the bronchoalveolar macrophages observed in the lung histopathology, macrophages of the BALF contained intracytoplasmic brown to black, granular to globular pigment (presumptive test article) in the 2, 15, and 30 mg/m³ groups (Figure 16C).

There were no statistically significant findings in the BALF differential cell counts of female mice exposed to nano-C₆₀ (Table 15). Similar to the histopathological findings, however, bronchoalveolar macrophages from mice exposed to 0.5 or 2 mg/m³ nano-C₆₀ fullerene often contained intracytoplasmic, brown to black, granular, to globular pigment.

Table 14. Bronchoalveolar Lavage Differential Results of Female Mice in the Three-month Nose-only Inhalation Study of Fullerene Micro-C₆₀ (1 μm)^a

	0 mg/m ³	2 mg/m ³	15 mg/m ³	30 mg/m ³
Macrophages (%)	99.8 ± 0.2	99.8 ± 0.1	94.3 ± 1.1**	71.9 ± 2.1**c
Neutrophils (%)	0.0 ± 0.0	0.3 ± 0.1	5.6 ± 1.1**	25.6 ± 2.0**
Lymphocytes (%)	0.0 ± 0.0	0.0 ± 0.0	0.1 ± 0.1*	2.5 ± 0.5**
Eosinophils (%)	0.2 ± 0.2	0.0 ± 0.0	0.0 ± 0.0	0.0 ± 0.0
Basophils (%)	0.0 ± 0.0	0.0 ± 0.0	0.0 ± 0.0	0.0 ± 0.0

*Significantly different ($p \leq 0.05$) from the control group by Shirley's test; ** $p \leq 0.01$.

^aData presented as mean ± standard error.

Table 15. Bronchoalveolar Lavage Differential Results of Female Mice in the Three-month Nose-only Inhalation Study of Fullerene Nano-C₆₀ (50 nm)^a

	0 mg/m ³	0.5 mg/m ³	2 mg/m ³
Macrophages (%)	99.8 ± 0.1	99.8 ± 0.1	99.7 ± 0.1
Neutrophils (%)	0.2 ± 0.01	0.1 ± 0.0	0.1 ± 0.1
Lymphocytes (%)	0.0 ± 0.0	0.1 ± 0.0	0.2 ± 0.1
Eosinophils (%)	0.0 ± 0.0	0.0 ± 0.0	0.1 ± 0.0
Basophils (%)	0.0 ± 0.0	0.0 ± 0.0	0.0 ± 0.0

*Significantly different ($p \leq 0.05$) from the control group by Shirley's test; ** $p \leq 0.01$.

^aData presented as mean ± standard error.

Spleen Cell Phenotype

Results of the spleen cell phenotype analysis in female mice are presented in Table C-1. In the micro-C₆₀ studies, significantly fewer (approximately 22%) splenic macrophages (Mac-3⁺) were measured in mice exposed to 15 or 30 mg/m³, and a significant negative trend in cytotoxic

T cells (T_{CTL}, CD4⁻CD8⁺) also occurred. The percentage of macrophages was significantly decreased in mice exposed to 30 mg/m³, which coincided with a significantly decreasing trend in the same animals. In the nano-C₆₀ studies, significantly fewer absolute numbers of B cells (Ig⁺) (18% and 24%) were noted in mice exposed to 0.5 and 2 mg/m³, respectively, relative to controls; a significant negative trend also occurred. Significantly fewer total T cells (CD3⁺) (approximately 20%) also were observed in mice exposed to 0.5 mg/m³ relative to the control group; a significant negative trend in the percentage of B cells was also observed.

There were no effects on the number of IgM PFC/10⁶ splenocytes (specific activity) or PFC/spleen (total spleen activity) in the plaque assay in mice exposed to either micro- or nano-C₆₀ particles. Serum levels of anti-sRBC IgM antibodies in mice were not affected by exposure to either size of C₆₀ particles.

Spleen cells from exposed mice were cultured with and without anti-CD3 antibody to evaluate anti-CD3 antibody-mediated T cell proliferative response as a marker of cell-mediated immunity (Table C-3). There were no statistically significant changes in the basal proliferative response of spleen cells from mice exposed to the micro-C₆₀ particles with the exception of mice in the 2 mg/m³ group, where a 47% decrease occurred in the basal proliferative response relative to control animals. There were no statistically significant changes in the basal proliferative response of spleen cells from mice exposed to the nano-C₆₀ particles. There was an exposure-concentration-dependent decrease in the anti-CD3-stimulated proliferative response; however, the decrease did not reach statistical significance. The total number of spleen cells was significantly lower in mice exposed to 2 mg/m³; this coincided with a significant negative trend in the same animals.

In the micro-C₆₀ study, a significant increase in MIP-1 α occurred in female mice following exposure to 15 or 30 mg/m³ (Table C-7). In contrast, in the nano-C₆₀ study there were no significant increases in MIP-1 α in female mice following exposure up to 2 mg/m³.

Genetic Toxicology

Micro-C₆₀ particles, administered by nose-only inhalation for 3 months at concentrations of 2, 15, or 30 mg/m³ did not increase the frequencies of micronucleated reticulocytes (polychromatic erythrocytes) or erythrocytes (normochromatic erythrocytes) in peripheral blood of male or female rats or mice (Table D-1 and Table D-3). Similarly, nano-C₆₀ particles administered by nose-only inhalation for 3 months at concentrations of 0.5 or 2 mg/m³ did not increase the frequencies of micronucleated reticulocytes or erythrocytes in peripheral blood of male or female rats or mice (Table D-2 and Table D-4). Neither size particle affected the percentage of reticulocytes in peripheral blood, suggesting no exposure-related bone marrow toxicity.

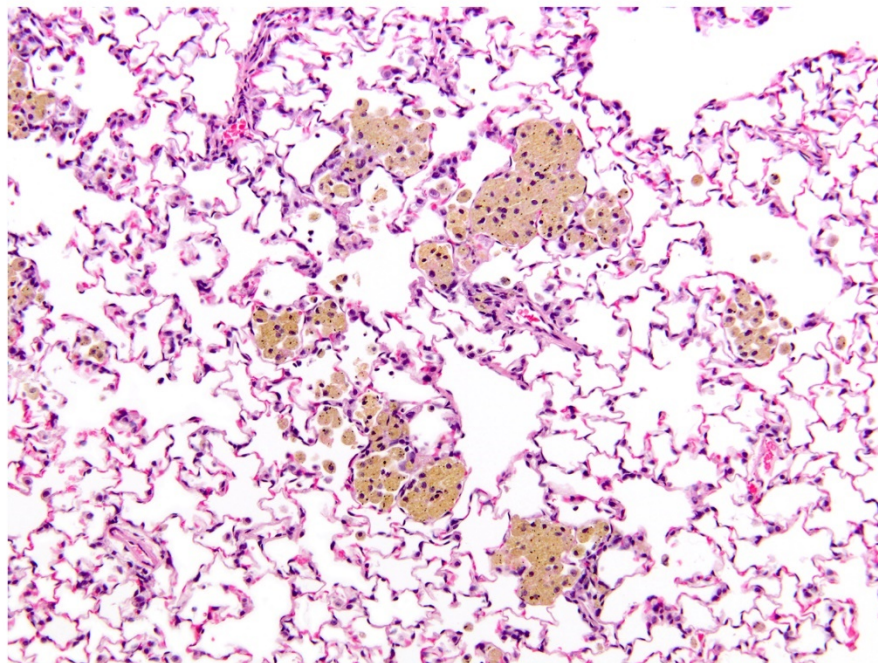


Figure 8. Infiltration Cellular, Histiocyte and Pigmentation in the Lung of a Male Wistar Han Rat Exposed to 30 mg/m³ Micro-C60 by Nose-only Inhalation for Three Months (H&E, 20×)

The golden-brown pigment within the alveolar macrophages is presumed to be the test article.

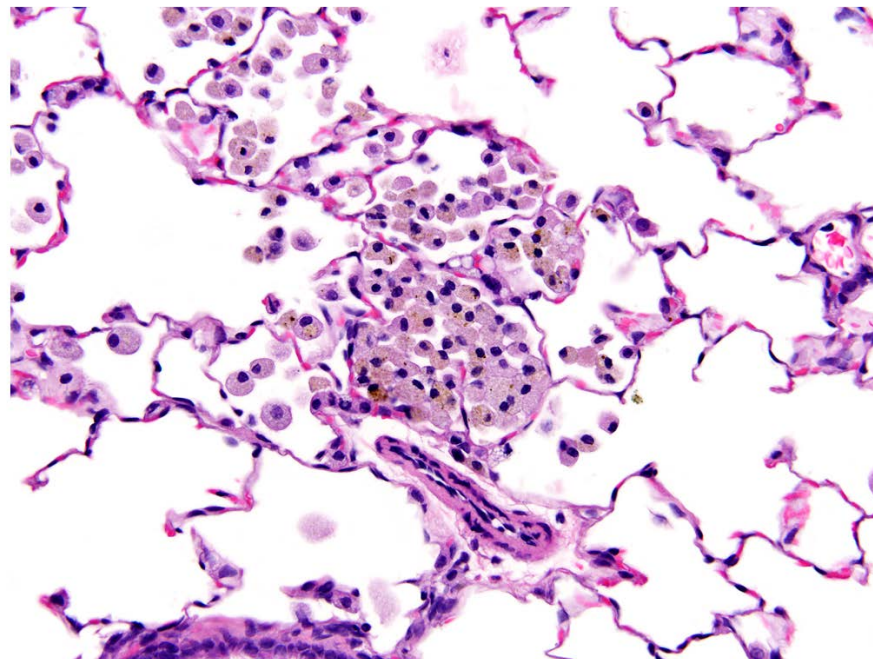


Figure 9. Infiltration Cellular, Histiocyte and Pigmentation in the Lung of a Male Wistar Han Rat Exposed to 2 mg/m³ Nano-C60 by Nose-only Inhalation for Three Months (H&E, 40×)

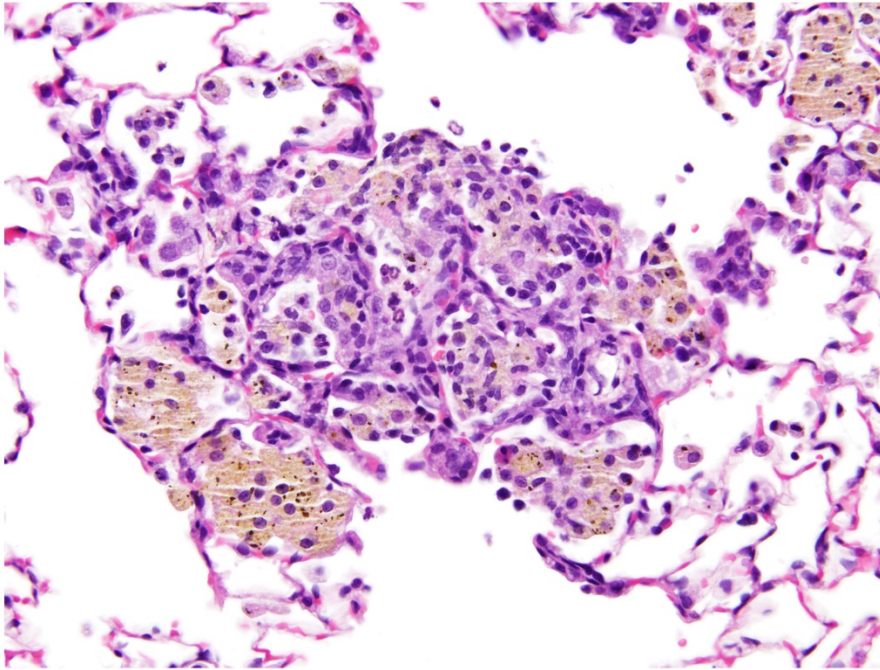


Figure 10. Chronic Active Inflammation in the Lung of a Male Wistar Han Rat Exposed to 30 mg/m³ micro-C₆₀ by Nose-only Inhalation for Three Months (H&E, 40×)

In addition to the macrophages, lymphocytes, neutrophils, and increased numbers of alveolar type II cells are present.

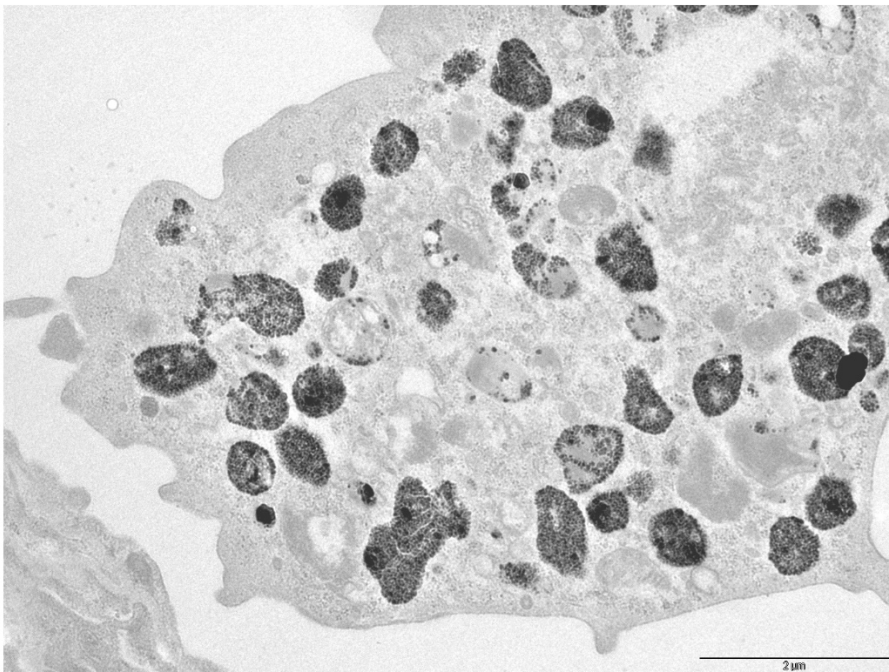


Figure 11. Transmission Electron Micrograph of an Alveolar Macrophage in the Lung of a Male Wistar Han Rat Exposed by Nose-only Inhalation to 2 mg/m³ Nano-C₆₀ for Three Months (9900×)

Note the electron-dense material within the macrophage.

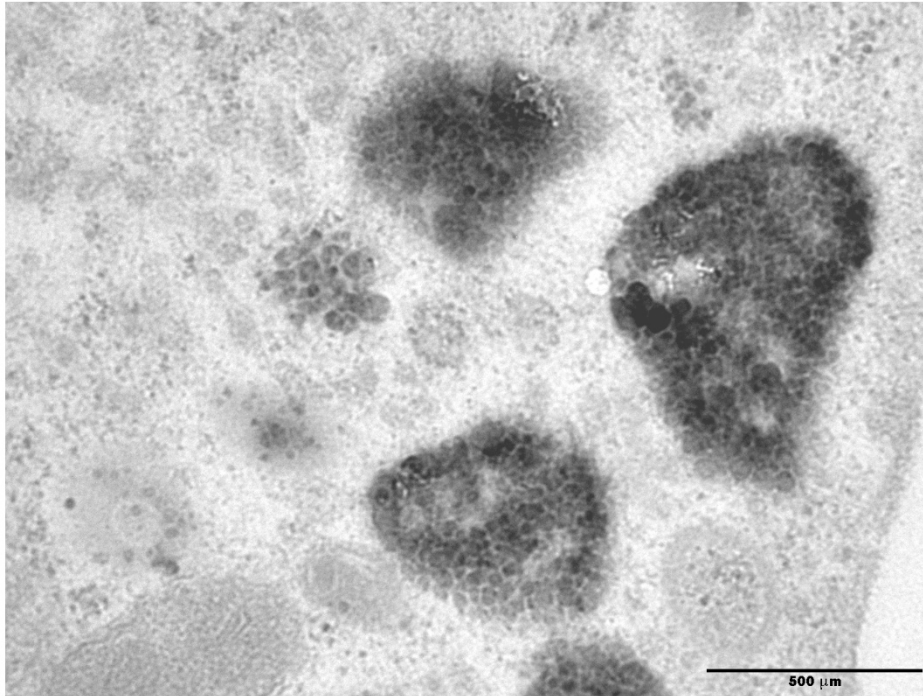


Figure 12. Transmission Electron Micrograph of an Alveolar Macrophage in the Lung of a Male Wistar Han Rat Exposed by Nose-only Inhalation to 2 mg/m³ Nano-C₆₀ for Three Months (43,000×)

Higher magnification of Figure 11. The electron-dense material is consistent with the test article.

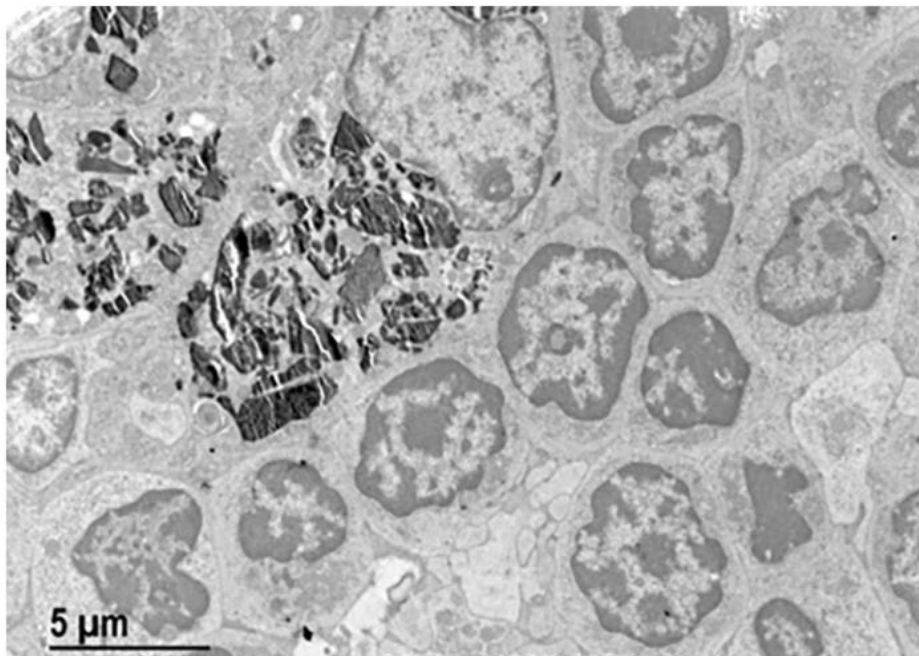


Figure 13. Transmission Electron Micrograph of a Macrophage in the Bronchial Lymph Node of a Male Wistar Han Rat Exposed to 30 mg/m³ Micro-C₆₀ by Nose-only Inhalation for Three Months

Note the electron-dense material within the macrophage.

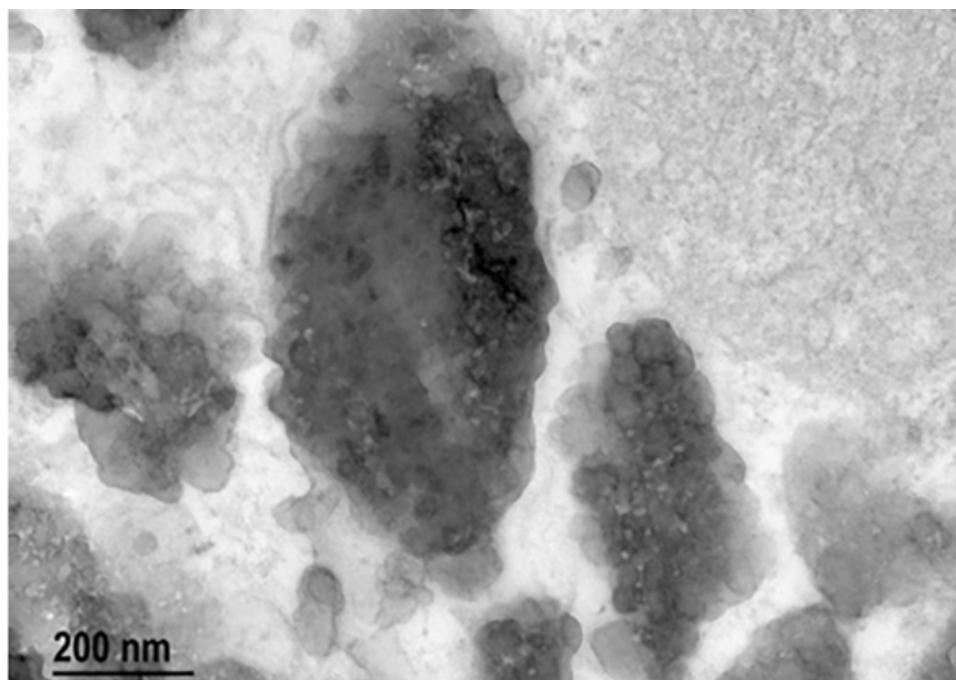


Figure 14. Transmission Electron Micrograph of a Macrophage in the Bronchial Lymph Node of a Male Wistar Han Rat Exposed by Nose-only Inhalation to 30 mg/m³ Micro-C₆₀ for Three Months

Higher magnification of Figure 13. The electron-dense material is consistent with micro-C₆₀ and appears identical to that seen in Figure 12.

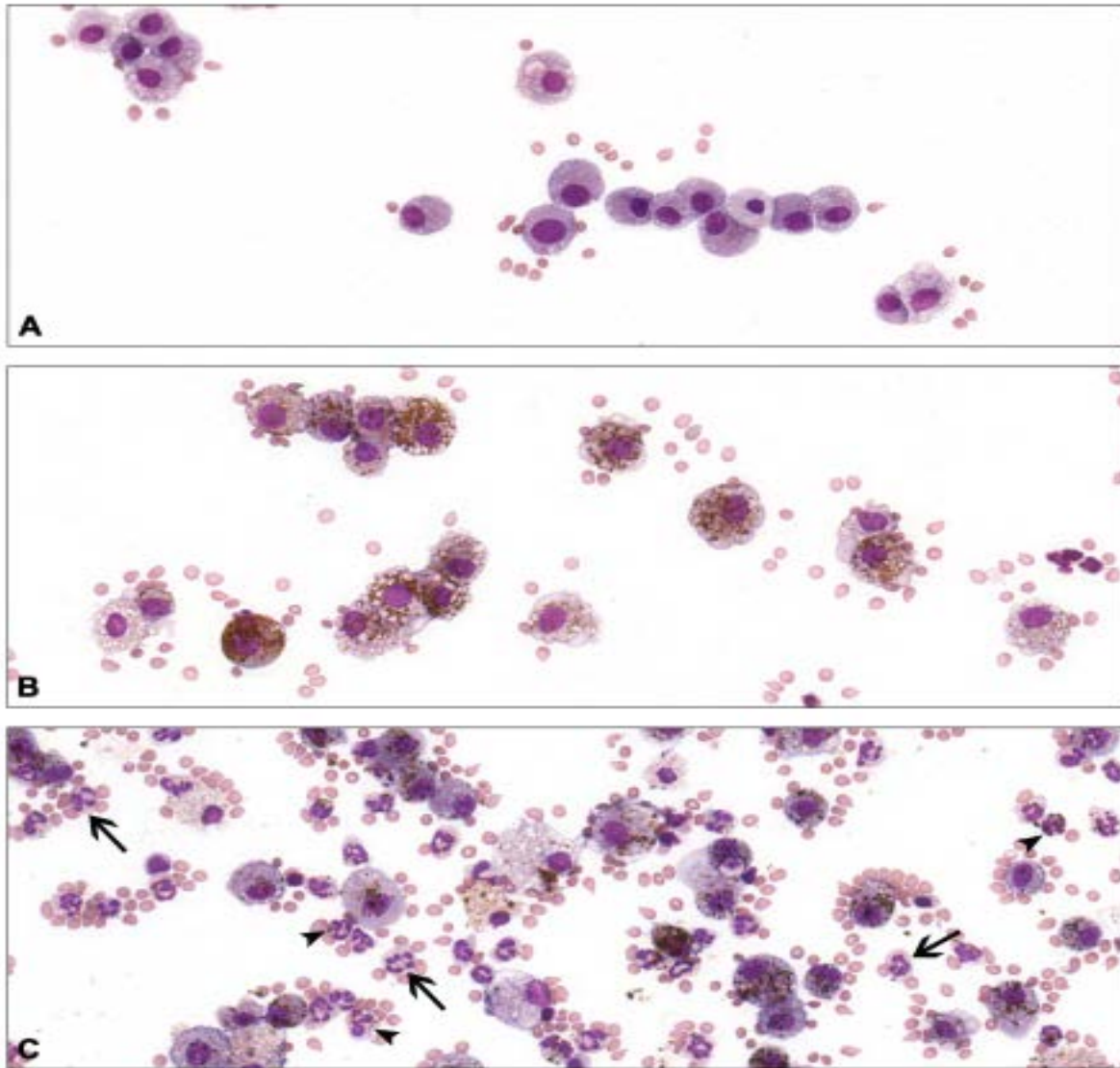


Figure 15. Cell Morphology of Bronchoalveolar Lavage Fluid in Rats

(A) BALF cell morphology representative of control rats of both the nano- and micro-C₆₀ studies; (B) Rat BALF cell morphology of the 2 mg/m³ nano-C₆₀ consisting predominantly of macrophages containing variable amounts of granular to globular, brown to black intracytoplasmic granules (i.e., presumptive test article); (C) Rat BALF cell morphology of the 30 mg/m³ micro-C₆₀ consisting predominantly of macrophages containing variable amounts of brown to black intracytoplasmic granules (i.e., presumptive test article).

BALF = bronchoalveolar lavage fluid. Note, increased numbers of neutrophils (arrows), many of which contain intracytoplasmic brown to black granules (arrowheads). Photomicrographs are of BALF cytospin preparations stained with a Romanowsky-type stain and examined microscopically (original magnification 40×).

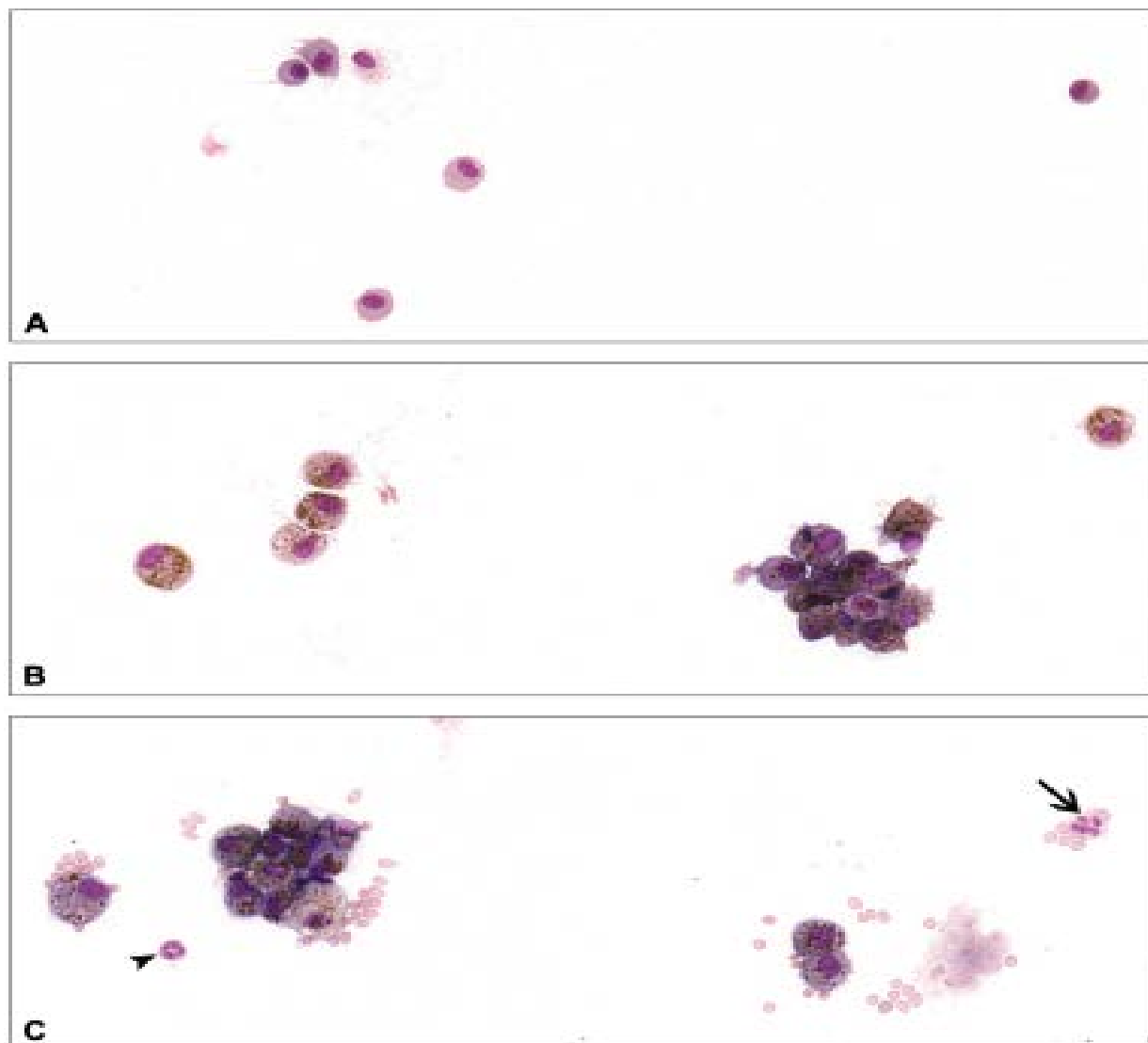


Figure 16. Cell Morphology of Bronchoalveolar Lavage Fluid in Mice

(A) BALF cell morphology representative of control mice of both the nano- and micro-C₆₀ Studies; (B) Mouse BALF cell morphology of the 2 mg/m³ nano-C₆₀ consisting predominantly of macrophages containing variable amounts of granular to globular, brown to black intracytoplasmic granules (i.e., presumptive test article); (C) Mouse BALF cell morphology of the 30 mg/m³ micro-C₆₀ consisting predominantly of macrophages containing variable amounts of brown to black intracytoplasmic granules (i.e., presumptive test article).

BALF = bronchoalveolar lavage fluid. Note increased numbers of neutrophils (arrow), many of which contain intracytoplasmic brown to black granules (arrowhead). Photomicrographs are of BALF cytopsin preparations stained with a Romanowsky-type stain and examined microscopically (original magnification 40×).

Discussion

Differential pathological effects have been previously observed between nanoscale and microscale titanium dioxide (TiO₂) particles of the same chemical composition and the same mass dose in the lungs of rodents.^{33; 87} When the dose is expressed as surface area instead of mass, however, nanoscale and microscale particles share the same dose-response curve.^{88; 28} Those observations, along with subsequent research in nanotoxicology, have highlighted the importance of understanding how chemical composition and physical properties influence toxicokinetics and toxicity.⁸⁹ The current studies were designed to allow for comparisons of tissue burden and clearance kinetics between nanoscale and microscale C₆₀ fullerenes. The exposure concentrations in these studies were selected to allow for comparison between the two particle sizes using either mass or estimated surface area as the dose metric.

In the current studies, initial lung burdens generally increased in proportion to exposure concentrations for both nano- and micro-C₆₀ particles. In addition, rapid clearance of C₆₀ from the lung was observed during the first 14 days of the postexposure period for both particle sizes at all exposure concentrations except for 30 mg/m³ micro-C₆₀ groups in both species. Relatively large lung burdens and increased retention half-lives are characteristic of lung overload. Morrow's overload hypothesis^{90; 91} is applicable to poorly soluble particles of low toxicity (e.g., carbon black, coal dust, diesel soot, talc, and titanium dioxide). Experiments in F344 rats demonstrated a slowing of pulmonary clearance when the volume of particles in the lung reaches 6% of the volume of alveolar macrophages and a ceasing of clearance when the particle volume reaches 60%.^{90; 91} In rats, but not mice or hamsters, inhalation exposure to certain particles at concentrations that result in lung overload has been associated with a variety of nonneoplastic lung lesions including inflammation, fibrosis, epithelial hyperplasia, and lung tumors.⁹² Lung burdens, similar to those that result in lung overload in rats, have been observed in humans. Induction of lung fibrosis has been observed in both rats and humans, whereas lung tumors were observed only in rats.

The possibility that lung overload resulted from exposure to nano- or micro-C₆₀ was evaluated in the present studies.⁹³ Using a density of 1.72 g/cm³ and the lung burdens determined immediately after exposure, Sayers et al. calculated the volume of particles in the lungs and compared it to the volume corresponding to 6% of the volume of alveolar macrophages (1.8×10^9 for rats and 2.4×10^8 for mice) using a lung alveolar macrophage cell number derived for Sprague Dawley rats and scaled to mice using relative lung weights.⁹³ The volume of particles exceeded the overload volume in male rats and mice exposed to 30 mg/m³ of micro-C₆₀. Tran et al.⁹⁴ demonstrated that surface area of the retained lung burden is also an appropriate metric for determining if lung overload has occurred. Using the average estimated surface-area-to-mass ratios and the lung burdens determined immediately after exposure, the estimated surface area of particles in the lungs was calculated by Sayers et al. and compared to the particle surface area thought to result in overload (300 cm² for rats scaled to 32 cm² for mice using relative lung weights).⁹⁴ The estimated surface area of particles exceeded this surface area at 30 mg/m³ for micro-C₆₀ and at 2 mg/m³ for nano-C₆₀, in both rats and mice. Overall, the estimated surface-area-based lung overload calculations were in good agreement with the pulmonary clearance data. Although both volumetric and surface-area-based lung overload were apparent at the higher exposure concentrations following exposure to both particle sizes in the present studies, a notable finding is that the retention half-lives observed with both nano- and

micro-C₆₀, in particular following exposure to lower concentrations of either particle size, were shorter than those typically observed with poorly soluble particles (~70 days in rats).⁹⁵ The retention half-life data in the current study are similar to those observed in a previous study, where retention half-lives of 26 and 29 days were observed in rats following exposure to nano- or micro-C₆₀, respectively.¹¹

At an equivalent exposure concentration (2 mg/m³), the lung burden of C₆₀ on postexposure day 0 was consistently greater in both species following inhalation of nano-C₆₀ particles compared to micro-C₆₀. In rats, nano-C₆₀ exposure resulted in lung burdens 32% (males) and 87% (females) greater than C₆₀ lung burdens following micro-C₆₀ exposure. Similar findings were observed in a 10-day nose-only inhalation study comparing nano-C₆₀ (count median diameter [CMD]: 55 nm) and micro-C₆₀ particles (mass median aerodynamic diameter [MMAD]: 0.93 μm); the lung burden immediately after exposure to nano-C₆₀ particles was 41% greater than micro-C₆₀ particle exposure in male rats.¹¹ In the present studies, the difference in lung burden between the two particle sizes (nano-C₆₀ versus micro-C₆₀) was greater in mice than in rats; in mice, the lung burden immediately after exposure was approximately threefold greater following nano-C₆₀ exposure compared to following micro-C₆₀ exposure in both sexes. Of note, however, is that although steady-state lung burden was likely achieved in rats exposed to micro-C₆₀ particles at 2 mg/m³, this was not the case in rats exposed to nano-C₆₀ particles at the same exposure concentration. As such, the difference in lung concentrations and burdens between the two different particle sizes likely would have been greater in rats following longer exposure duration.

The differences in C₆₀ lung deposition between the two particle sizes at the same exposure concentration (2 mg/m³) were greater in mice than in rats, but the opposite pattern was observed in terms of clearance parameters between the species. In mice, the clearance rate constants (0.047, nano-C₆₀; 0.044 days⁻¹, micro-C₆₀; respectively) and half-lives (15 days, nano-C₆₀; 16 days, micro-C₆₀; respectively) were very similar. In rats, the C₆₀ clearance rate was about twofold greater (0.026 days) following micro-C₆₀ exposure than following nano-C₆₀ exposure (0.011 days⁻¹). Likewise, the half-life of C₆₀ following nano-C₆₀ exposure (61 days) was about twofold longer than the half-life of C₆₀ following micro-C₆₀ exposure (27 days). In a previous study, following a 10-day inhalation exposure in male rats, the half-lives of C₆₀ particles were very similar, 26 days compared to 29 days for nano-C₆₀ or micro-C₆₀ particles, respectively, at the same exposure concentration (2 mg/m³) for both particle sizes.¹¹ These observations, along with the current studies, highlight the effect of interspecies differences and exposure duration on particle elimination kinetics between the nanometer and micrometer particles. Interestingly, in rats, the half-life of C₆₀ particles following nano-C₆₀ exposure at 2 mg/cm³ was similar to the half-life of C₆₀ particles following micro-C₆₀ exposure at higher exposure concentrations (15 and 30 mg/cm³).

Shinohara et al.,⁸⁶ proposed a two-compartment model to describe the clearance of inhaled C₆₀ particles from the lung, with compartment one representing the alveolar surface and compartment two representing the lung interstitium or alveolar epithelial cells. According to this model, phagocytosis by alveolar macrophages is responsible for rapid clearance of C₆₀ from compartment one. C₆₀ particles that penetrate the epithelial barrier are slowly cleared by translocation to the lymph nodes. Important to note is that some fraction of the measured retained dose was likely also localized to compartments other than macrophages, like the interstitium or within epithelial cells. This suggests that 90% of instilled C₆₀ particles in the current study were

eliminated by rapid clearance from compartment one. Shinohara et al.⁸⁶ also used the two-compartment model to calculate the half-life of C₆₀ from data originally reported using a one-compartment model by Baker et al.¹¹ The half-life calculated by both models is similar, suggesting that the one-compartment and two-compartment models estimate similar clearance dynamics of C₆₀ from the lung.

Previous reports suggest the translocation of inhaled particles to extrapulmonary tissues is minimal (<1%).^{96; 97} In the current study, C₆₀ fullerenes were detected in bronchial lymph nodes, liver tissue, and spleen tissue following both nano- and micro-C₆₀ particle exposure, but most of the samples were below the estimated limit of quantitation (ELOQ). The ELOQ concentrations (0.06 to 0.61 mg C₆₀/g tissue) indicate that the C₆₀ burdens in liver and spleen tissues were less than 1% of the C₆₀ burdens measured in lung tissue (≥130 mg C₆₀/g tissue). C₆₀ was not detected in blood, brain, or kidney tissues following exposure to either particle size. In a similar study comparing the toxicity and tissue burden between nano- and micro-C₆₀ particle inhalation exposure for 10 days, C₆₀ fullerenes were not detected in blood samples for either particle size.¹¹ In another whole-body inhalation study, ¹³C elemental carbon nanoparticles (22 to 30 nm) were used to evaluate extrapulmonary translocation.⁹⁸ In this study, ¹³C was detected in liver tissue but not heart, brain, or kidney tissues. As noted by these authors, the extrapulmonary translocation of ¹³C could be the result of a combination of direct particle deposition into the lungs and translocation into the blood, and also translocation up into the gastrointestinal tract by the mucociliary escalator. In the present studies, C₆₀ was not detected in the blood, which suggests that either extrapulmonary translocation did not occur to the blood, C₆₀ concentrations in the blood were below the limit of detection, or C₆₀ was rapidly cleared from the blood.

The only extrapulmonary site of potential toxicity was the testis. A low incidence of germinal epithelium degeneration was observed in the testes of male rats in each micro-C₆₀ exposure group. Germinal epithelium degeneration also was observed in testes of three male rats exposed to 2 mg/m³ nano-C₆₀. Germinal epithelium degeneration was not seen in air controls in the study. This lesion is generally a relatively common background lesion in rats, so these occurrences alone do not indicate a treatment-related effect. Because sperm motility was slightly lower in male rats and mice in all micro-C₆₀ exposed groups, however, an effect of micro-C₆₀ on the rat testis cannot be ruled out.

The toxicity of C₆₀ fullerene nanoparticles and microparticles following nose-only inhalation was evaluated in the current studies. The results demonstrated that inhalation of C₆₀ at concentrations up to 2 mg/m³ (nano-C₆₀) and 30 mg/m³ (micro-C₆₀) did not affect systemic immune function in mice or rats, as indicated by a lack of effects on the antibody-forming cell (AFC) assay and minimal effects on the numbers of specific cell types in the spleen. The AFC assay, as described in Luster et al.,⁹⁹ is considered the most sensitive and predictive test of immune function, and, when combined with other immune assays (i.e., plaque-forming cell responses and surface marker analysis), is an accurate predictor (91%) of systemic immunotoxicity. In addition, NTP has historically used only female rodents for immunotoxicology studies, as females tend to be more immunologically responsive than their male counterparts, which allows for the detection of subtle immunological effects. Decreased spleen cell numbers were observed (on a mass basis) in mice exposed to 2 mg/m³ nano-C₆₀; however, the total spleen cell number of the control group of mice assigned (randomly) to the nano-C₆₀ study was higher than in any other group, including the control animals in the micro-C₆₀ test group, and thus the difference in total spleen cell numbers does not appear to be biologically relevant. Although minimal effects on observational

parameters (spleen cell numbers and phenotypes in mice) were noted, those effects were not supported by functional changes. Given the observed effects on the immune system were minimal, additional immunologic effects are unlikely to have been observed if male animals had been included in the immunotoxicity study.

In the current studies, inflammatory effects (histiocytic infiltration, pigmentation, and chronic inflammation) were noted in lung histopathology. These findings are consistent with previous reports of inflammation induced by C₆₀ particles.^{59; 6; 39} By comparison, the inflammatory response in the 15 mg/m³ and 30 mg/m³ micro-C₆₀ was more pronounced than that of the 2 mg/m³ nano-C₆₀, consistent with the more highly deposited mass of C₆₀ in the lung with the micro-C₆₀ at 15 and 30 mg/m³ compared to that observed in the nano-C₆₀ study at 2 mg/m³. Comparisons of the incidence and average severity results from evaluations of lung histopathology in both rats and mice indicated that the nano-C₆₀ test article initiated a greater inflammatory response compared to micro-C₆₀ test article at the same mass-based exposure concentration (2 mg/m³). The higher measured surface area/mass of the nano-C₆₀ particle suggests the inflammatory response is driven by a surface area dose. As noted by Sayers et al.⁶³ using the data from this study, the surface areas of the exposure atmospheres for the 2 mg/m³ nano-C₆₀ (0.112 m²/m³) was within the range of the calculated surface areas of the 15 mg/m³ (0.084 m²/m³) and 30 mg/m³ (0.167 m²/m³) micro-C₆₀ exposure atmospheres. Estimates of the surface area of the deposited C₆₀, made by Sayers et al.⁶⁴ using the lung burden data and surface areas of the respective C₆₀ particles, indicated that at the 2 mg/m³ the estimated surface area of deposited C₆₀ in the lung was higher for nano-C₆₀ exposed animals as compared to animals exposed to micro-C₆₀ at the 15 mg/m³ and 30 mg/m³. This implies that the inflammatory response is not driven by the surface area. That the estimates made by Sayers et al. of the surface area of the deposited C₆₀ in the lung assumes lack of aggregation *in vivo*, however, should be noted and thus might be inaccurate and likely overestimate the deposited surface area of the nano-C₆₀.

Significant, concentration-related increases in MCP-1 (rats) and MIP-1 α (mice) following C₆₀ inhalation were observed in the present studies. These data are consistent with a study demonstrating that C₆₀ inhalation (0.2 mg/m³) for 4 weeks increased the expression of genes associated with MCP-1 and MIP-1 α .²⁷ Interestingly, differential effects were observed in BALF levels of both MIP-1 α and MCP-1 between animals exposed to nano-C₆₀ and micro-C₆₀ that could not be accounted for by using surface area as the basis of exposure. MCP-1, also known as chemokine (C-C motif) ligand 2 (CCL2), is a potent chemoattractant for monocytes.¹⁰⁰ However, MCP-1 has also been shown to have chemoattractant effects on other immune cells, including T cells¹⁰¹ and NK cells.¹⁰² MIP-1 α , another chemokine, can be secreted by a wide variety of immune cell types, including monocytes and macrophages, T and B lymphocytes, NK cells, dendritic cells, neutrophils, and eosinophils.¹⁰³ Increased production of MIP-1 α is associated with inflammation due to its chemotactic effects on several cell types, including monocytes, T cells, neutrophils, eosinophils, basophils, dendritic cells, and NK cells.

The use of CD11b and CD163 in these studies for delineating cell types in the BALF did not allow distinct cell types to be determined, as both the double-positive and double-negative cell populations could contain numerous cell types. Most likely is that the double-negative (i.e., CD163⁻CD11b⁻) population of rat BALF cells in the present studies consisted primarily of alveolar macrophages (AM), in addition to a smaller population of other cell types, including T and B lymphocytes, NK cells, eosinophils, and mast cells, which can all be recovered from

BALF in low numbers.¹⁰⁴ Cells staining positive for both CD163 and CD11b were most likely a combination of resident airway macrophages, which have been identified throughout the respiratory tract,¹⁰⁵ and macrophages recruited to the lung. Cells staining positive for CD11b only (i.e., CD163⁻CD11b⁺) were neutrophils and other myeloid cells. Significant increases in the percentage and absolute numbers of CD163⁻CD11b⁺ neutrophils were observed in rats exposed to 30 mg/m³ micro-C₆₀, which correlated with a significant increase in neutrophils in rats in the same exposure group identified by BALF differential cell counting. Unfortunately, cellular origin is not determined for macrophages identified by differential cell counting.

These studies demonstrated that the immune effects of C₆₀ fullerene inhalation in rats and mice were limited primarily to the lung, where dramatically increased levels of the monocyte/macrophage chemotactic and inflammatory cytokines MCP-1 and MIP-1 α were detected in BALF. Increases in MCP-1 and MIP-1 α have been linked to the formation of pulmonary fibrosis in rodents and humans.^{106; 103; 107} In fact, the absence of MCP-1 in CCL2^{-/-} mice conferred protection against bleomycin-induced pulmonary fibrosis.¹⁰⁸ In humans, pneumoconiosis, or particle-induced pulmonary fibrosis, has been documented in several cases of occupational exposure to particulates, although no human cases of pulmonary fibrosis directly linked to nanomaterial exposure have been documented.¹⁰⁹ Nanomaterial-mediated pulmonary fibrosis, however, has been observed in Sprague Dawley rats as soon as 21 days and persisting for at least 60 days following a single intratracheal instillation of multiwalled carbon nanotubes.^{110; 111} Further, that nanoparticles are the fraction of inhaled particulates that contribute most significantly to pulmonary fibrosis in humans has been suggested.¹⁰⁹

In conclusion, the lung deposition of nano-C₆₀ particles was greater than lung deposition of micro-C₆₀ particles in both rats and mice following exposure to the same mass-based exposure concentration for both particle sizes (2 mg/m³). Although the clearance kinetics were similar between nano- and micro-C₆₀ particles in male mice, in male rats, the elimination rate of nano-C₆₀ particles was about half that of micro-C₆₀ particles. On an estimated surface-area basis, exposure to 2 mg/m³ nano-C₆₀ resulted in a similar lung burden as exposure to 30 mg/m³ of micro-C₆₀. This was also the case for 0.5 mg/m³ nano-C₆₀ and 15 mg/m³ micro-C₆₀. The data from these studies provide comparative information regarding how particle size influences the deposition and clearance of C₆₀ fullerenes.

The mild pulmonary inflammation observed in rats and mice exposed to fullerenes is consistent with the response observed following inhalation of other nanoparticles. Pulmonary inflammation is the most commonly reported effect of inhaled nanoparticles.¹¹² Lung inflammatory responses were observed, primarily at the higher exposure concentrations. Inflammatory effects of nano-C₆₀ exposure were, in general, more severe than micro-C₆₀ exposure when comparing both particle sizes at the same mass-based exposure concentration.

References

1. Hirsch A. The era of carbon allotropes. *Nat Mater.* 2010; 9:868-871. <http://dx.doi.org/10.1038/nmat2885>
2. Kroto HW, Allaf AW, Balm SP. C₆₀: Buckminsterfullerene. *Chem Rev.* 1991; 91:1213-1235. <http://dx.doi.org/10.1021/cr00006a005>
3. Terrones H, Mackay AL. The geometry of hypothetical curved graphite structures. *Carbon.* 1992; 30:1251-1260. [http://dx.doi.org/10.1016/0008-6223\(92\)90066-6](http://dx.doi.org/10.1016/0008-6223(92)90066-6)
4. National Center for Biotechnology Information (NCBI). PubChem Open Chemistry Database. CID = 123591, Fullerene C₆₀. Bethesda, MD: National Institutes of Health, National Library of Medicine; 2017. <https://pubchem.ncbi.nlm.nih.gov/compound/123591#Section=Top>
5. Sigma Aldrich. Safety Data Sheet: Fullerene-C₆₀, Product Number 379646. 2017. www.sigmaaldrich.com
6. Johnston HJ, Hutchinson GR, Christensen FM, Aschberger K, Stone V. The biological mechanisms and physiochemical characteristics responsible for driving fullerene toxicity. *Toxicol Sci.* 2010; 114:162-182. <http://dx.doi.org/10.1093/toxsci/kfp265>
7. Bleeker EAJ, de Jong WH, Geertsma RE, Groenewold M, Heugens EHW, Koers-Jacquemijns M, van de Meent D, Popma JR, Rietveld AG, Wijnhoven SWP et al. Considerations on the EU definition of a nanomaterial: Science to support policy making. *Regul Toxicol Pharm.* 2013; 65:119-125. <http://dx.doi.org/10.1016/j.yrtph.2012.11.007>
8. European Commission. Commission recommendation of 18 October 2011 on the definition of nanomaterial (2011/696/EU). *Off J Eur Union.* 2011; L275:38-40.
9. Fortner JD, Lyon DY, Sayes CM, Boyd AM, Falkner JC, Hotze EM, Alemany LB, Tao YJ, Guo W, Ausman KD et al. C₆₀ in water: Nanocrystal formation and microbial response. *Environ Sci Technol.* 2005; 39:4307-4316. <http://dx.doi.org/10.1021/es048099n>
10. Materials Electrochemical Research Corporation. MER fullerene products. 2017. <http://www.mercorp.com/fullbro.pdf>
11. Baker GL, Gupta A, Clark ML, Valenzuela BR, Staska LM, Harbo SJ, Pierce JT, Dill JA. Inhalation toxicity and lung toxicokinetics of C₆₀ fullerene nanoparticles and microparticles. *Toxicol Sci.* 2008; 101:122-131. <http://dx.doi.org/10.1093/toxsci/kfm243>
12. Deguchi S, Alargova RG, Tsujii K. Stable dispersions of fullerenes, C₆₀ and C₇₀, in water. Preparation and characterization. *Langmuir.* 2001; 17:6013-6017. <http://dx.doi.org/10.1021/la010651o>
13. Gharbi N, Pressac M, Hadchouel M, Szwarc H, Wilson SR, Moussa F. [60]Fullerene is a powerful antioxidant in vivo with no acute or subacute toxicity. *Nano Lett.* 2005; 5:2578-2585. <http://dx.doi.org/10.1021/nl051866b>

14. Scott LT, Boorum MM, McMahon BJ, Hagen S, Mack J, Blank J, Wegner H, de Meijere A. A rational chemical synthesis of C₆₀. *Science*. 2002; 295:1500-1503. <http://dx.doi.org/10.1126/science.1068427>
15. Hendren CO, Mesnard X, Dröge J, Wiesner MR. Estimating production data for five engineered nanomaterials as a basis for exposure assessment. *Environ Sci Technol*. 2011; 45:2562-2569. <http://dx.doi.org/10.1021/es103300g>
16. Murr LE, Esquivel EV, Bang JJ, de la Rosa G, Gardea-Torresdey JL. Chemistry and nanoparticulate compositions of a 10,000 year-old ice core melt water. *Water Res*. 2004; 38:4282-4296. <http://dx.doi.org/10.1016/j.watres.2004.08.010>
17. Wang Z, Xuepeng L, Wenmin W, Xunjiang X, Tang ZC, Huang RB, Zheng LS. Fullerenes in the fossil of dinosaur egg. *Fullerene Sci Technol*. 1998; 6:715-720. <http://dx.doi.org/10.1080/10641229809350232>
18. Food and Drug Administration (FDA). Guidance for industry: Safety of nanomaterials in cosmetic products. United States Department of Health and Human Services, Food and Drug Administration, Center for Food Safety and Applied Nutrition; 2014.
19. Gwinn MR, Vallyathan V. Nanoparticles: Health effects – pros and cons. *Environ Health Perspect*. 2006; 114:1818-1825. <http://dx.doi.org/10.1289/ehp.8871>
20. Nel A, Xia T, Mädler L, Li N. Toxic potential of materials at the nanolevel. *Science*. 2006; 311:622-627. <http://dx.doi.org/10.1126/science.1114397>
21. Bonner JC. Nanoparticles as a potential cause of pleural and interstitial lung disease. *Proc Am Thorac Soc*. 2010; 7:138-141. <http://dx.doi.org/10.1513/pats.200907-061RM>
22. Lockman PR, Koziara JM, Mumper RJ, Allen DD. Nanoparticle surface charges alter blood brain barrier integrity and permeability. *J Drug Target*. 2008; 12:635-641. <http://dx.doi.org/10.1080/10611860400015936>
23. Halford B. Fullerene for the face. *Chem Eng News*. 2006; 84:47. <http://dx.doi.org/10.1021/cen-v084n013.p047>
24. Singh R, and Lillard JW, Jr. Nanoparticle-based targeted drug delivery. *Exp Mol Pathol*. 2009; 86:215-223. <http://dx.doi.org/10.1016/j.yexmp.2008.12.004>
25. Benn TM, Westorhoff P, Herckes P. Detection of fullerene (C₆₀ and C₇₀) in commercial cosmetics. *Environ Pollut*. 2011; 159:1334-1342. <http://dx.doi.org/10.1016/j.envpol.2011.01.018>
26. Kato S, Taira H, Aoshima H, Saitoh Y, Miwa N. Clinical evaluation of fullerene-C₆₀ dissolved in squalene for anti-wrinkle cosmetics. *J Nanosci Nanotechnol*. 2010; 10:6769-6774. <http://dx.doi.org/10.1166/jnn.2010.3053>
27. Fujita K, Morimoto Y, Ogami A, Myojyo T, Tanaka I, Shimada M, Wang WN, Endoh S, Uchida K, Nakazato T et al. Gene expression profiles in rat lung after inhalation exposure to C₆₀ fullerene particles. *Toxicology*. 2009; 258:47-55. <http://dx.doi.org/10.1016/j.tox.2009.01.005>

28. Oberdörster G, Oberdörster E, Oberdörster J. Nanotechnology: An emerging discipline evolving from studies of ultrafine particles. *Environ Health Perspect.* 2005; 113:823-838. <http://dx.doi.org/10.1289/ehp.7339>
29. Utsunomiya S, Jensen KA, Keeler GJ, Ewing RC. Uraninite and fullerene in atmospheric particulates. *Environ Sci Technol.* 2002; 36:4943-4947. <http://dx.doi.org/10.1021/es025872a>
30. Mercer RR, Scabilloni J, Wang L, Kisin E, Murray AR, Schwegler-Berry D, Shvedova AA, Castranova V. Alteration of deposition pattern and pulmonary response as a result of improved dispersion of aspirated single-walled carbon nanotubes in a mouse model. *Am J Physiol Lung Cell Mol Physiol.* 2008; 294:L87-L97. <http://dx.doi.org/10.1152/ajplung.00186.2007>
31. Oberdörster G, Ferin J, Lehnert BE. Correlation between particle size, in vivo particle persistence, and lung injury. *Environ Health Perspect.* 1994; 102:173-179.
32. Oberdörster G, Ferin J, Gelein R, Soderholm SC, Finkelstein J. Role of the alveolar macrophage in lung injury: Studies with ultra-fine particles. *Environ Health Perspect.* 1992; 97:193-199.
33. Ferin J, Oberdörster G, Penney DP, Soderholm SC, Glein RPHC. Increased pulmonary toxicity of ultrafine particles? I. Particle clearance, translocation, and morphology. *J Aerosol Sci.* 1990; 21:381-384. [http://dx.doi.org/10.1016/0021-8502\(90\)90064-5](http://dx.doi.org/10.1016/0021-8502(90)90064-5)
34. Harmsen AG, Muggenburg BA, Snipes MB, Bice DE. The role of macrophages in particle translocation from lungs to lymph nodes. *Science.* 1985; 230:1277-1280. <http://dx.doi.org/10.1126/science.4071052>
35. Mercer RR, Scabilloni JF, Hubbs AF, Wang L, Battelli L, McKinney W, Castranova V, Porter DW. Extrapulmonary transport of MWCNT following inhalation exposure. *Part Fibre Toxicol.* 2013; 10:38-51. <http://dx.doi.org/10.1186/1743-8977-10-38>
36. Shipkowski KA, Sanders JM, McDonald JD, Walker NJ, Waidyanatha S. Disposition of fullerene C₆₀ in rats following intratracheal or intravenous administration. *Xenobiotica.* 2019; 49(9):1078-1085. <http://dx.doi.org/10.1080/00498254.2018.1528646>
37. Ema M, Kobayashi N, Naya M, Hanai S, Nakanishi J. Reproductive and developmental toxicity studies of manufactured nanomaterials. *Reprod Toxicol.* 2010; 30:343-352. <http://dx.doi.org/10.1016/j.reprotox.2010.06.002>
38. Sumner SC, Fennell TR, Snyder RW, Taylor GF, Lewin AH. Distribution of carbon-14 labeled C₆₀ ([¹⁴C]C₆₀) in the pregnant and in the lactating dam and the effect of C₆₀ exposure on the biochemical profile of urine. *J Appl Toxicol.* 2010; 30:354-360.
39. Park EJ, Kim H, Kim Y, Yi J, Choi K, Park K. Carbon fullerenes (C₆₀s) can induce inflammatory responses in the lung of mice. *Toxicol Appl Pharmacol.* 2010; 244:226-233. <http://dx.doi.org/10.1016/j.taap.2009.12.036>
40. Sayes CM, Marchione AA, Reed KL, Warheit DB. Comparative pulmonary toxicity assessments of C₆₀ water suspensions in rats: Few differences in fullerene toxicity in vivo in contrast to in vitro profiles. *Nano Lett.* 2007; 7:2399-2406. <http://dx.doi.org/10.1021/nl0710710>

41. Roursgaard M, Poulsen SS, Kepley CL, Hammer M, Nielsen GD, Larsen ST. Polyhydroxylated C₆₀ fullerene (fullerenol) attenuates neutrophilic lung inflammation in mice. *Basic Clin Pharmacol Toxicol*. 2008; 103:386-388. <http://dx.doi.org/10.1111/j.1742-7843.2008.00315.x>
42. Chen HHC, Yu C, Ueng TH, Chen S, Chen BJ, Huang KJ, Chiang LY. Acute and subacute toxicity study of water-soluble polyalkylsulfonated C₆₀ in rats. *Toxicol Pathol*. 1998; 26:143-151. <http://dx.doi.org/10.1177/019262339802600117>
43. Moussa F, Trivin F, Céolin R, Hadchouel M, Sizarert PY, Greungny V, Fabre C, Rassat A, Szwarc H. Early effects of C₆₀ administration in Swiss mice: A preliminary account for in vivo C₆₀ toxicity. *Fullerene Sci Technol*. 1996; 4:21-29. <http://dx.doi.org/10.1080/10641229608001534>
44. Mori T, Takada H, Ito S, Matsubayashi K, Miwa N, Sawaguchi T. Preclinical studies on safety of fullerene upon acute oral administration and evaluation for no mutagenesis. *Toxicology*. 2006; 225:48-54. <http://dx.doi.org/10.1016/j.tox.2006.05.001>
45. Baati T, Bourasset F, Gharbi N, Njim L, Abderrabba M, Kerkeni A, Szwarc H, Moussa F. The prolongation of the lifespan of rats by repeated oral administration of [60] fullerene. *Biomaterials*. 2012; 33:4936-4946. <http://dx.doi.org/10.1016/j.biomaterials.2012.03.036>
46. Patri A, Dobrovolskaia MA, Stern ST, McNeil SE. Preclinical characterization of engineered nanoparticles intended for cancer therapeutics. *Nanotechnology for Cancer Therapy*. Boca Raton, FL: CRC Press, Taylor & Francis Group; 2007. p. 105-137.
47. Smith MJ, McLoughlin CE, White KL, Jr, Germolec DR. Evaluating the adverse effects of nanomaterials on the immune system with animal models In: Dobrovolskaia MA, McNeil SE, editors. *Handbook of Immunological Properties of Engineered Nanomaterials*. Hackensack, NJ: World Scientific Publishing Co.; 2013. p. 639-670. http://dx.doi.org/10.1142/9789814390262_0020
48. Yamashita K, Sakai M, Takemoto N, Tsukimoto M, Uchida K, Yajima H, Oshio S, Takeda K, Kojima S. Attenuation of delayed-type hypersensitivity by fullerene treatment. *Toxicology*. 2009; 261:19-24. <http://dx.doi.org/10.1016/j.tox.2009.04.034>
49. Zogovic NS, Nikolic NS, Vranjes-Djuric SD, Harhaji LM, Vucicevic LM, Janjetovic KD, Misirkic MS, Todorovic-Markovic BM, Markovic ZM, Milonjic SK et al. Opposite effect of nanocrystalline fullerene (C₆₀) on tumour cell growth in vitro and in vivo and a possible role of immunosuppression in the cancer-promoting activity of C₆₀. *Biomaterials*. 2009; 30:6940-6946. <http://dx.doi.org/10.1016/j.biomaterials.2009.09.007>
50. Chen BX, Wilson SR, Das M, Coughlin DJ, Erlanger BF. Antigenicity of fullerenes: Antibodies specific for fullerenes and their characteristics. *Proc Natl Acad Sci USA*. 1998; 95:10,809-810,813. <https://www.pnas.org/content/95/18/10809.long>
51. Tsuchiya T, Oguri I, Yamakoshi YN, Miyata N. Novel harmful effects of [60]fullerene on mouse embryos in vitro and in vivo. *FEBS Lett*. 1996; 393:139-145. [http://dx.doi.org/10.1016/0014-5793\(96\)00812-5](http://dx.doi.org/10.1016/0014-5793(96)00812-5)

52. Zhu X, Zhu L, Li Y, Duan Z, Chen W, Alvarez PJJ. Developmental toxicity in zebrafish (*Danio rerio*) embryos after exposure to manufactured nanomaterials: Buckminsterfullerene aggregates (nC₆₀) and fullerol. *Environ Toxicol Chem.* 2007; 26:976-979. <http://dx.doi.org/10.1897/06-583.1>
53. Nelson MA, Domann FE, Bowden GT, Hooser SB, Fernando Q, Carter DE. Effects of acute and subchronic exposure of topically applied fullerene extracts on the mouse skin. *Toxicol Ind Health.* 1993; 9:623-630. <http://dx.doi.org/10.1177/074823379300900405>
54. Roller M. In vitro genotoxicity data of nanomaterials compared to carcinogenic potency of inorganic substances after inhalational exposure. *Mutat Res.* 2011; 727:72-85. <http://dx.doi.org/10.1016/j.mrrev.2011.03.002>
55. Matsuda S, Matsui S, Shimizu Y, Matsuda T. Genotoxicity of colloidal fullerene C₆₀. *Environ Sci Technol.* 2011; 45:4133-4138. <http://dx.doi.org/10.1021/es1036942>
56. Shinohara N, Matsumoto K, Endoh S, Maru J, Nakanishi J. In vitro and in vivo genotoxicity tests on fullerene C₆₀ particles. *Toxicol Lett.* 2009; 191:289-296. <http://dx.doi.org/10.1016/j.toxlet.2009.09.012>
57. Totsuka Y, Higuchi T, Imai T, Nishikawa A, Nohmi T, Kato T, Masuda S, Kinoshita N, Hiyoshi K, Ogo S et al. Genotoxicity of nano/microparticles in in vitro micronuclei, in vivo comet and mutations assay systems. Part Fibre Toxicol. 2009; 6:23. <http://dx.doi.org/10.1186/1743-8977-6-23>
58. Jacobsen NR, Pojana G, White P, Møller P, Cohn CA, Korsholm KS, Vogel U, Marcomini A, Loft S, Wallin H. Genotoxicity, cytotoxicity, and reactive oxygen species induced by single-walled carbon nanotubes and C (60) fullerenes in the FE1-MutaMouse™ lung epithelial cells. *Environ Mol Mutagen.* 2008; 49:476-487. <http://dx.doi.org/10.1002/em.20406>
59. Ema M, Tanaka J, Kobayashi NN, Endoh S, Maru J, Hosoi M, Nagai M, Nakajima M, Hayashi M, Nakanishi J. Genotoxicity evaluation of fullerene C₆₀ nanoparticles in a comet assay using lung cells of intratracheally instilled rats. *Regul Toxicol Pharmacol.* 2012; 62:419-424. <http://dx.doi.org/10.1016/j.yrtph.2012.01.003>
60. Jacobsen NR, Møller P, Jensen KA, Vogel U, Ladefoged O, Loft S, Wallin H. Lung inflammation and genotoxicity following pulmonary exposure to nanoparticles in ApoE -/- mice. Part Fibre Toxicol. 2009; 6:2. <http://dx.doi.org/10.1186/1743-8977-6-2>
61. Folkmann JK, Risom L, Jacobsen NR, Wallin H, Loft S, Møller P. Oxidatively damaged DNA in rats exposed by oral gavage to C₆₀ fullerenes and single-walled carbon nanotubes. *Environ Health Perspect.* 2009; 117:703-708. <http://dx.doi.org/10.1289/ehp.11922>
62. Aoshima H, Yamana S, Nakamura S, Mashino T. Biological safety of water-soluble fullerenes evaluated using tests for genotoxicity, phototoxicity, and pro-oxidant activity. *J Toxicol Sci.* 2010; 35:401-409. <http://dx.doi.org/10.2131/jts.35.401>
63. Sayers BC, Germolec DR, Walker NJ, Shipkowski KA, Stout MD, Cesta MF, Roycroft JH, White KL, Baker GL, Dill JA et al. Respiratory toxicity and immunotoxicity evaluations of microparticle and nanoparticle C₆₀ fullerene aggregates in mice and rats following nose-only

inhalation for 13 weeks. *Nanotoxicology*. 2016; 10:1458-1468.

<http://dx.doi.org/10.1080/17435390.2016.1235737>

64. Sayers BC, Walker NJ, Roycroft JH, Germolec DR, Baker GL, Clark ML, Hayden BK, DeFord H, Dill JA, Gupta A et al. Lung deposition and clearance of microparticle and nanoparticle C60 fullerene aggregated in B6C3F1 mice and Wistar Han rats following nose-only inhalation for 13 weeks. *Toxicology*. 2016; 339:87-96.

<http://dx.doi.org/10.1016/j.tox.2015.11.003>

65. Nakamoto K, McKinney MA. Application of the correlation method to vibrational spectra of C60 and other fullerenes: Predicting the number of IR-and Raman-active bands. *J Chem Educ*. 2000; 77:775-780. <http://dx.doi.org/10.1021/ed077p775>

66. Hill MA, Watson CR, Moss OR. NEWCAS—An interactive computer program for particle size analysis. Richland, WA: Pacific Northwest Laboratory; 1977. PNL-2405, UC-32.

67. Brecher G, Schneiderman M. Time saving device for the counting of reticulocytes. *Am J Clin Pathol*. 1950; 20:2079-2084. http://dx.doi.org/10.1093/ajcp/20.11_ts.1079

68. National Toxicology Program (NTP). Specifications for the conduct of studies to evaluate the reproductive and developmental toxicity of chemical, biological and physical agents in laboratory animals for the National Toxicology Program (NTP). Research Triangle Park, NC: U.S. Department of Health and Human Services, National Institutes of Health, National Toxicology Program; 2011.

https://ntp.niehs.nih.gov/ntp/test_info/finalntp_reprospecsmay2011_508.pdf

69. Maronpot RR, Boorman GA. Interpretation of rodent hepatocellular proliferative alterations and hepatocellular tumors in chemical safety assessment. *Toxicol Pathol*. 1982; 10:71-80.

<http://dx.doi.org/10.1177/019262338201000210>

70. Boorman GA, Montgomery CA, Jr., Eustis SL, Wolfe MJ, McConnell EE, Hardisty JF. Quality assurance in pathology for rodent carcinogenicity studies. *Handbook of Carcinogen Testing*. Park Ridge, NJ: Noyes Publications; 1985. p. 345-357.

71. Gart JJ, Chu KC, Tarone RE. Statistical issues in interpretation of chronic bioassay tests for carcinogenicity. *JNCI*. 1979; 62:957-974.

72. Dunnett CW. A multiple comparison procedure for comparing several treatments with a control. *J Am Stat Assoc*. 1955; 50:1096-1121.

<http://dx.doi.org/10.1080/01621459.1955.10501294>

73. Williams DA. A test for differences between treatment means when several dose levels are compared with a zero dose control. *Biometrics*. 1971; 27:103-117.

<http://dx.doi.org/10.2307/2528930>

74. Williams DA. The comparison of several dose levels with a zero dose control. *Biometrics*. 1972; 28:519-531. <http://dx.doi.org/10.2307/2556164>

75. Shirley E. A non-parametric equivalent of Williams' test for contrasting increasing dose levels of a treatment. *Biometrics*. 1977; 33:386-389. <http://dx.doi.org/10.2307/2529789>

76. Williams DA. A note on Shirley's nonparametric test for comparing several dose levels with a zero-dose control. *Biometrics*. 1986; 42:183-186. <http://dx.doi.org/10.2307/2531254>
77. Dunn OJ. Multiple comparisons using rank sums. *Technometrics*. 1964; 6:241-252. <http://dx.doi.org/10.1080/00401706.1964.10490181>
78. Jonckheere AR. A distribution-free k-sample test against ordered alternatives. *Biometrika*. 1954; 41:133-145. <http://dx.doi.org/10.1093/biomet/41.1-2.133>
79. Dixon WJ, Massey FJ, Jr. Introduction to statistical analysis. New York: McGraw Hill Book Company, Inc.; 1957. <http://dx.doi.org/10.2307/2332898>
80. Girard DM, Sager DB. The use of Markov chains to detect subtle variation in reproductive cycling. *Biometrics*. 1987; 43:225-234. <http://dx.doi.org/10.2307/2531963>
81. Code of Federal Regulations (CFR). 21(Part 58).
82. Witt KL, Livanos E, Kissling GE, Torous DK, Caspary W, Tice RR, Recio L. Comparison of flow cytometry and microscopy-based methods for measuring micronucleated reticulocyte frequencies in rodents treated with nongenotoxic and genotoxic chemicals. *Mutat Res*. 2008; 649:101-113. <http://dx.doi.org/10.1016/j.mrgentox.2007.08.004>
83. Kissling GE, Dertinger SD, Hayashi M, MacGregor JT. Sensitivity of the erythrocyte micronucleus assay: Dependence on number of cells scored and inter-animal variability. *Mutat Res*. 2007; 634:235-240. <http://dx.doi.org/10.1016/j.mrgentox.2007.07.010>
84. National Toxicology Program (NTP). TOX-87: Pathology tables, survival and growth curves from NTP short-term studies. Research Triangle Park, NC; 2020. <https://doi.org/10.22427/NTP-DATA-TOX-87>
85. Yamawaki H, Iwai N. Cytotoxicity of water-soluble fullerene in vascular endothelial cells. *Am J Physiol Cell Physiol*. 2006; 290:C1495-C1502. <http://dx.doi.org/10.1152/ajpcell.00481.2005>
86. Shinohara N, Nakazato T, Tamura M, Endoh S, Fukui H, Morimoto Y, Myojo T, Shimada M, Yamamoto K, Tao H et al. Clearance kinetics of fullerene C₆₀ nanoparticles from rat lungs after intratracheal C₆₀ instillation and inhalation C₆₀ exposure. *Toxicol Sci*. 2010; 118:564-573. <http://dx.doi.org/10.1093/toxsci/kfq288>
87. Oberdörster G, Ferin J, Finkelstein G, Wade P, Corson N. Increased pulmonary toxicity of ultrafine particles? II. Lung lavage studies. *J Aerosol Sci*. 1990; 21:384-387. [http://dx.doi.org/10.1016/0021-8502\(90\)90065-6](http://dx.doi.org/10.1016/0021-8502(90)90065-6)
88. Oberdörster G. Toxicology of ultrafine particles: In vivo studies. *Philosoph Trans R Soc*. 2000; A 358:2719-2740.
89. Maynard AD, Warheit DB, Philbert MA. The new toxicology of sophisticated materials: Nanotoxicology and beyond. *Toxicol Sci*. 2011; 120:S109-S129. <http://dx.doi.org/10.1093/toxsci/kfq372>

90. Morrow PE. Possible mechanisms to explain dust overloading of the lungs. *Fundam Appl Toxicol.* 1988; 10:369-384. [http://dx.doi.org/10.1016/0272-0590\(88\)90284-9](http://dx.doi.org/10.1016/0272-0590(88)90284-9)
91. Morrow PE. Dust overloading of the lungs: Update and appraisal. *Toxicol Appl Pharmacol.* 1992; 113:1-12. [http://dx.doi.org/10.1016/0041-008X\(92\)90002-A](http://dx.doi.org/10.1016/0041-008X(92)90002-A)
92. Olin SS. The relevance of the rat lung response to particle overload for human risk assessment: A workshop consensus report. *Inhal Toxicol.* 2000; 12:1-17. <http://dx.doi.org/10.1080/08958370050029725>
93. Masse R, Fritsch P, Nolike D, LaFuma J, Chretien J. Cytokinetic study of alveolar macrophage renewal in rats. *Pulmonary Macrophages and Epithelial Cells.* Washington, D.C.: Energy Research and Development Administration, Technical Information Center; 1977. p. 106-114.
94. Tran CL, Buchanan D, Cullen RT, Searl A, Jones AD, Donaldson K. Inhalation of poorly soluble particles. II. Influence of particle surface area on inflammation and clearance. *Inhal Toxicol.* 2000; 12:1113-1126. <http://dx.doi.org/10.1080/08958370050166796>
95. Oberdörster G. Lung particle overload: Implications for occupational exposures to particles. *Regul Toxicol Pharmacol.* 1995; 21:123-135. <http://dx.doi.org/10.1006/rtp.1995.1017>
96. Kreyling WG, Semmler M, Erbe F, Mayer P, Takenaka S, Schulz H, Oberdörster G, Ziesenis A. Translocation of ultrafine insoluble iridium particles from lung epithelium to extrapulmonary organs is size dependent but very low. *J Toxicol Environ Health A.* 2002; 65:1513-1530. <http://dx.doi.org/10.1080/00984100290071649>
97. Möller W, Felten K, Sommerer K, Scheuch G, Meyer G, Meyer P, Häussinger K, Kreyling WG. Deposition, retention, and translocation of ultrafine particles from the central airways and lung periphery. *Am J Respir Crit Care Med.* 2008; 177:426-432. <http://dx.doi.org/10.1164/rccm.200602-301OC>
98. Oberdörster G, Sharp Z, Atudorei V, Elder A, Gelein R, Lunts A, Kreyling W, Cox C. Extrapulmonary translocation of ultrafine carbon particles following whole-body inhalation exposure of rats. *J Toxicol Environ Health.* 2002; A 65:1531-1543. <http://dx.doi.org/10.1080/00984100290071658>
99. Luster MI, Portier C, Pait DG, White KL, Jr, Gennings C, Munson AE, Rosenthal GJ. Risk assessment in immunotoxicology. I. Sensitivity and predictability of immune tests. *Fundam Appl Toxicol.* 1992; 18:200-210. [http://dx.doi.org/10.1016/0272-0590\(92\)90047-L](http://dx.doi.org/10.1016/0272-0590(92)90047-L)
100. Uguccioni M, D'Apuzzo M, Loetscher M, Dewald B, Baggiolini M. Actions of the chemotactic cytokines MCP-1, MCP-2, MCP-3, RANTES, MIP-1 alpha and MIP-1 beta on human monocytes. *Eur J Immunol.* 1995; 25:64-68. <http://dx.doi.org/10.1002/eji.1830250113>
101. Loetscher P, Seitz M, Clark-Lewis I, Baggiolini M, Moser B. Monocyte chemotactic protein MCP-1, MCP-2, and MCP-3 are major attractants for human CD4⁺ and CD⁺ T lymphocytes. *FASEB J.* 1994; 8:1055-1060. <http://dx.doi.org/10.1096/fasebj.8.13.7926371>

102. Loetscher P, Seitz M, Clark-Lewis I, Baggiolini M, Moser B. Activation of NK cells by CC chemokines. Chemotaxis, CA²⁺ mobilization, and enzyme release. *J Immunol*. 1996; 156:322-327.
103. Menten P, Wuyts A, Van Damme J. Macrophage inflammatory protein-1. Cytokine Growth Factor Rev. 2002; 13:455-481. [http://dx.doi.org/10.1016/S1359-6101\(02\)00045-X](http://dx.doi.org/10.1016/S1359-6101(02)00045-X)
104. Dörger M, Münzing S, Allmeling AM, Messmer K, Krombach F. Phenotypic and functional differences between rat alveolar, pleural, and peritoneal macrophages. *Exp Lung Res*. 2001; 27:65-76. <http://dx.doi.org/10.1080/019021401459770>
105. Sibille Y, Reynolds HY. Macrophages and polymorphonuclear neutrophils in lung defense and injury. *Am Rev Respir Dis*. 1990; 141:471-501. <http://dx.doi.org/10.1164/ajrccm/141.2.471>
106. Hasegawa M, Sato S, Takehara K. Augmented production of chemokines (monocyte chemoattractant protein-1 (MCP-1), macrophage inflammatory protein-1alpha (MIP-1alpha) and MIP-1beta) in patients with systemic sclerosis: MCP-1 and MIP-1alpha may be involved in the development of pulmonary fibrosis. *Clin Exp Immunol*. 1999; 117:159-165. <http://dx.doi.org/10.1046/j.1365-2249.1999.00929.x>
107. Smith RE, Strieter RM, Zhang K, Phan SH, Standiford TJ, Lukacs NW, Kunkel SL. A role for C-C chemokines in fibrotic lung disease. *J Leukoc Biol*. 1995; 57:782-787. <http://dx.doi.org/10.1002/jlb.57.5.782>
108. Baran CP, Opalek JM, McMaken S, Newland CA, O'Brien JM, Jr., Hunter MG, Bringardner BD, Monick MM, Brigstock DR, Stromberg PC et al. Important roles for macrophage colony-stimulating factor, CC chemokine ligand 2, and mononuclear phagocytes in the pathogenesis of pulmonary fibrosis. *Am J Respir Crit Care Med*. 2007; 176(78-89). <http://dx.doi.org/10.1164/rccm.200609-1279OC>
109. Byrne JD, Baugh JA. The significance of nanoparticles in particle-induced pulmonary fibrosis. *Mcgill J Med*. 2008; 11:43-50.
110. Cesta MF, Ryman-Rasmussen JP, Wallace DG, Masinde T, Hurlburt G, Taylor AJ, Bonner JC. Bacterial lipopolysaccharide enhances PDGF signaling and pulmonary fibrosis in rats exposed to carbon nanotubes. *Am J Respir Cell Mol Biol*. 2010; 43:142-151. <http://dx.doi.org/10.1165/rcmb.2009-0113OC>
111. Muller J, Huaux F, Moreau N, Mission P, Heilier JF, Delos M, Aras M, Fonseca A, Nagy JB, Lison D. Respiratory toxicity of multi-wall carbon nanotubes. *Toxicol Appl Pharmacol*. 2005; 207:221-231. <http://dx.doi.org/10.1016/j.taap.2005.01.008>
112. Braakhuis HM, Park MVDZ, Gosens I, De Jong WH, Cassee FR. Physicochemical characteristics of nanomaterials that affect pulmonary inflammation. *Part Fibre Toxicol*. 2014; 11:18. <http://dx.doi.org/10.1186/1743-8977-11-18>

Appendix A. Reproductive Tissue Evaluations and Estrous Cycle Characterization

Tables

Table A-1. Summary of Reproductive Tissue Evaluations for Male Rats in the Three-month Nose-only Inhalation Study of Fullerene Micro-C ₆₀ (1 μm).....	A-2
Table A-2. Summary of Reproductive Tissue Evaluations for Male Rats in the Three-month Nose-only Inhalation Study of Fullerene Nano-C ₆₀ (50 nm)	A-2
Table A-3 . Summary of Reproductive Tissue Evaluations for Male Mice in the Three-month Nose-only Inhalation Study of Fullerene Micro-C ₆₀ (1 μm).....	A-3
Table A-4. Estrous Cycle Characterization for Female Mice in the Three-month Nose-only Inhalation Study of Fullerene Micro-C ₆₀ (1 μm)	A-3
Table A-5. Results of Vaginal Cytology Study Using the Transition Matrix Approach for Female Mice in the Three-month Nose-only Inhalation Study of Fullerene Micro-C ₆₀ (1 μm).....	A-4
Table A-6. Summary of Reproductive Tissue Evaluations for Male Mice in the Three-month Nose-only Inhalation Study of Fullerene Nano-C ₆₀ (50 nm)	A-5
Table A-7. Estrous Cycle Characterization for Female Mice in the Three-month Nose-only Inhalation Study of Fullerene Nano-C ₆₀ (50 nm).....	A-5
Table A-8. Results of Vaginal Cytology Study Using the Transition Matrix Approach for Female Mice in the Three-month Nose-only Inhalation Study of Fullerene Nano-C ₆₀ (50 nm).....	A-6

Figures

Figure A-1. Vaginal Cytology Plots for Female Mice in the Three-month Nose-only Inhalation Study of Fullerene Micro-C ₆₀ (1 μm)	A-7
Figure A-2. Vaginal Cytology Plots for Female Mice in the Three-month Nose-only Inhalation Study of Fullerene Nano-C ₆₀ (50 nm).....	A-8

Table A-1. Summary of Reproductive Tissue Evaluations for Male Rats in the Three-month Nose-only Inhalation Study of Fullerene Micro-C₆₀ (1 μm)^a

	0 mg/m ³	2 mg/m ³	15 mg/m ³	30 mg/m ³
n	10	10	10	10
Weights (g)				
Necropsy body wt.	353 ± 12	350 ± 10	373 ± 16	368 ± 9
L. Cauda epididymis	0.2400 ± 0.0092	0.2430 ± 0.0088	0.2476 ± 0.0203	0.2443 ± 0.0068
L. Epididymis	0.6829 ± 0.0220	0.6594 ± 0.0227	0.6727 ± 0.0443	0.6749 ± 0.0187
L. Testis	1.8296 ± 0.0434	1.8348 ± 0.0563	1.8040 ± 0.1605	1.8206 ± 0.0318
Spermatid Measurements				
Spermatid heads (10 ³ /mg testis)	137.9 ± 7.1	138.1 ± 4.4	118.0 ± 15.0	122.3 ± 3.2
Spermatid heads (10 ⁶ /testis)	250.8 ± 11.3	252.9 ± 9.6	228.3 ± 27.5	222.1 ± 4.8
Epididymal Spermatozoal Measurements				
Sperm motility (%)	84 ± 1	80 ± 1**	74 ± 8*	79 ± 1**
Sperm (10 ³ /mg cauda epididymis)	529 ± 19	587 ± 36	468 ± 66	532 ± 18
Sperm (10 ⁶ /cauda epididymis)	128 ± 7	143 ± 11	122 ± 17	130 ± 4

*Significantly different ($p \leq 0.05$) from the control group by Shirley's test; ** $p \leq 0.01$.

^aData are presented as mean ± standard error. Differences from the control group are not significant by Dunnett's test (body weights and tissue weights) or Dunn's test (spermatid measurements and sperm/mg cauda epididymis and per cauda epididymis).

Table A-2. Summary of Reproductive Tissue Evaluations for Male Rats in the Three-month Nose-only Inhalation Study of Fullerene Nano-C₆₀ (50 nm)^a

	0 mg/m ³	0.5 mg/m ³	2 mg/m ³
n	10	10	10
Weights (g)			
Necropsy body wt.	362 ± 10	360 ± 12	356 ± 9
L. Cauda epididymis	0.2403 ± 0.0099	0.2325 ± 0.0123	0.2384 ± 0.0141
L. Epididymis	0.6741 ± 0.0235	0.6392 ± 0.0218	0.6498 ± 0.0274
L. Testis	1.8168 ± 0.0465	1.7605 ± 0.0819	1.8299 ± 0.0551
Spermatid Measurements			
Spermatid heads (10 ³ /mg testis)	141.8 ± 9.0	128.8 ± 5.6	134.2 ± 12.1
Spermatid heads (10 ⁶ /testis)	256.40 ± 15.65	225.73 ± 11.63	248.76 ± 24.41
Epididymal Spermatozoal Measurements			
Sperm motility (%)	85 ± 1	82 ± 1	71 ± 8**
Sperm (10 ³ /mg cauda epididymis)	625 ± 39	626 ± 54	479 ± 68
Sperm (10 ⁶ /cauda epididymis)	150 ± 10	145 ± 15	122 ± 19

**Significantly different ($p \leq 0.01$) from the control group by Shirley's test.

^aData are presented as mean ± standard error. Differences from the control group are not significant by Dunnett's test (body weights and tissue weights) or Dunn's test (spermatid measurements and sperm/mg cauda epididymis and per cauda epididymis).

Table A-3 . Summary of Reproductive Tissue Evaluations for Male Mice in the Three-month Nose-only Inhalation Study of Fullerene Micro-C₆₀ (1 µm)^a

	0 mg/m ³	2 mg/m ³	15 mg/m ³	30 mg/m ³
n	10	9	10	10
Weights (g)				
Necropsy body wt.	31.6 ± 0.7	32.1 ± 0.9	30.9 ± 0.5	31.3 ± 0.7
L. Cauda epididymis	0.0156 ± 0.0005	0.0176 ± 0.0021	0.0193 ± 0.0015	0.0172 ± 0.0013
L. Epididymis	0.0483 ± 0.0019	0.0458 ± 0.0009	0.0489 ± 0.0021	0.0476 ± 0.0026
L. Testis	0.1088 ± 0.0021	0.0978 ± 0.0109	0.1056 ± 0.0025	0.1092 ± 0.0013
Spermatid Measurements				
Spermatid heads (10 ³ /mg testis)	323.3 ± 21.2	274.8 ± 35.0	283.0 ± 10.9	321.4 ± 21.6
Spermatid heads (10 ⁶ /testis)	35.14 ± 2.29	29.82 ± 3.98	29.88 ± 1.35	34.89 ± 1.98
Epididymal Spermatozoal Measurements				
Sperm motility (%)	83 ± 1	72 ± 9*	78 ± 1**	76 ± 3*
Sperm (10 ³ /mg cauda epididymis)	527 ± 38	429 ± 70	477 ± 32	552 ± 71
Sperm (10 ⁶ /cauda epididymis)	8 ± 0	7 ± 1	9 ± 1	9 ± 1

*Significantly different ($p \leq 0.05$) from the control group by Shirley's test; ** $p \leq 0.01$.

^aData are presented as mean ± standard error. Differences from the control group are not significant by Dunnett's test (body weights and left epididymis weights) or Dunn's test (spermatid measurements and sperm/mg cauda epididymis and per cauda epididymis).

Table A-4. Estrous Cycle Characterization for Female Mice in the Three-month Nose-only Inhalation Study of Fullerene Micro-C₆₀ (1 µm)^a

	0 mg/m ³	2 mg/m ³	15 mg/m ³	30 mg/m ³
Number Weighed at Necropsy	10	10	10	10
Necropsy body wt. (g)	28.1 ± 0.6	28.4 ± 0.7	27.9 ± 0.5	28.6 ± 0.8
Proportion of Regular Cycling Females ^b	10/10	10/10	9/10	10/10
Estrous Cycle Length (days)	4.5 ± 0.18	4.1 ± 0.21	4.6 ± 0.16	4.4 ± 0.14
Estrous Stages (% of cycle)				
Diestrus	34.4	32.5	26.9	28.1
Proestrus	0.6	1.3	1.9	0.6
Estrus	51.3	52.5	50.6	51.9
Metestrus	8.1	8.1	6.9	9.4
Uncertain diagnosis	5.6	5.6	13.8	10.0

^aNecropsy body weights and estrous cycle length data are presented as mean ± standard error. Differences from the control group are not significant by Dunnett's test (body weights) or Dunn's test (estrous cycle length). Tests for equality of transition probability matrices among all groups and between the control group and each exposed group indicated females exposed to 15 mg/m³ had increased probability of extended estrus compared to the control group.

^bNumber of females with a regular cycle/number of females cycling.

Table A-5. Results of Vaginal Cytology Study Using the Transition Matrix Approach for Female Mice in the Three-month Nose-only Inhalation Study of Fullerene Micro-C₆₀ (1 µm)

Stage	Comparison	P Value	Trend ^a
Overall Tests	Overall	0.065	
Overall Tests	2 mg/m ³ vs. controls	0.829	–
Overall Tests	15 mg/m ³ vs. controls	0.008	–
Overall Tests	30 mg/m ³ vs. controls	0.408	–
Extended Estrus	Overall	0.24	
Extended Estrus	2 mg/m ³ vs. controls	0.93	N
Extended Estrus	15 mg/m ³ vs. controls	0.034	–
Extended Estrus	30 mg/m ³ vs. controls	0.586	–
Extended Diestrus	Overall	0.587	
Extended Diestrus	2 mg/m ³ vs. controls	0.217	–
Extended Diestrus	15 mg/m ³ vs. controls	0.447	–
Extended Diestrus	30 mg/m ³ vs. controls	0.996	–
Extended Metestrus	Overall	0.92	
Extended Metestrus	2 mg/m ³ vs. controls	1	–
Extended Metestrus	15 mg/m ³ vs. controls	0.607	–
Extended Metestrus	30 mg/m ³ vs. controls	0.607	–
Extended Proestrus	Overall	1	
Extended Proestrus	2 mg/m ³ vs. controls	1	–
Extended Proestrus	15 mg/m ³ vs. controls	1	–
Extended Proestrus	30 mg/m ³ vs. controls	1	–
Skipped Estrus	Overall	1	
Skipped Estrus	2 mg/m ³ vs. controls	0.931	–
Skipped Estrus	15 mg/m ³ vs. controls	1	–
Skipped Estrus	30 mg/m ³ vs. controls	1	–
Skipped Diestrus	Overall	0.1	
Skipped Diestrus	2 mg/m ³ vs. controls	0.043	–
Skipped Diestrus	15 mg/m ³ vs. controls	0.359	N
Skipped Diestrus	30 mg/m ³ vs. controls	0.251	–
Summary of Significant Groups			
Overall Tests	15 mg/m ³ vs. controls	0.008	–
Extended Estrus	15 mg/m ³ vs. controls	0.034	–
Skipped Diestrus	2 mg/m ³ vs. controls	0.043	–

^aN means that the exposed group had a lower probability of transitioning to the relevant abnormal state (extended estrus, extended metestrus, extended proestrus, skipped estrus, or skipped diestrus) than did the control group.

Table A-6. Summary of Reproductive Tissue Evaluations for Male Mice in the Three-month Nose-only Inhalation Study of Fullerene Nano-C₆₀ (50 nm)^a

	0 mg/m ³	0.5 mg/m ³	2 mg/m ³
n	10	10	10
Weights (g)			
Necropsy body wt.	31.5 ± 0.8	31.7 ± 1.1	31.3 ± 0.6
L. Cauda epididymis	0.0181 ± 0.0010	0.0164 ± 0.0012	0.0163 ± 0.0006
L. Epididymis	0.0479 ± 0.0017	0.0445 ± 0.0020	0.0459 ± 0.0019
L. Testis	0.1057 ± 0.0015	0.1065 ± 0.0020	0.1076 ± 0.0018
Spermatid Measurements			
Spermatid heads (10 ³ /mg testis)	355.6 ± 21.7	322.2 ± 23.4	319.3 ± 28.5
Spermatid heads (10 ⁶ /testis)	37.42 ± 1.91	34.24 ± 2.46	34.43 ± 3.12
Epididymal Spermatozoal Measurements			
Sperm motility (%)	78 ± 2	71 ± 5	75 ± 2
Sperm (10 ³ /mg cauda epididymis)	477 ± 55	623 ± 61	846 ± 141
Sperm (10 ⁶ /cauda epididymis)	9 ± 1	10 ± 1	14 ± 2

^aData are presented as mean ± standard error. Differences from the control group are not significant by Dunnett's test (body weights and tissue weights) or Dunn's test (spermatid and epididymal spermatozoal measurements).

Table A-7. Estrous Cycle Characterization for Female Mice in the Three-month Nose-only Inhalation Study of Fullerene Nano-C₆₀ (50 nm)^a

	0 mg/m ³	0.5 mg/m ³	2 mg/m ³
Number Weighed at Necropsy	10	10	10
Necropsy Body Wt. (g)	26.5 ± 0.5	27.9 ± 0.7	26.6 ± 0.4
Proportion of Regular Cycling Females ^b	10/10	10/10	10/10
Estrous Cycle Length (days)	4.2 ± 0.13	4.5 ± 0.20	4.5 ± 0.13
Estrous stages (% of cycle)			
Diestrus	26.3	31.3	33.8
Proestrus	3.8	2.5	3.1
Estrus	45.6	51.9	52.5
Metestrus	16.9	8.8	8.8
Uncertain diagnosis	7.5	5.6	1.9

^aNecropsy body weights and estrous cycle length data are presented as mean ± standard error. Differences from the control group are not significant by Dunnett's test (body weights) or Dunn's test (estrous cycle length). Tests for equality of transition probability matrices among all groups and between the control group and each exposed group indicated exposed females had an increased probability of extended estrus compared to the control group.

^bNumber of females with a regular cycle/number of females cycling.

Table A-8. Results of Vaginal Cytology Study Using the Transition Matrix Approach for Female Mice in the Three-month Nose-only Inhalation Study of Fullerene Nano-C₆₀ (50 nm)

Stage	Comparison	P Value	Trend ^a
Overall Tests	Overall	0.122	
Overall Tests	0.5 mg/m ³ vs. controls	0.52	–
Overall Tests	2 mg/m ³ vs. controls	0.051	–
Extended Estrus	Overall	<0.001	
Extended Estrus	0.5 mg/m ³ vs. controls	0.002	–
Extended Estrus	2 mg/m ³ vs. controls	<0.001	–
Extended Diestrus	Overall	0.909	
Extended Diestrus	0.5 mg/m ³ vs. controls	0.604	–
Extended Diestrus	2 mg/m ³ vs. controls	1	–
Extended Metestrus	Overall	1	
Extended Metestrus	0.5 mg/m ³ vs. controls	1	–
Extended Metestrus	2 mg/m ³ vs. controls	1	–
Extended Proestrus	Overall	1	
Extended Proestrus	0.5 mg/m ³ vs. controls	1	–
Extended Proestrus	2 mg/m ³ vs. controls	1	–
Skipped Estrus	Overall	1	
Skipped Estrus	0.5 mg/m ³ vs. controls	1	–
Skipped Estrus	2 mg/m ³ vs. controls	1	–
Skipped Diestrus	Overall	0.993	
Skipped Diestrus	0.5 mg/m ³ vs. controls	0.931	–
Skipped Diestrus	2 mg/m ³ vs. controls	0.934	–
Summary of Significant Groups			
Extended Estrus	0.5 mg/m ³ vs. controls	0.002	–
Extended Estrus	2 mg/m ³ vs. controls	<0.001	–

^aN means that the exposed group had a lower probability of transitioning to the relevant abnormal state (extended estrus, extended metestrus, extended proestrus, skipped estrus, or skipped diestrus) than did the control group.

Fullerene C₆₀, TOX 87

Concentration (mg/m ³)																				
0			P	E	E	D	D	E	E	M	IC	E	E	M	D	E	E	M		
0				E	M	M	D	E	E	M	IC	E	M	M	IC	E	E	D	D	
0					E	D	D	E	E	E	D	D	E	E	M	D	E	E	D	D
0					E	D	P	E	E	E	D	IC	IC	E	E	M	D	P	E	E
0			P	E	E	M	D	E	E	D	IC	E	E	D	D	E	E	M		
0	M	D	P	E	E	M	IC	E	E	D	D	E	M	M	D	E				
0		D	IC	E	E	M	D	E	E	M	D	E	E	D	D	E	E			
0	M	D	P	E	E	M	IC	E	IC	E	D	D	E	E	D	D				
0				E	E	D	IC	E	E	M	IC	E	E	M	D	E	E	M	D	
0	M	D	E	E	E	D	D	E	E	M	M	D	E	E	M	D				
0.5			D	E	E	D	D	E	E	D	D	E	E	M	D	E	E	M		
0.5					E	D	IC	E	E	E	D	D	E	E	E	D	D	E	E	E
0.5					E	D	IC	E	E	M	D	E	E	M	D	E	E	D	D	E
0.5				E	M	D	D	E	E	E	D	D	P	E	E	M	D	P	E	
0.5				E	E	D	D	E	E	E	D	IC	E	E	E	D	P	IC	E	M
0.5			D	E	E	D	D	E	E	D	IC	E	E	E	D	D	E	E		
0.5			E	E	D	D	D	E	E	D	IC	E	E	E	M	D	P	E		
0.5		D	D	E	E	M	IC	E	E	M	D	E	E	M	D	E	E			
0.5				E	E	D	D	E	E	D	D	E	E	M	D	IC	E	E	E	
0.5			D	E	E	D	D	E	E	D	IC	E	E	M	D	E	M	D		
2					E	D	IC	E	M	M	E	E	E	E	D	P	E	M	D	D
2			E	E	M	D	D	E	E	D	P	E	E	D	D	E	E	E		
2	M	D	E	E	D	D	D	E	E	M	D	E	E	E	D	D	E			
2			E	E	D	D	D	E	E	D	D	P	E	E	M	D	E	E	E	
2			E	E	M	D	D	E	E	E	D	D	E	E	E	M	D	E	E	
2			E	E	D	IC	E	E	D	D	E	E	D	D	E	E	D	D		
2		D	E	E	E	M	IC	E	E	E	D	D	P	E	E	D	D			
2			E	E	E	D	D	E	E	E	M	D	E	E	E	M	D	E		
2			E	E	E	D	D	E	E	D	D	E	E	D	D	E	E	E		
2		D	D	E	E	D	D	E	M	D	D	P	E	E	M	D	D			

Figure A-2. Vaginal Cytology Plots for Female Mice in the Three-month Nose-only Inhalation Study of Fullerene Nano-C₆₀ (50 nm)

P = proestrus; E = estrus; M = metestrus; D = diestrus; IC = insufficient number of cells to determine stage.

Appendix B. Tissue Burden Results

Table of Contents

B.1. Lung Deposition and Clearance Equations Used in the Three-month Nose-only Inhalation Studies of Fullerene C ₆₀ (1 μm and 50 nm).....	B-2
B.2. Results for Rats	B-3
B.3. Results for Mice	B-10

Tables

Table B-1. Tissue Weights, Fullerene C ₆₀ Concentrations, and Fullerene C ₆₀ Burdens for Rats in the Three-month Nose-only Inhalation Study of Fullerene Micro-C ₆₀ (1 μm)	B-3
Table B-2. Lung Deposition and Clearance Parameter Estimates for Male Rats in the Three-month Nose-only Inhalation Study of Fullerene Micro-C ₆₀ (1 μm)	B-6
Table B-3. Tissue Weights, Fullerene C ₆₀ Concentrations, and Fullerene C ₆₀ Burdens for Rats in the Three-month Nose-only Inhalation Study of Fullerene Nano-C ₆₀ (50 nm)	B-6
Table B-4. Lung Deposition and Clearance Parameter Estimates for Male Rats in the Three-month Nose-only Inhalation Study of Fullerene Nano-C ₆₀ (50 nm).....	B-9
Table B-5. Tissue Weights, Fullerene C ₆₀ Concentrations, and Fullerene C ₆₀ Burdens for Mice in the Three-month Nose-only Inhalation Study of Fullerene Micro-C ₆₀ (1 μm)	B-10
Table B-6. Lung Deposition and Clearance Parameter Estimates for Male Mice in the Three-month Nose-only Inhalation Study of Fullerene Micro-C ₆₀ (1 μm)	B-12
Table B-7. Tissue Weights, Fullerene C ₆₀ Concentrations, and Fullerene C ₆₀ Burdens for Mice in the Three-month Nose-only Inhalation Study of Fullerene Nano-C ₆₀ (50 nm)	B-13
Table B-8. Lung Deposition and Clearance Parameter Estimates for Male Mice in the Three-month Nose-only Inhalation Study of Fullerene Nano-C ₆₀ (50 nm).....	B-15

B.1. Lung Deposition and Clearance Equations Used in the Three-month Nose-only Inhalation Studies of Fullerene C₆₀ (1 μm and 50 nm)

Lung burdens at $t = 0$ days postexposure and lung clearance rates were determined using the clearance model shown in Equation (1):

$$\text{Equation (1): } A(t) = A_0(e^{-kt})$$

where $A(t)$ is the lung burden (μg fullerene C₆₀) at each postexposure time point t ($t = \text{days}$ postexposure), A_0 is the lung burden at $t = 0$ days postexposure, and k is the lung clearance rate constant (fraction cleared per day [day^{-1}]).

Lung clearance half-lives in days ($t_{1/2}$) were calculated from Equation (2):

$$\text{Equation (2): } t_{1/2} = \ln 2/k$$

Deposition rates were calculated from lung burdens using Equation (3). The lung burden and time at terminal kill and the calculated lung clearance rate constant were used to solve for the deposition rate α ($\mu\text{g}/\text{day}$).

$$\text{Equation (3): } A(t) = (\alpha/k)(1 - e^{-kt})$$

In Equation (3), $A(t)$ is the lung burden (μg fullerene C₆₀) at time t ; α is the amount of fullerene C₆₀ deposited ($\mu\text{g}/\text{day}$); and k is the first-order clearance rate constant derived from Equation (1). Steady-state or equilibrium lung burdens (A_e , μg fullerene C₆₀) were calculated according to Equation (4):

$$\text{Equation (4): } A_e = \alpha/k$$

B.2. Results for Rats**Table B-1. Tissue Weights, Fullerene C₆₀ Concentrations, and Fullerene C₆₀ Burdens for Rats in the Three-month Nose-only Inhalation Study of Fullerene Micro-C₆₀ (1 µm)^a**

	0 mg/m ³	2 mg/m ³	15 mg/m ³	30 mg/m ³
Male				
n	6	6	6	6
Bronchial Lymph Node				
Absolute bronchial lymph node wt. (g)				
Day 88	0.030 ± 0.005	0.029 ± 0.006	0.031 ± 0.002	0.051 ± 0.005*
µg Fullerene C ₆₀ /g bronchial lymph node				
Day 88	0.526 ± 0.097 ^b	1.889 ± 0.544 ^{**b}	82.661 ± 49.095 ^{**}	1,188.098 ± 421.212 ^{**b}
µg Fullerene C ₆₀ /total bronchial lymph node				
Day 88	0.014 ± 0.001 ^b	0.045 ± 0.011 ^b	2.704 ± 1.641 ^{**}	61.886 ± 22.164 ^{**b}
µg Fullerene C ₆₀ /total bronchial lymph node per mg fullerene C ₆₀ /m ³				
Day 88	NA	0.023 ± 0.005 ^b	0.180 ± 0.109	2.063 ± 0.739 ^b
Spleen				
Absolute spleen wt. (g)				
Day 88	0.624 ± 0.031	0.561 ± 0.023	0.632 ± 0.051	0.566 ± 0.026
µg Fullerene C ₆₀ /g spleen				
Day 88	0.003 ± 0.000 ^c	0.011 ± 0.009 ^c	0.026 ± 0.011	0.046 ± 0.017 ^{*c}
µg Fullerene C ₆₀ /total spleen				
Day 88	0.002 ± 0.000 ^b	0.006 ± 0.004 ^c	0.018 ± 0.008	0.027 ± 0.010 ^c
µg Fullerene C ₆₀ /total spleen per mg fullerene C ₆₀ /m ³				
Day 88	NA	0.003 ± 0.02 ^c	0.001 ± 0.001	0.001 ± 0.000 ^c
Liver				
Absolute liver wt. (g)				
Day 88	12.507 ± 0.496	11.639 ± 0.431	11.886 ± 0.261	10.426 ± 0.387 ^{**}
µg Fullerene C ₆₀ /g liver				
Day 88	0.004 ± 0.000 ^b	0.004 ± 0.000 ^b	0.007 ± 0.002	0.015 ± 0.006 ^{**b}
µg Fullerene C ₆₀ /total liver				
Day 88	0.050 ± 0.002 ^b	0.047 ± 0.002 ^b	0.088 ± 0.031	0.161 ± 0.066 ^b
µg Fullerene C ₆₀ /total liver per mg fullerene C ₆₀ /m ³				
Day 88	NA	0.023 ± 0.01 ^b	0.006 ± 0.002	0.005 ± 0.002 ^b
Lung				
Absolute lung wt. (g)				
Day 88	1.413 ± 0.093	1.229 ± 0.049	1.281 ± 0.053	1.221 ± 0.044

Fullerene C₆₀, TOX 87

	0 mg/m ³	2 mg/m ³	15 mg/m ³	30 mg/m ³
PE Day 14	1.483 ± 0.060	1.552 ± 0.091	1.631 ± 0.114	2.012 ± 0.210**
PE Day 28	1.639 ± 0.160	1.746 ± 0.096	1.661 ± 0.100	1.728 ± 0.188
PE Day 56	1.437 ± 0.067	1.591 ± 0.102	1.712 ± 0.039**	1.694 ± 0.040**
µg Fullerene C ₆₀ /g lung				
Day 88	0.122 ± 0.027 ^b	358.103 ± 19.667** ^b	1,681.645 ± 233.880**	4,659.764 ± 344.713** ^b
PE Day 14	0.025 ± 0.010	157.113 ± 17.980**	901.140 ± 103.671**	2,796.07 ± 315.546**
PE Day 28	0.027 ± 0.012	128.255 ± 15.397**	1,088.54 ± 223.310**	2,388.87 ± 291.212**
PE Day 56	0.042 ± 0.018 ^b	73.285 ± 11.566** ^b	669.586 ± 138.945**	1,660.43 ± 198.512** ^b
µg Fullerene C ₆₀ /total lung				
Day 88	0.181 ± 0.046 ^b	438.806 ± 26.973** ^b	2,182.396 ± 358.886**	5,748.744 ± 582.344** ^b
PE Day 14	0.039 ± 0.018	242.932 ± 27.575**	1,419.92 ± 127.344**	5,521.69 ± 633.566**
PE Day 28	0.044 ± 0.019	228.353 ± 36.470**	1,754.34 ± 337.908**	4,084.52 ± 556.664**
PE Day 56	0.057 ± 0.024 ^b	109.333 ± 14.820** ^b	1,150.20 ± 238.847**	2,879.47 ± 371.692** ^b
µg Fullerene C ₆₀ /total lung per mg fullerene C ₆₀ /m ³				
Day 88	NA	219.4 ± 13.56 ^b	145.5 ± 23.96	191.6 ± 19.41 ^b
PE Day 14	NA	121.466 ± 13.787	94.661 ± 8.490	184.056 ± 21.119
PE Day 28	NA	114.176 ± 18.235	116.956 ± 22.527	136.151 ± 18.555
PE Day 56	NA	54.667 ± 7.410 ^b	76.680 ± 15.923	95.982 ± 12.390 ^b
Female				
n	8	8	8	8
Bronchial Lymph Node				
Absolute bronchial lymph node wt. (g)				
Day 88	0.021 ± 0.002	0.020 ± 0.001	0.023 ± 0.003	0.030 ± 0.002
µg Fullerene C ₆₀ /g bronchial lymph node				
Day 88	0.602 ± 0.028 ^d	2.844 ± 0.389** ^d	53.488 ± 13.325**	1,766.176 ± 391.460** ^d
µg Fullerene-C ₆₀ /total bronchial lymph node				
Day 88	0.013 ± 0.001 ^d	0.056 ± 0.010** ^d	1.012 ± 0.187**	54.527 ± 12.944** ^d
µg Fullerene C ₆₀ /total lymph node per mg fullerene C ₆₀ /m ³				
Day 88	NA	0.028 ± 0.005 ^d	0.067 ± 0.012	1.821 ± 0.431 ^d
Spleen				
Absolute spleen wt. (g)				
Day 88	0.415 ± 0.012	0.416 ± 0.021	0.405 ± 0.026	0.388 ± 0.011
µg Fullerene C ₆₀ /g spleen				
Day 88	0.003 ± 0.000 ^e	0.003 ± 0.000 ^e	0.003 ± 0.000	0.136 ± 0.118 ^d
µg Fullerene C ₆₀ /total spleen				
Day 88	0.001 ± 0.000 ^e	0.001 ± 0.000 ^e	0.001 ± 0.000	0.056 ± 0.048 ^d

Fullerene C₆₀, TOX 87

	0 mg/m ³	2 mg/m ³	15 mg/m ³	30 mg/m ³
μg Fullerene C ₆₀ /total spleen per mg fullerene C ₆₀ /m ³				
Day 88	NA	0.001 ± 0.000 ^e	0.000 ± 0.000	0.002 ± 0.002 ^d
Liver				
Absolute liver wt. (g)				
Day 88	7.205 ± 0.290	6.448 ± 0.271	6.510 ± 0.307	6.161 ± 0.310
μg Fullerene C ₆₀ /g liver				
Day 88	0.004 ± 0.000 ^d	0.004 ± 0.000 ^d	0.008 ± 0.003	0.007 ± 0.002 ^d
μg Fullerene C ₆₀ /total liver				
Day 88	0.029 ± 0.001 ^d	0.026 ± 0.001 ^d	0.050 ± 0.018	0.045 ± 0.010 ^d
μg Fullerene C ₆₀ /total liver per mg fullerene C ₆₀ /m ³				
Day 88	NA	0.013 ± 0.001 ^d	0.003 ± 0.001	0.001 ± 0.000 ^d
Lung				
Absolute lung wt. (g)				
Day 88	0.919 ± 0.030	0.936 ± 0.033	0.997 ± 0.052	0.978 ± 0.034
μg Fullerene C ₆₀ /g lung				
Day 88	0.259 ± 0.026 ^d	252.037 ± 13.281 ^{***d}	1,769.746 ± 84.185 ^{**}	4,706.482 ± 230.457 ^{***d}
μg Fullerene C ₆₀ /total lung				
Day 88	0.239 ± 0.026 ^d	234.274 ± 13.648 ^{***d}	1,763.436 ± 126.305 ^{**}	4,657.878 ± 372.741 ^{***d}
μg Fullerene C ₆₀ /total lung per mg fullerene C ₆₀ /m ³				
Day 88	NA	117.137 ± 6.824 ^d	117.562 ± 8.420	115.263 ± 12.425 ^d

*Significantly different ($p \leq 0.05$) from the control group by Shirley's test; ** $p \leq 0.01$.

^aData are presented as mean ± standard error. Statistical tests were not performed on data that were normalized to fullerene C₆₀ exposure concentration. NA = not applicable; PE = postexposure.

^bn = 5.

^cn = 4.

^dn = 7.

^en = 6.

Table B-2. Lung Deposition and Clearance Parameter Estimates for Male Rats in the Three-month Nose-only Inhalation Study of Fullerene Micro-C₆₀ (1 μm)^a

Parameter	2 mg/m ³	15 mg/m ³	30 mg/m ³
A ₀ (μg fullerene C ₆₀ /total lung)	416	2,037	6,032
k (days ⁻¹)	0.026	0.010	0.013
t _{1/2} (days)	27	69	55
α (μg fullerene C ₆₀ /total lung per day)	12	35	113
A _e (μg fullerene C ₆₀ /total lung)	465	3,472	9,010

A₀=lung burden at t = 0 days postexposure; k = first-order lung clearance rate constant; t_{1/2}=lung clearance half-life; α = lung deposition rate; A_e=steady-state lung burden.

^aData are presented as mean values.

Table B-3. Tissue Weights, Fullerene C₆₀ Concentrations, and Fullerene C₆₀ Burdens for Rats in the Three-month Nose-only Inhalation Study of Fullerene Nano-C₆₀ (50 nm)^a

	0 mg/m ³	0.5 mg/m ³	2 mg/m ³
Male			
n	6	6	6
Bronchial Lymph Node			
Absolute bronchial lymph node wt. (g)			
Day 89	0.032 ± 0.004	0.033 ± 0.002	0.041 ± 0.003
μg Fullerene C ₆₀ /g bronchial lymph node			
Day 89	0.617 ± 0.161 ^b	0.734 ± 0.059 ^b	2.332 ± 0.461 ^{**b}
μg Fullerene C ₆₀ /total bronchial lymph node			
Day 89	0.016 ± 0.002 ^b	0.025 ± 0.002 ^{**b}	0.095 ± 0.018 ^{**b}
μg Fullerene C ₆₀ /total bronchial lymph node per mg fullerene C ₆₀ /m ³			
Day 89	NA	0.050 ± 0.003 ^b	0.047 ± 0.009 ^b
Spleen			
Absolute spleen wt. (g)			
Day 89	0.531 ± 0.041	0.544 ± 0.025	0.509 ± 0.025
μg Fullerene C ₆₀ /g spleen			
Day 89	0.003 ± 0.000 ^c	0.003 ± 0.00 ^c	0.022 ± 0.014 ^c
μg Fullerene C ₆₀ /total spleen			
Day 89	0.001 ± 0.000 ^c	0.001 ± 0.000 ^c	0.012 ± 0.008 ^c
μg Fullerene C ₆₀ /total spleen per mg fullerene C ₆₀ /m ³			
Day 89	NA	0.003 ± 0.000 ^c	0.006 ± 0.004 ^c
Liver			
Absolute liver wt. (g)			
Day 89	10.641 ± 0.584	10.011 ± 0.298	9.948 ± 0.278
μg Fullerene C ₆₀ /g liver			

Fullerene C₆₀, TOX 87

	0 mg/m ³	0.5 mg/m ³	2 mg/m ³
Day 89	0.004 ± 0.000 ^b	0.004 ± 0.000 ^b	0.006 ± 0.001 ^b
µg Fullerene C ₆₀ /total liver			
Day 89	0.042 ± 0.003 ^b	0.040 ± 0.001 ^b	0.058 ± 0.012 ^b
µg Fullerene C ₆₀ /total liver per mg fullerene C ₆₀ /m ³			
Day 89	NA	0.080 ± 0.003 ^b	0.029 ± 0.006 ^b
Lung			
Absolute lung wt. (g)			
Day 89	1.447 ± 0.101	1.424 ± 0.064	1.404 ± 0.077
PE Day 14	1.489 ± 0.103	1.797 ± 0.083	1.776 ± 0.102
PE Day 28	1.517 ± 0.110	2.113 ± 0.161 ^{**}	1.629 ± 0.067
PE Day 56	1.649 ± 0.139	1.645 ± 0.027	1.846 ± 0.074 [*]
µg Fullerene C ₆₀ /g lung			
Day 89	0.069 ± 0.031 ^b	103.574 ± 5.358 ^{**b}	414.382 ± 33.979 ^{**b}
PE Day 14	0.021 ± 0.006	68.509 ± 3.173 ^{**}	274.966 ± 8.506 ^{**}
PE Day 28	0.115 ± 0.024	63.371 ± 7.730 ^{**}	334.298 ± 38.944 ^{**}
PE Day 56	0.046 ± 0.020 ^b	31.973 ± 4.134 ^{**b}	141.400 ± 20.492 ^{**b}
µg Fullerene C ₆₀ /total lung			
Day 89	0.086 ± 0.034 ^b	189.217 ± 4.928 ^{**b}	580.890 ± 45.767 ^{**b}
PE Day 14	0.031 ± 0.009	122.324 ± 5.302 ^{**}	487.523 ± 30.124 ^{**}
PE Day 28	0.176 ± 0.035	136.756 ± 24.762 ^{**}	538.166 ± 53.556 ^{**}
PE Day 56	0.076 ± 0.032 ^b	52.629 ± 6.201 ^{**b}	248.916 ± 31.078 ^{**b}
µg Fullerene C ₆₀ /total lung per mg fullerene C ₆₀ /m ³			
Day 89	NA	378.43 ± 9.86 ^b	290.45 ± 22.88 ^b
PE Day 14	NA	244.649 ± 10.60	243.761 ± 15.062
PE Day 28	NA	273.511 ± 49.523	269.083 ± 26.778
PE Day 56	NA	105.259 ± 12.403 ^b	124.458 ± 15.539 ^b
Female			
n	8	8	8
Bronchial Lymph Node			
Absolute bronchial lymph node wt. (g)			
Day 89	0.024 ± 0.002	0.028 ± 0.005	0.025 ± 0.004
µg Fullerene C ₆₀ /g bronchial lymph node			
Day 89	0.570 ± 0.044 ^d	0.860 ± 0.141 ^d	4.926 ± 1.537 ^{**d}
µg Fullerene C ₆₀ /total bronchial lymph node			
Day 89	0.014 ± 0.001 ^d	0.023 ± 0.003 ^{*d}	0.100 ± 0.012 ^{**d}

Fullerene C₆₀, TOX 87

	0 mg/m ³	0.5 mg/m ³	2 mg/m ³
μg Fullerene C ₆₀ /total bronchial lymph node per mg fullerene C ₆₀ /m ³			
Day 89	NA	0.046 ± 0.006 ^d	0.050 ± 0.006 ^d
Spleen			
Absolute spleen wt. (g)			
Day 89	0.394 ± 0.018	0.422 ± 0.031	0.391 ± 0.026
μg Fullerene C ₆₀ /g spleen			
Day 89	0.003 ± 0.000 ^e	0.020 ± 0.017 ^e	0.003 ± 0.000 ^e
μg Fullerene C ₆₀ /total spleen			
Day 89	0.001 ± 0.000 ^e	0.007 ± 0.006 ^e	0.001 ± 0.000 ^e
μg Fullerene C ₆₀ /total spleen per mg fullerene C ₆₀ /m ³			
Day 89	NA	0.015 ± 0.012 ^e	0.000 ± 0.000 ^e
Liver			
Absolute liver wt. (g)			
Day 89	6.259 ± 0.221	6.644 ± 0.386	6.015 ± 0.277
μg Fullerene C ₆₀ /g liver			
Day 89	0.005 ± 0.001 ^d	0.004 ± 0.000 ^d	0.006 ± 0.001 ^d
μg Fullerene C ₆₀ /total liver			
Day 89	0.034 ± 0.009 ^d	0.027 ± 0.002 ^d	0.034 ± 0.006 ^d
μg Fullerene C ₆₀ /total liver per mg fullerene C ₆₀ /m ³			
Day 89	NA	0.054 ± 0.003 ^d	0.017 ± 0.003 ^d
Lung			
Absolute lung wt. (g)			
Day 89	1.065 ± 0.066	1.266 ± 0.077	0.971 ± 0.057
μg Fullerene C ₆₀ /g lung			
Day 89	0.086 ± 0.030 ^d	102.128 ± 12.142 ^{**d}	442.346 ± 33.335 ^{**d}
μg Fullerene C ₆₀ /total lung			
Day 89	0.088 ± 0.031 ^d	128.396 ± 9.442 ^{**d}	433.868 ± 27.467 ^{**d}
μg Fullerene C ₆₀ /total lung per mg fullerene C ₆₀ /m ³			
Day 89	NA	256.792 ± 18.884 ^d	216.934 ± 13.733 ^d

*Significantly different ($p \leq 0.05$) from the control group by Dunn's or Shirley's test; ** $p \leq 0.01$.

^aData are presented as mean ± standard error. Statistical tests were not performed on data that were normalized to fullerene C₆₀ exposure concentration. NA = not applicable; PE = postexposure.

^bn = 5.

^cn = 4.

^dn = 7.

^en = 6.

Table B-4. Lung Deposition and Clearance Parameter Estimates for Male Rats in the Three-month Nose-only Inhalation Study of Fullerene Nano-C₆₀ (50 nm)^a

Parameter	0.5 mg/m ³	2 mg/m ³
A ₀ (µg fullerene C ₆₀ /total lung)	185	604
k (days ⁻¹)	0.018	0.011
t _{1/2} (days)	38	61
α (µg fullerene C ₆₀ /total lung per day)	4.2	10.8
A _e (µg fullerene C ₆₀ /total lung)	229	946

A₀ = lung burden at t = 0 days postexposure; k = first-order lung clearance rate constant; t_{1/2} = lung clearance half-life; α = lung deposition rate; A_e = steady-state lung burden.

^aData are presented as mean values.

B.3. Results for Mice**Table B-5. Tissue Weights, Fullerene C₆₀ Concentrations, and Fullerene C₆₀ Burdens for Mice in the Three-month Nose-only Inhalation Study of Fullerene Micro-C₆₀ (1 μm)^a**

	0 mg/m ³	2 mg/m ³	15 mg/m ³	30 mg/m ³
Male				
n	6	6	6	6
Bronchial Lymph Node				
Absolute bronchial lymph node wt. (g)				
Day 88	0.012 ± 0.002	0.010 ± 0.001	0.016 ± 0.004	0.012 ± 0.003
μg Fullerene C ₆₀ /g bronchial lymph node				
Day 88	0.718 ± 0.113 ^b	1.964 ± 0.136 ^{**b}	142.650 ± 54.106 ^{**}	1,692.370 ± 454.458 ^{**b}
μg Fullerene C ₆₀ /total bronchial lymph node				
Day 88	0.008 ± 0.000 ^b	0.020 ± 0.002 ^{**b}	1.753 ± 0.425 ^{**}	16.035 ± 2.311 ^{**b}
μg Fullerene C ₆₀ /total bronchial lymph node per mg fullerene C ₆₀ /m ³				
Day 88	NA	0.010 ± 0.001 ^b	0.117 ± 0.028	0.535 ± 0.077 ^b
Spleen				
Absolute spleen wt. (g)				
Day 88	0.057 ± 0.002	0.064 ± 0.002	0.058 ± 0.001	0.061 ± 0.002
μg Fullerene C ₆₀ /g spleen				
Day 88	0.114 ± 0.000 ^c	0.114 ± 0.000 ^c	1.673 ± 1.209	2.840 ± 2.220 ^c
μg Fullerene C ₆₀ /total spleen				
Day 88	0.006 ± 0.000 ^c	0.008 ± 0.000 ^c	0.099 ± 0.072	0.185 ± 0.151 ^c
μg Fullerene C ₆₀ /total spleen per mg fullerene C ₆₀ /m ³				
Day 88	NA	0.004 ± 0.000 ^c	0.007 ± 0.005	0.006 ± 0.005 ^c
Liver				
Absolute liver wt. (g)				
Day 88	1.265 ± 0.030	1.320 ± 0.043 ^d	1.186 ± 0.034	1.196 ± 0.048
μg Fullerene C ₆₀ /g liver				
Day 88	0.006 ± 0.000 ^d	0.006 ± 0.000	0.272 ± 0.161 [*]	0.529 ± 0.456 ^{*d}
μg Fullerene C ₆₀ /total liver				
Day 88	0.007 ± 0.000 ^d	0.008 ± 0.000 ^d	0.309 ± 0.182 ^{**}	0.679 ± 0.601 ^{*d}
μg Fullerene C ₆₀ /total liver per mg fullerene C ₆₀ /m ³				
Day 88	NA	0.004 ± 0.000 ^d	0.021 ± 0.012	0.023 ± 0.020 ^d
Lung				
Absolute lung wt. (g)				
Day 88	0.159 ± 0.015	0.159 ± 0.005	0.159 ± 0.008	0.177 ± 0.004 [*]

Fullerene C₆₀, TOX 87

	0 mg/m ³	2 mg/m ³	15 mg/m ³	30 mg/m ³
PE Day 14	0.153 ± 0.006	0.154 ± 0.002	0.154 ± 0.002	0.168 ± 0.006
PE Day 28	0.155 ± 0.006	0.160 ± 0.008	0.169 ± 0.004	0.179 ± 0.016*
PE Day 56	0.158 ± 0.005	0.170 ± 0.005	0.175 ± 0.005*	0.188 ± 0.003**
µg Fullerene C ₆₀ /g lung				
Day 88	0.090 ± 0.000 ^b	245.990 ± 20.016 ^{**b}	1,331.375 ± 79.440 ^{**}	3,335.689 ± 246.179 ^{**b}
PE Day 14	0.090 ± 0.000	118.681 ± 7.618 ^{**}	674.684 ± 20.066 ^{**}	3,425.57 ± 340.797 ^{**}
PE Day 28	0.090 ± 0.000	72.130 ± 3.682 ^{**}	425.722 ± 39.064 ^{**}	2,605.80 ± 361.820 ^{**}
PE Day 56	0.090 ± 0.000 ^b	33.851 ± 3.454 ^{**b}	195.155 ± 38.049	1,846.59 ± 128.572 ^{**b}
µg Fullerene C ₆₀ /total lung				
Day 88	0.015 ± 0.00 ^b	38.316 ± 2.033 ^{**b}	209.469 ± 8.387 ^{**}	595.138 ± 40.532 ^{**b}
PE Day 14	0.014 ± 0.001	18.202 ± 1.027 ^{**}	103.728 ± 3.788 ^{**}	572.117 ± 53.954 ^{**}
PE Day 28	0.014 ± 0.001	11.423 ± 0.409 ^{**}	72.064 ± 7.087 ^{**}	440.291 ± 25.214 ^{**}
PE Day 56	0.014 ± 0.000 ^b	5.683 ± 0.471 ^{**b}	34.169 ± 6.639 ^{**}	347.127 ± 28.898 ^{**b}
µg Fullerene C ₆₀ /total lung per mg fullerene C ₆₀ /m ³				
Day 88	NA	19.16 ± 1.02 ^b	13.97 ± 0.56	19.84 ± 1.35 ^b
PE Day 14	NA	9.101 ± 0.513	6.915 ± 0.253	19.071 ± 1.798
PE Day 28	NA	5.712 ± 0.204	4.804 ± 0.472	14.676 ± 0.840
PE Day 56	NA	2.842 ± 0.236 ^b	2.278 ± 0.443	11.571 ± 0.963 ^b
Female				
n	8	8	8	8
Bronchial Lymph Node				
Absolute bronchial lymph node wt. (g)				
Day 88	0.009 ± 0.001	0.012 ± 0.003	0.009 ± 0.001	0.011 ± 0.001
µg Fullerene C ₆₀ /g bronchial lymph node				
Day 88	1.111 ± 0.110 ^e	2.092 ± 0.356 ^{*e}	80.680 ± 17.315 ^{**}	1,696.586 ± 255.975 ^{**e}
µg Fullerene C ₆₀ /total bronchial lymph node				
Day 88	0.009 ± 0.000 ^e	0.021 ± 0.002 ^{**e}	0.609 ± 0.063 ^{**}	17.415 ± 1.470 ^{**e}
µg Fullerene C ₆₀ /total bronchial lymph node per mg fullerene C ₆₀ /m ³				
Day 88	NA	0.010 ± 0.001 ^e	0.041 ± 0.004	0.580 ± 0.049 ^e
Spleen				
Absolute spleen wt. (g)				
Day 88	0.086 ± 0.005	0.076 ± 0.002	0.082 ± 0.005	0.078 ± 0.001
µg Fullerene C ₆₀ /g spleen				
Day 88	0.114 ± 0.000 ^f	0.114 ± 0.000 ^f	0.288 ± 0.117	2.180 ± 1.945 ^{*f}
µg Fullerene C ₆₀ /total spleen				
Day 88	0.010 ± 0.001 ^f	0.009 ± 0.000 ^f	0.022 ± 0.009	0.159 ± 0.140 ^f

Fullerene C₆₀, TOX 87

	0 mg/m ³	2 mg/m ³	15 mg/m ³	30 mg/m ³
μg Fullerene C ₆₀ /total spleen per mg fullerene C ₆₀ /m ³				
Day 88	NA	0.004 ± 0.000 ^f	0.001 ± 0.001	0.005 ± 0.005 ^f
Liver				
Absolute liver wt. (g)				
Day 88	1.208 ± 0.051	1.108 ± 0.028	1.075 ± 0.037*	1.086 ± 0.012
μg Fullerene C ₆₀ /g liver				
Day 88	0.006 ± 0.000 ^b	0.006 ± 0.000 ^b	0.097 ± 0.039**	0.112 ± 0.018** ^b
μg Fullerene C ₆₀ /total liver				
Day 88	0.007 ± 0.000 ^b	0.007 ± 0.000 ^b	0.106 ± 0.043**	0.123 ± 0.021** ^b
μg Fullerene C ₆₀ /total liver per mg fullerene C ₆₀ /m ³				
Day 88	NA	0.003 ± 0.000 ^b	0.007 ± 0.003	0.004 ± 0.001 ^b
Lung				
Absolute lung wt. (g)				
Day 88	0.147 ± 0.003	0.151 ± 0.003	0.147 ± 0.003	0.167 ± 0.003**
μg Fullerene C ₆₀ /g lung				
Day 88	0.090 ± 0.000 ^e	242.169 ± 8.996** ^e	1,294.840 ± 41.845**	3,386.537 ± 100.480** ^e
μg Fullerene C ₆₀ /total lung				
Day 88	0.013 ± 0.000 ^e	36.109 ± 1.111** ^e	189.975 ± 5.211**	560.250 ± 14.158** ^e
μg Fullerene C ₆₀ /total liver per mg fullerene C ₆₀ /m ³				
Day 88	NA	18.055 ± 0.556 ^e	12.665 ± 0.347	18.675 ± 0.472 ^e

*Significantly different ($p \leq 0.05$) from the control group by Dunn's or Shirley's test; ** $p \leq 0.01$.

NA = not applicable; PE = postexposure.

^aData are presented as mean ± standard error. Statistical tests were not performed on data that were normalized to fullerene C₆₀ exposure concentration.

^bn = 5.

^cn = 4.

^dn = 3.

^en = 7.

^fn = 6.

Table B-6. Lung Deposition and Clearance Parameter Estimates for Male Mice in the Three-month Nose-only Inhalation Study of Fullerene Micro-C₆₀ (1 μm)^a

Parameter	2 mg/m ³	15 mg/m ³	30 mg/m ³
A ₀ (μg fullerene C ₆₀ /total lung)	37	204	615
k (days ⁻¹)	0.044	0.039	0.010
t _{1/2} (days)	16	18	68
α (μg fullerene C ₆₀ /total lung per day)	2	8	11
A _e (μg fullerene C ₆₀ /total lung)	38	211	1,038

A₀ = lung burden at t = 0 days postexposure; k = first-order lung clearance rate constant; t_{1/2} = lung clearance half-life; α = lung deposition rate; A_e = steady-state lung burden.

^aData are presented as mean values.

Table B-7. Tissue Weights, Fullerene C₆₀ Concentrations, and Fullerene C₆₀ Burdens for Mice in the Three-month Nose-only Inhalation Study of Fullerene Nano-C₆₀ (50 nm)^a

	0 mg/m ³	0.5 mg/m ³	2 mg/m ³
Male			
n	6	6	6
Bronchial Lymph Node			
Absolute bronchial lymph node wt. (g)			
Day 89	0.009 ± 0.001	0.022 ± 0.008	0.016 ± 0.002
µg Fullerene C ₆₀ /g bronchial lymph node			
Day 89	0.596 ± 0.243 ^b	2.040 ± 0.626 ^{*b}	39.160 ± 26.831 ^{*b}
µg Fullerene C ₆₀ /bronchial lymph node			
Day 89	0.005 ± 0.002 ^b	0.025 ± 0.003 ^{**b}	0.760 ± 0.548 ^{**b}
µg Fullerene C ₆₀ /total bronchial lymph node per mg fullerene C ₆₀ /m ³			
Day 89	NA	0.050 ± 0.007 ^b	0.380 ± 0.274 ^b
Spleen			
Absolute spleen wt. (g)			
Day 89	0.049 ± 0.010	0.056 ± 0.002	0.060 ± 0.003
µg Fullerene C ₆₀ /g spleen			
Day 89	0.114 ± 0.000 ^c	0.114 ± 0.000 ^c	0.166 ± 0.052 ^c
µg Fullerene C ₆₀ /total spleen			
Day 89	0.005 ± 0.002 ^c	0.007 ± 0.000 ^c	0.010 ± 0.003 ^c
µg Fullerene C ₆₀ /total spleen per mg fullerene C ₆₀ /m ³			
Day 89	NA	0.013 ± 0.001 ^c	0.005 ± 0.002 ^c
Liver			
Absolute liver wt. (g)			
Day 89	1.133 ± 0.042	1.225 ± 0.043	1.171 ± 0.025
µg Fullerene C ₆₀ /g liver			
Day 89	0.006 ± 0.000 ^d	0.006 ± 0.000 ^d	0.037 ± 0.011 ^{*d}
µg Fullerene C ₆₀ /total liver			
Day 89	0.007 ± 0.000 ^d	0.008 ± 0.000 ^d	0.042 ± 0.011 ^d
µg Fullerene C ₆₀ /total liver per mg fullerene C ₆₀ /m ³			
Day 89	NA	0.015 ± 0.001 ^d	0.021 ± 0.006 ^d
Lung			
Absolute lung wt. (g)			
Day 89	0.153 ± 0.006	0.151 ± 0.009	0.159 ± 0.004
PE day 14	0.148 ± 0.004	0.171 ± 0.005 ^{**}	0.161 ± 0.003
PE day 28	0.148 ± 0.003	0.174 ± 0.005 ^{**}	0.167 ± 0.009

Fullerene C₆₀, TOX 87

	0 mg/m ³	0.5 mg/m ³	2 mg/m ³
PE day 56	0.154 ± 0.003	0.175 ± 0.005**	0.186 ± 0.007**
μg Fullerene C ₆₀ /g lung			
Day 89	0.090 ± 0.000 ^b	157.971 ± 10.880** ^b	732.025 ± 28.837** ^b
PE day 14	0.090 ± 0.000	70.457 ± 4.027**	396.547 ± 19.776**
PE day 28	0.090 ± 0.000	46.434 ± 3.036**	172.877 ± 12.197**
PE day 56	0.090 ± 0.000 ^b	20.290 ± 1.415** ^b	45.875 ± 2.941** ^b
μg Fullerene C ₆₀ /total lung			
Day 89	0.014 ± 0.001 ^b	23.714 ± 2.158** ^b	115.390 ± 2.747** ^b
PE day 14	0.013 ± 0.000	12.112 ± 0.815**	63.659 ± 0.815**
PE day 28	0.013 ± 0.000	8.104 ± 0.575**	28.571 ± 1.784**
PE day 56	0.014 ± 0.000 ^b	3.513 ± 0.248** ^b	8.548 ± 0.689** ^b
μg Fullerene C ₆₀ /total lung per mg fullerene C ₆₀ /m ³			
Day 89	NA	47.43 ± 4.32 ^b	57.70 ± 1.37 ^b
PE day 14	NA	24.224 ± 1.631	31.829 ± 1.711
PE day 28	NA	16.207 ± 1.149	14.285 ± 0.892
PE day 56	NA	7.026 ± 0.495 ^b	4.274 ± 0.345 ^b
Female			
n	8	8	8
Bronchial Lymph Node			
Absolute bronchial lymph node wt. (g)			
Day 89	0.009 ± 0.003	0.013 ± 0.004	0.010 ± 0.002
μg Fullerene C ₆₀ /g bronchial lymph node			
Day 89	1.144 ± 0.233 ^e	3.463 ± 0.757** ^e	17.177 ± 4.699** ^e
μg Fullerene C ₆₀ /total bronchial lymph node			
Day 89	0.008 ± 0.001 ^e	0.036 ± 0.007** ^e	0.140 ± 0.031** ^e
μg Fullerene C ₆₀ /total bronchial lymph node per mg fullerene C ₆₀ /m ³			
Day 89	NA	0.071 ± 0.013 ^e	0.070 ± 0.015 ^e
Spleen			
Absolute spleen wt. (g)			
Day 89	0.076 ± 0.002	0.078 ± 0.002	0.075 ± 0.002
μg Fullerene C ₆₀ /g spleen			
Day 89	0.114 ± 0.000 ^f	0.114 ± 0.000 ^f	0.114 ± 0.003 ^f
μg Fullerene C ₆₀ /total spleen			
Day 89	0.009 ± 0.000 ^f	0.009 ± 0.000 ^f	0.009 ± 0.000 ^f
μg Fullerene C ₆₀ /total spleen per mg fullerene C ₆₀ /m ³			

Fullerene C₆₀, TOX 87

	0 mg/m ³	0.5 mg/m ³	2 mg/m ³
Day 89	NA	0.018 ± 0.001 ^f	0.004 ± 0.000 ^f
Liver			
Absolute liver wt. (g)			
Day 89	1.095 ± 0.015	1.063 ± 0.016	1.007 ± 0.017**
µg Fullerene C ₆₀ /g liver			
Day 89	0.006 ± 0.000 ^b	0.006 ± 0.000 ^b	0.070 ± 0.003** ^b
µg Fullerene C ₆₀ /total liver			
Day 89	0.006 ± 0.000 ^b	0.006 ± 0.000 ^b	0.071 ± 0.004** ^b
µg Fullerene C ₆₀ /total liver per mg fullerene C ₆₀ /m ³			
Day 89	NA	0.013 ± 0.000 ^b	0.035 ± 0.002 ^b
Lung			
Absolute lung wt. (g)			
Day 89	0.140 ± 0.008	0.151 ± 0.004	0.144 ± 0.006
µg Fullerene C ₆₀ /g lung			
Day 89	0.090 ± 0.000 ^e	169.635 ± 4.139** ^e	685.230 ± 31.611** ^e
µg Fullerene C ₆₀ /total lung			
Day 89	0.012 ± 0.001 ^e	25.658 ± 1.006** ^e	97.530 ± 5.935** ^e
µg Fullerene C ₆₀ /total lung per mg fullerene C ₆₀ /m ³			
Day 89	NA	57.317 ± 2.011 ^e	48.765 ± 2.967 ^e

*Significantly different ($p \leq 0.05$) from the control group by Dunn's or Shirley's test; ** $p \leq 0.01$.

^aData are presented as mean ± standard error. Statistical tests were not performed on data that were normalized to fullerene C₆₀ exposure concentration. NA = not applicable; PE = postexposure.

^bn = 5.

^cn = 4.

^dn = 3.

^en = 7.

^fn = 6.

Table B-8. Lung Deposition and Clearance Parameter Estimates for Male Mice in the Three-month Nose-only Inhalation Study of Fullerene Nano-C₆₀ (50 nm)^a

Parameter	0.5 mg/m ³	2 mg/m ³
A ₀ (µg fullerene C ₆₀ /total lung)	23	116
k (days ⁻¹)	0.040	0.047
t _{1/2} (days)	17	15
α (µg fullerene C ₆₀ /total lung per day)	0.9	5.5
A _e (µg fullerene C ₆₀ /total lung)	24	118

A₀ = lung burden at t = 0 days postexposure; k = first-order lung clearance rate constant; t_{1/2} = lung clearance half-life; α = lung deposition rate; A_e = steady-state lung burden.

^aData are presented as mean values.

Appendix C. Immunotoxicity Results

Tables

Table C-1. Spleen Cell Immunophenotypes in Female Rats and Mice in the Three-month Nose-only Inhalation Studies of Fullerene Nano-C ₆₀ (50 nm) and Micro-C ₆₀ (1 μm).....	C-2
Table C-2. T-Dependent Antibody Response to Sheep Red Blood Cells in the Spleen of Female Rats and the Spleen and Serum of Female Mice in the Three-month Nose-only Inhalation Studies of Fullerene Nano-C ₆₀ (50 nm) and Micro-C ₆₀ (1 μm).....	C-4
Table C-3. Proliferative Response to Anti-CD3 Antibody in the Spleen of Female Rats and Mice in the Three-month Nose-only Inhalation Studies of Fullerene Nano-C ₆₀ (50 nm) and Micro-C ₆₀ (1 μm).....	C-5
Table C-4. Natural Killer Cell Activity in the Spleen of Female Rats and Mice in the Three-month Nose-only Inhalation Studies of Fullerene Nano-C ₆₀ (50 nm) and Micro-C ₆₀ (1 μm).....	C-6
Table C-5. Mixed Leukocyte Response to DBA/2 Mouse Spleen Cells in Female Mice in the Three-month Nose-only Inhalation Studies of Fullerene Nano-C ₆₀ (50 nm) and Micro-C ₆₀ (1 μm).....	C-7
Table C-6. Bronchoalveolar Lavage Cell Phenotypes of Female Rats in the Three-month Nose-only Inhalation Studies of Fullerene Nano-C ₆₀ (50 nm) and Micro-C ₆₀ (1 μm).....	C-8
Table C-7. Cytokine Levels in the Bronchoalveolar Lavage Fluid of Female Rats and Mice in the Three-month Nose-only Inhalation Studies of Fullerene Nano-C ₆₀ (50 nm) and Micro-C ₆₀ (1 μm).....	C-9

Table C-1. Spleen Cell Immunophenotypes in Female Rats and Mice in the Three-month Nose-only Inhalation Studies of Fullerene Nano-C₆₀ (50 nm) and Micro-C₆₀ (1 µm)^a

	50 nm C ₆₀ 0 mg/m ³	50 nm C ₆₀ 0.5 mg/m ³	50 nm C ₆₀ 2 mg/m ³	1.0 µm C ₆₀ 0 mg/m ³	1.0 µm C ₆₀ 2 mg/m ³	1.0 µm C ₆₀ 15 mg/m ³	1.0 µm C ₆₀ 30 mg/m ³
n	8	8	8	8	8	8	8
Female Rats							
Total Spleen Cells (×10 ⁷)	31.82 ± 2.27	31.68 ± 3.45	29.57 ± 2.86	28.27 ± 1.14	31.68 ± 1.75	31.46 ± 1.55	33.22 ± 2.95
CD45+							
Absolute	124.3 ± 8.9	130.7 ± 16.2	110.0 ± 13.2	106.7 ± 4.5	121.1 ± 11.3	119.4 ± 6.8	133.1 ± 12.0
Percent	39.2 ± 1.4	41.6 ± 2.5	36.9 ± 1.4	38.0 ± 1.9	38.1 ± 2.5	38.0 ± 1.5	40.1 ± 1.4
CD5+							
Absolute	106.0 ± 7.2	103.6 ± 13.7	86.6 ± 12.4	84.0 ± 10.2	99.4 ± 7.2	94.3 ± 4.2	101.5 ± 10.5
Percent	33.4 ± 1.2	33.3 ± 3.2	28.9 ± 2.4	29.5 ± 3.2	32.0 ± 2.7	30.1 ± 1.1	30.3 ± 0.7
CD4+CD5+							
Absolute	62.9 ± 3.7 [▲]	59.8 ± 6.6	50.3 ± 7.7	47.9 ± 5.7	57.1 ± 3.4	52.6 ± 3.8	61.1 ± 6.7
Percent	20.0 ± 0.7 [▲]	19.4 ± 1.5	16.7 ± 1.2	16.8 ± 1.8	18.3 ± 1.3	16.7 ± 1.0	18.2 ± 0.7
CD8+CD5+							
Absolute	40.6 ± 4.2	39.7 ± 6.4	33.9 ± 5.4	31.6 ± 4.6	39.7 ± 5.3	33.1 ± 2.1	35.5 ± 4.6
Percent	12.6 ± 0.8	12.8 ± 1.7	11.3 ± 1.3	11.1 ± 1.5	12.8 ± 1.8	10.6 ± 0.7	10.5 ± 0.6
NK+CD8+							
Absolute	9.0 ± 0.9	10.3 ± 1.3	9.0 ± 0.7	10.2 ± 1.0	10.8 ± 1.2	12.1 ± 1.9	9.9 ± 1.5
Percent	2.9 ± 0.3	3.3 ± 0.3	3.1 ± 0.2	3.6 ± 0.4	3.4 ± 0.4	3.8 ± 0.5	3.1 ± 0.6
HIS6+							
Absolute	14.3 ± 1.2	12.0 ± 1.4	13.5 ± 1.2	9.6 ± 1.0	14.6 ± 1.9	15.7 ± 1.9 ^{*b}	11.8 ± 1.6
Percent	4.5 ± 0.3	3.9 ± 0.5	4.8 ± 0.4	3.4 ± 0.3	4.5 ± 0.4	5.1 ± 0.5 ^{*b}	3.5 ± 0.2
Female Mice							
Total Spleen Cells (×10 ⁷)	17.40 ± 0.82 ^{▲▲}	16.13 ± 0.70	14.48 ± 0.45 ^{**}	14.77 ± 0.70	15.12 ± 1.04	14.75 ± 0.65	14.9 ± 0.75
Ig+							
Absolute	112.5 ± 4.3 ^{▲▲}	92.4 ± 4.0 ^{**}	85.4 ± 3.4 ^{**}	107.6 ± 4.8	100.6 ± 5.9	99.2 ± 5.0	101.9 ± 5.3

Fullerene C₆₀, TOX 87

	50 nm C ₆₀ 0 mg/m ³	50 nm C ₆₀ 0.5 mg/m ³	50 nm C ₆₀ 2 mg/m ³	1.0 μm C ₆₀ 0 mg/m ³	1.0 μm C ₆₀ 2 mg/m ³	1.0 μm C ₆₀ 15 mg/m ³	1.0 μm C ₆₀ 30 mg/m ³
Percent	65.0 ± 1.8 [▲]	58.0 ± 3.2	59.1 ± 2.0	72.9 ± 1.0 [▲]	67.0 ± 2.3	67.4 ± 2.5	68.0 ± 1.0*
CD3+							
Absolute	28.2 ± 1.7	22.5 ± 1.1*	23.1 ± 1.2	20.2 ± 1.4	18.7 ± 2.2	20.5 ± 1.7	19.6 ± 2.1
Percent	16.3 ± 1.0	14.1 ± 0.9	16.0 ± 0.8	13.6 ± 0.5	12.2 ± 0.7	13.8 ± 0.6	12.9 ± 0.9
CD4+CD8-							
Absolute	18.4 ± 1.2	15.5 ± 0.8	15.8 ± 0.8	13.6 ± 0.9	12.3 ± 1.9	13.5 ± 1.3	11.8 ± 1.3
Percent	10.6 ± 0.6	9.7 ± 0.5	10.9 ± 0.6	9.1 ± 0.2	7.9 ± 0.8	9.1 ± 0.6	7.8 ± 0.6
CD4-CD8+							
Absolute	7.1 ± 0.4	6.4 ± 0.2	6.1 ± 0.5	6.2 ± 0.3 ^{▲▲}	5.4 ± 0.8	4.8 ± 0.5	3.5 ± 0.4**
Percent	4.1 ± 0.3	4.0 ± 0.2	4.2 ± 0.3	4.2 ± 0.1 ^{▲▲}	3.5 ± 0.3	3.3 ± 0.3*	2.4 ± 0.2**
CD4+CD8+							
Absolute	0.1 ± 0.0	0.1 ± 0.0	0.0 ± 0.0	0.0 ± 0.0	0.0 ± 0.0	0.1 ± 0.0	0.0 ± 0.0
Percent	0.0 ± 0.0	0.0 ± 0.0	0.0 ± 0.0	0.0 ± 0.0	0.0 ± 0.0	0.1 ± 0.0	0.0 ± 0.0
NK1.1+CD3-							
Absolute	2.3 ± 0.2 [▲]	2.2 ± 0.2	1.9 ± 0.1	1.9 ± 0.1	1.8 ± 0.1	2.2 ± 0.2	1.9 ± 0.2
Percent	1.4 ± 0.1	1.4 ± 0.1	1.3 ± 0.1	1.3 ± 0.0	1.2 ± 0.0	1.4 ± 0.1	1.3 ± 0.1
MAC-3+							
Absolute	8.0 ± 0.3	8.2 ± 0.9	6.8 ± 0.4	7.2 ± 0.4 ^{▲▲}	6.8 ± 0.2	5.9 ± 0.4*	5.6 ± 0.5*
Percent	4.6 ± 0.2	5.0 ± 0.5	4.7 ± 0.2	4.9 ± 0.4 ^{▲▲}	4.6 ± 0.3	4.0 ± 0.2	3.8 ± 0.3*

[▲]Significant trend (p ≤ 0.05) by Jonckheere's test.

^{▲▲}p ≤ 0.01.

*Significantly different (p ≤ 0.05) from the respective control group by Shirley's or Dunn's test; **p ≤ 0.01.

^aAll values are presented as mean ± standard error.

^bn = 7.

Table C-2. T-Dependent Antibody Response to Sheep Red Blood Cells in the Spleen of Female Rats and the Spleen and Serum of Female Mice in the Three-month Nose-only Inhalation Studies of Fullerene Nano-C₆₀ (50 nm) and Micro-C₆₀ (1 µm)^a

	50 nm C ₆₀ 0 mg/m ³	50 nm C ₆₀ 0.5 mg/m ³	50 nm C ₆₀ 2 mg/m ³	1.0 µm C ₆₀ 0 mg/m ³	1.0 µm C ₆₀ 2 mg/m ³	1.0 µm C ₆₀ 15 mg/m ³	1.0 µm C ₆₀ 30 mg/m ³
Female Rats							
n	8	8	8	8	8	8	8
Spleen Weight (mg)	451 ± 19 [▲]	467 ± 19	549 ± 31*	441 ± 26	476 ± 23	513 ± 25	503 ± 28
Spleen Cells (×10 ⁷)	36.93 ± 2.20 ^{▲▲}	39.68 ± 2.82	53.53 ± 2.30**	43.00 ± 3.38	44.26 ± 2.93	42.64 ± 4.37	44.13 ± 4.07
IgM PFC/ 10 ⁶ Spleen Cells	3,196 ± 635	3,038 ± 738	3,617 ± 711	3,246 ± 750	2,838 ± 406	4,348 ± 972	3,781 ± 697
IgM PFC/ Spleen (×10 ³)	1,190 ± 274	1,241 ± 316	1,963 ± 384	1,173 ± 34 ^b	1,231 ± 166	1,742 ± 354	1,502 ± 187
Female Mice							
n	8	8	8	8	8	8	7
Spleen Weight (mg)	105 ± 4	107 ± 6	104 ± 5	99 ± 9	107 ± 4	94 ± 10	96 ± 8
Total Spleen Cells (×10 ⁷)	17 ± 1	17 ± 1	17 ± 1	18 ± 1	19 ± 1	17 ± 1	20 ± 1
IgM PFC/ 10 ⁶ Spleen Cells	1,799 ± 83	1,884 ± 159	1,978 ± 157	1,985 ± 196	1,995 ± 84	1,934 ± 48	1,855 ± 98
IgM PFC/ Spleen (×10 ³)	305 ± 21	330 ± 32	340 ± 31	359 ± 35	382 ± 24	336 ± 16	369 ± 28
Serum IgM Titer (log ₂)	6.79 ± 0.12	6.86 ± 0.14	6.97 ± 0.11	6.91 ± 0.14	7.05 ± 0.13	6.73 ± 0.10	6.93 ± 0.12

[▲]Significant trend (p ≤ 0.01) by Jonckheere's test.

^{▲▲}p ≤ 0.01.

*Significantly different (p ≤ 0.05) from the respective control group by Dunnett's test; **significantly different (p ≤ 0.01) from the respective control group by Shirley's test. PFC = plaque-forming cell.

^aAll values are presented as mean ± standard error. All endpoints were measured on the day of sacrifice, 4 days following IV administration of sRBCs.

^bn = 6.

Table C-3. Proliferative Response to Anti-CD3 Antibody in the Spleen of Female Rats and Mice in the Three-month Nose-only Inhalation Studies of Fullerene Nano-C₆₀ (50 nm) and Micro-C₆₀ (1 μm)^a

	50 nm C ₆₀ 0 mg/m ³	50 nm C ₆₀ 0.5 mg/m ³	50 nm C ₆₀ 2 mg/m ³	1.0 μm C ₆₀ 0 mg/m ³	1.0 μm C ₆₀ 2 mg/m ³	1.0 μm C ₆₀ 15 mg/m ³	1.0 μm C ₆₀ 30 mg/m ³
n	8	8	8	8	8	8	8
Female Rats							
Total Spleen Cells (×10 ⁷)	31.8 ± 2.27	31.68 ± 3.45	29.57 ± 2.86	28.27 ± 1.14	31.68 ± 1.75	31.46 ± 1.55	33.22 ± 2.95
Responders (CPM/2 × 10 ⁵ spleen cells)	5,990 ± 829	7,062 ± 666	8,720 ± 1,157	8,018 ± 761	9,184 ± 1,078	7,440 ± 713	8,102 ± 1,670
Responders + Anti-CD3 (CPM/2 × 10 ⁵ spleen cells)	77,244 ± 3,931	67,462 ± 4,778	77,916 ± 5,009	72,199 ± 5,041	79,720 ± 7,380	83,267 ± 4,823	80,855 ± 11,144
Mice							
Total Spleen Cells (×10 ⁷)	17.40 ± 0.82 ^{▲▲}	16.13 ± 0.70	14.48 ± 0.45 ^{**}	14.77 ± 0.70	15.12 ± 1.04	14.75 ± 0.65	14.98 ± 0.75
Responders (CPM/2 × 10 ⁵ spleen cells)	166 ± 22 ^b	167 ± 31	173 ± 24	203 ± 31	108 ± 11 [*]	155 ± 15	166 ± 22
Responders + Anti-CD3 (CPM/2 × 10 ⁵ spleen cells)	37,571 ± 5,458	27,635 ± 4,506	24,416 ± 5,654	30,053 ± 5,922	11,958 ± 4,167	20,099 ± 4,249	24,046 ± 4,023

^{▲▲}Significant trend (p ≤ 0.01) by Jonckheere's test.

^{*}Significantly different (p ≤ 0.05) from the respective control group by Dunn's test; ^{**}significantly different (p ≤ 0.01) from the respective control group by Shirley's test.

^aAll values are presented as mean ± standard error.

^bn = 7.

Table C-4. Natural Killer Cell Activity in the Spleen of Female Rats and Mice in the Three-month Nose-only Inhalation Studies of Fullerene Nano-C₆₀ (50 nm) and Micro-C₆₀ (1 µm)^a

	50 nm C ₆₀ 0 mg/m ³	50 nm C ₆₀ 0.5 mg/m ³	50 nm C ₆₀ 2 mg/m ³	1.0 µm C ₆₀ 0 mg/m ³	1.0 µm C ₆₀ 2 mg/m ³	1.0 µm C ₆₀ 15 mg/m ³	1.0 µm C ₆₀ 30 mg/m ³
n	8	8	8	8	8	8	8
Female Rats							
Spleen Weight (mg)	429 ± 20	446 ± 22	410 ± 28	426 ± 16	406 ± 16	388 ± 12	430 ± 19
%CYT (200 E:T ratio) ^b	23.5 ± 2.4	23.6 ± 2.8	25.1 ± 1.7	24.3 ± 2.9	19.7 ± 2.5	23.7 ± 2.0	25.0 ± 0.7
%CYT (100 E:T ratio)	18.8 ± 2.8	22.8 ± 3.9	22.2 ± 2.3	16.5 ± 2.3	12.1 ± 2.1	15.7 ± 2.0	16.4 ± 1.1
%CYT (50 E:T ratio)	9.2 ± 1.8	12.8 ± 3.0	11.5 ± 1.6	9.5 ± 1.8	6.2 ± 1.3	8.9 ± 1.7	8.7 ± 1.3
%CYT (25 E:T ratio)	4.5 ± 1.6	6.4 ± 2.2	5.4 ± 1.5	3.1 ± 1.5	1.1 ± 1.1	3.1 ± 1.1	3.7 ± 0.8
%CYT (12.5 E:T ratio)	-1.3 ± 1.1	0.9 ± 1.7	0.5 ± 1.0	1.2 ± 1.3	-0.5 ± 0.8	0.6 ± 0.9	1.1 ± 0.7
%CYT (6.25 E:T ratio)	-4.8 ± 0.7	-3.7 ± 1.0	-3.7 ± 0.7	-2.5 ± 0.7	-4.0 ± 0.6	-2.9 ± 0.7	-2.5 ± 0.7
Female Mice							
Spleen Weight (mg)	84 ± 5	69 ± 8	86 ± 6	73 ± 5 [▲]	84 ± 3	87 ± 6	88 ± 4
%CYT (200 E:T ratio)	9.9 ± 1.7	10.1 ± 2.0	6.4 ± 1.5	8.6 ± 1.6	4.2 ± 1.8	7.8 ± 1.9	6.9 ± 1.7
%CYT (100 E:T ratio)	6.6 ± 1.2	5.0 ± 1.5	4.1 ± 1.3	5.1 ± 1.5	1.0 ± 1.7	3.7 ± 1.4	3.8 ± 0.8
%CYT (50 E:T ratio)	3.1 ± 0.9	3.2 ± 0.8	1.9 ± 0.7	1.8 ± 0.7	0.7 ± 0.8	2.6 ± 0.9	1.7 ± 0.6
%CYT (25 E:T ratio)	1.2 ± 0.6	1.0 ± 0.6	0.2 ± 0.5	1.1 ± 0.6	0.2 ± 0.3	1.2 ± 0.5	0.9 ± 0.5
%CYT (12.5 E:T ratio)	-0.9 ± 1.0	-1.0 ± 1.0	-1.2 ± 0.8	-0.6 ± 1.1	-2.8 ± 1.3	0.3 ± 0.5	0.4 ± 0.5
%CYT (6.25 E:T ratio)	-0.4 ± 0.3	-0.7 ± 0.3	-0.7 ± 0.3	0.1 ± 0.4	-0.4 ± 0.4	-0.1 ± 0.3	0.1 ± 0.4

[▲]Significant trend (p ≤ 0.05) by Jonckheere's test.

^aAll values are presented as mean ± standard error.

^bEffector-to-target-cell ratio.

Table C-5. Mixed Leukocyte Response to DBA/2 Mouse Spleen Cells in Female Mice in the Three-month Nose-only Inhalation Studies of Fullerene Nano-C₆₀ (50 nm) and Micro-C₆₀ (1 µm)^a

	50 nm C ₆₀ 0 mg/m ³	50 nm C ₆₀ 0.5 mg/m ³	50 nm C ₆₀ 2 mg/m ³	1.0 µm C ₆₀ 0 mg/m ³	1.0 µm C ₆₀ 2 mg/m ³	1.0 µm C ₆₀ 15 mg/m ³	1.0 µm C ₆₀ 30 mg/m ³
n	8	8	8	8	8	8	8
Total Spleen Cells (×10 ⁷)	17.40 ± 0.82 ^{▲▲}	16.13 ± 0.70	14.48 ± 0.45 ^{**}	14.77 ± 0.70	15.12 ± 1.04	14.75 ± 0.65	14.98 ± 0.75
Responders (CPM/10 ⁵ spleen cells)	545 ± 145	388 ± 63	358 ± 76	440 ± 65	314 ± 62	426 ± 56	278 ± 32
Responders + Stimulators (CPM/10 ⁵ spleen cells)	30,692 ± 4,731	33,844 ± 4,974	23,124 ± 5,550	56,399 ± 13,062	18,271 ± 5,240*	28,889 ± 4,600	28,460 ± 6,736

^{▲▲}Significant trend (p ≤ 0.01) by Jonckheere's test.

*Significantly different (p ≤ 0.05) from the respective control group by Dunn's test; **significantly different (p ≤ 0.01) from the respective control group by Shirley's test.

^aAll values are presented as mean ± standard error.

Table C-6. Bronchoalveolar Lavage Cell Phenotypes of Female Rats in the Three-month Nose-only Inhalation Studies of Fullerene Nano-C₆₀ (50 nm) and Micro-C₆₀ (1 µm)^a

	50 nm C ₆₀ 0 mg/m ³	50 nm C ₆₀ 0.5 mg/m ³	50 nm C ₆₀ 2 mg/m ³	1.0 µm C ₆₀ 0 mg/m ³	1.0 µm C ₆₀ 2 mg/m ³	1.0 µm C ₆₀ 15 mg/m ³	1.0 µm C ₆₀ 30 mg/m ³
n	8	8	8	8	8	8	8
BAL Cells (×10 ⁵)	10.77 ± 0.71	10.30 ± 0.72	9.80 ± 0.65	10.18 ± 0.71	9.90 ± 0.85	9.78 ± 1.12	14.92 ± 1.92
CD163+CD11b-							
Absolute	0.42 ± 0.09	0.53 ± 0.19	0.22 ± 0.06	0.47 ± 0.24	0.13 ± 0.02	0.21 ± 0.08	0.28 ± 0.06
Percent	0.38 ± 0.07	0.54 ± 0.18	0.24 ± 0.06	0.42 ± 0.20	0.13 ± 0.02	0.20 ± 0.07	0.23 ± 0.07
CD163+CD11b+							
Absolute	13.54 ± 3.76 ^{▲▲}	1.87 ± 0.88 ^{**}	1.16 ± 0.48 ^{**}	19.36 ± 8.71 [▲]	0.38 ± 0.11 ^{**}	0.35 ± 0.14 ^{**}	1.07 ± 0.34
Percent	12.37 ± 3.06 ^{▲▲}	1.79 ± 0.76 ^{**}	1.34 ± 0.63 ^{**}	17.25 ± 7.12 ^{▲▲}	0.37 ± 0.09 ^{**}	0.32 ± 0.12 ^{**}	0.88 ± 0.31 ^{**}
CD163-CD11b-							
Absolute	92.60 ± 6.54	95.77 ± 6.87	92.88 ± 7.85	80.39 ± 7.93 [▲]	97.45 ± 8.34	96.54 ± 10.93	137.2 ± 20.23 [*]
Percent	86.17 ± 3.39 [▲]	93.27 ± 3.02	94.07 ± 3.44	80.93 ± 7.64	98.50 ± 0.53 ^{**}	98.79 ± 0.31 ^{**}	90.52 ± 2.88
CD163-CD11b+							
Absolute	1.14 ± 0.28	4.82 ± 2.64	3.74 ± 2.13	1.59 ± 0.54 ^{▲▲}	1.04 ± 0.54	0.72 ± 0.20	10.62 ± 2.85 ^{**}
Percent	1.08 ± 0.29	4.40 ± 2.13	4.36 ± 2.77	1.40 ± 0.42 [▲]	0.99 ± 0.45	0.69 ± 0.16	8.37 ± 2.53 [*]

[▲]Significant trend (p ≤ 0.05) by Jonckheere's test.

^{▲▲}p ≤ 0.01.

^{*}Significantly different (p ≤ 0.05) from the respective control group by Shirley's or Dunn's test; ^{**}p ≤ 0.01.

^aAll values are presented as mean ± standard error. BAL = bronchoalveolar lavage.

Table C-7. Cytokine Levels in the Bronchoalveolar Lavage Fluid of Female Rats and Mice in the Three-month Nose-only Inhalation Studies of Fullerene Nano-C₆₀ (50 nm) and Micro-C₆₀ (1 µm)^a

	50 nm C ₆₀ 0 mg/m ³	50 nm C ₆₀ 0.5 mg/m ³	50 nm C ₆₀ 2 mg/m ³	1.0 µm C ₆₀ 0 mg/m ³	1.0 µm C ₆₀ 2 mg/m ³	1.0 µm C ₆₀ 15 mg/m ³	1.0 µm C ₆₀ 30 mg/m ³
n	8	8	8	8	8	8	8
Female Rats							
IL-1 (pg/mL)							
Neat	15.09 ± 7.89	17.18 ± 9.04	0.00 ± 0.00	35.88 ± 8.59	10.00 ± 6.56	11.50 ± 8.32	16.9 ± 7.23
Concentrated	17.86 ± 8.69	16.79 ± 8.35	2.83 ± 2.83	4.35 ± 4.35 ^{▲▲}	26.97 ± 12.37	35.28 ± 8.80*	73.72 ± 13.74**
MCP-1 (pg/mL)							
Neat	5.67 ± 2.56	4.24 ± 1.93	2.18 ± 1.49	13.70 ± 2.44	4.24 ± 1.99	4.00 ± 2.74	89.09 ± 31.32
Concentrated	93.41 ± 23.95	66.05 ± 13.36	74.88 ± 19.01	65.44 ± 21.71 ^{▲▲}	47.95 ± 7.01	68.64 ± 13.90	622.4 ± 146.8**
TNF-α (pg/mL)							
Neat	4.56 ± 3.05	2.42 ± 2.42	0.00 ± 0.00	21.89 ± 5.21 [▲]	6.50 ± 4.44	4.37 ± 4.37*	4.28 ± 2.80*
Concentrated	11.25 ± 3.45 [▲]	8.29 ± 4.23	0.00 ± 0.00*	4.71 ± 3.14	12.51 ± 6.72	14.70 ± 5.17	8.68 ± 4.30
IFN-γ (pg/mL)							
Neat	0.00 ± 0.00	0.00 ± 0.00	0.00 ± 0.00	0.00 ± 0.00	0.00 ± 0.00	0.00 ± 0.00	0.00 ± 0.00
Concentrated	0.00 ± 0.00	0.00 ± 0.00	0.00 ± 0.00	0.00 ± 0.00	0.00 ± 0.00	0.00 ± 0.00	0.00 ± 0.00
GM-CSF (pg/mL)							
Neat	22.10 ± 11.11	28.40 ± 11.11	0.00 ± 0.00	53.60 ± 12.62	16.97 ± 11.14	10.00 ± 10.00*	21.68 ± 10.62
Concentrated	36.56 ± 11.35 [▲]	21.75 ± 10.82	5.66 ± 5.66	12.80 ± 8.45	38.30 ± 15.56	42.58 ± 10.33	26.90 ± 13.49
IL-4							
Neat	0.19 ± 0.14	0.10 ± 0.10	0.00 ± 0.00	0.79 ± 0.31 [▲]	0.10 ± 0.10	0.20 ± 0.20	0.05 ± 0.05*
Concentrated	0.00 ± 0.00	0.00 ± 0.00	0.00 ± 0.00	0.00 ± 0.00	0.21 ± 0.21	0.00 ± 0.00	0.00 ± 0.00

Female Mice

Fullerene C₆₀, TOX 87

	50 nm C ₆₀ 0 mg/m ³	50 nm C ₆₀ 0.5 mg/m ³	50 nm C ₆₀ 2 mg/m ³	1.0 µm C ₆₀ 0 mg/m ³	1.0 µm C ₆₀ 2 mg/m ³	1.0 µm C ₆₀ 15 mg/m ³	1.0 µm C ₆₀ 30 mg/m ³
IL-13 (pg/mL)							
Neat	45.38 ± 5.89	35.67 ± 4.64	50.68 ± 5.29	35.61 ± 3.94	49.11 ± 4.77	33.84 ± 3.78	39.69 ± 7.41
Concentrated	77.41 ± 17.23	74.28 ± 9.63	48.29 ± 7.68	37.90 ± 9.18	47.7 ± 8.93	46.51 ± 4.95	51.75 ± 11.02
IL-1 (pg/mL)							
Neat	79.04 ± 12.18	68.83 ± 10.14	85.32 ± 7.81	52.60 ± 8.69	86.96 ± 12.47	62.73 ± 9.96	68.73 ± 16.05
Concentrated	138.5 ± 16.37	141.2 ± 8.28	108.2 ± 16.22	99.89 ± 11.97	111.5 ± 8.56	111.4 ± 4.90	106.5 ± 17.37
IL-2 (pg/mL)							
Neat	187.5 ± 14.66	151.4 ± 9.67	180.0 ± 17.76	149.8 ± 13.96	196.5 ± 19.50	137.7 ± 19.12	164.1 ± 29.50
Concentrated	233.7 ± 24.62	235.4 ± 10.91	183.0 ± 27.17	186.8 ± 18.67	201.3 ± 12.46	201.4 ± 9.48	204.7 ± 22.67
IL-5 (pg/mL)							
Neat	119.5 ± 19.56	106.9 ± 13.64	119.5 ± 15.42	86.97 ± 14.80	129.9 ± 17.21	102.0 ± 15.73	104.7 ± 22.74
Concentrated	222.2 ± 26.73	224.7 ± 13.64	167.7 ± 25.58	152.5 ± 18.28	183.6 ± 13.96	181.8 ± 11.01	172.6 ± 27.86
MCP-1 (pg/mL)							
Neat	429.7 ± 82.27	253.7 ± 68.57	388.7 ± 75.37	345.2 ± 69.45	531.3 ± 89.76	283.2 ± 70.15	507.3 ± 97.61
Concentrated	1,096 ± 152.1	1,171 ± 59.37	846.3 ± 125.7	861.0 ± 86.15	959.0 ± 88.24	902.9 ± 44.02	1,223 ± 142.9
IL-6 (pg/mL)							
Neat	16.30 ± 5.60	7.23 ± 4.51	18.25 ± 6.83	8.50 ± 4.84	21.36 ± 6.88	4.93 ± 2.64	19.13 ± 6.08
Concentrated	68.62 ± 7.93 [▲]	68.89 ± 4.59	52.70 ± 4.61	50.91 ± 4.08	55.97 ± 4.40	55.57 ± 2.22	60.56 ± 6.04
MIP-1α (pg/mL)							
Neat	0.18 ± 0.18	0.0 ± 0.0	2.06 ± 1.37	0.0 ± 0.0 ^{▲▲}	0.65 ± 0.65	2.36 ± 0.95 ^{**}	94.09 ± 12.25 ^{**}
Concentrated	6.76 ± 3.28	6.17 ± 1.79	11.89 ± 2.84	0.74 ± 0.74 ^{▲▲}	1.95 ± 1.13	23.12 ± 3.16 ^{**}	236.6 ± 38.38 ^{**}
IL-10 (pg/mL)							
Neat	32.37 ± 9.88	9.91 ± 9.91	21.83 ± 9.04	27.45 ± 9.32	53.53 ± 18.89	10.02 ± 3.80	42.86 ± 11.87
Concentrated	130.8 ± 25.95	122.3 ± 16.79	79.04 ± 12.85	62.00 ± 11.64	77.01 ± 14.03	84.70 ± 8.97	91.78 ± 18.51
RANTES (pg/mL)							

Fullerene C₆₀, TOX 87

	50 nm C₆₀ 0 mg/m³	50 nm C₆₀ 0.5 mg/m³	50 nm C₆₀ 2 mg/m³	1.0 μm C₆₀ 0 mg/m³	1.0 μm C₆₀ 2 mg/m³	1.0 μm C₆₀ 15 mg/m³	1.0 μm C₆₀ 30 mg/m³
Neat	35.99 ± 12.15	14.64 ± 12.00	41.43 ± 12.01	12.76 ± 9.72	46.85 ± 15.51	9.65 ± 4.52	42.03 ± 13.15
Concentrated	78.07 ± 21.26	74.14 ± 12.82	39.05 ± 5.94	26.58 ± 8.72	31.54 ± 9.36	32.25 ± 6.79	47.54 ± 12.60
IFN-γ (pg/mL)							
Neat	34.00 ± 10.17	19.72 ± 7.25	36.39 ± 9.59	15.01 ± 7.81	42.16 ± 14.22	15.4 ± 3.70	35.17 ± 9.08
Concentrated	98.55 ± 19.47	90.58 ± 10.29	59.32 ± 9.26	45.30 ± 9.45	62.23 ± 8.24	59.81 ± 4.36	67.26 ± 14.59
TNF-α (pg/mL)							
Neat	16.46 ± 6.77	5.75 ± 5.75	15.18 ± 6.94	7.68 ± 4.74	20.86 ± 7.67	3.26 ± 2.00	20.14 ± 5.93
Concentrated	55.24 ± 14.23	53.74 ± 6.73	30.26 ± 4.53	25.29 ± 3.96	31.46 ± 4.00	29.15 ± 1.74	38.04 ± 8.32
GM-CSF (pg/mL)							
Neat	109.2 ± 18.14	95.19 ± 11.29	137.9 ± 12.91	90.46 ± 17.38	133.8 ± 16.50	79.47 ± 12.36	107.7 ± 24.82
Concentrated	194.3 ± 22.56	193.8 ± 11.31	144.3 ± 21.27	145.2 ± 12.26	158.5 ± 11.68	159.2 ± 4.25	153.4 ± 24.56
IL-4							
Neat	21.78 ± 8.10	10.20 ± 7.89	26.36 ± 11.50	14.91 ± 7.29	42.06 ± 15.07	6.83 ± 3.59	35.06 ± 10.51
Concentrated	102.1 ± 21.65	98.18 ± 13.09	60.20 ± 10.76	49.82 ± 10.60	59.47 ± 11.67	57.64 ± 5.44	63.33 ± 14.39
IL-17 (pg/mL)							
Neat	3.35 ± 3.21	2.40 ± 2.40	8.10 ± 5.73	3.80 ± 3.80	14.87 ± 8.21	0.00 ± 0.00	12.73 ± 4.01
Concentrated	43.89 ± 14.20	44.08 ± 8.66	22.09 ± 5.37	12.60 ± 5.37	20.88 ± 6.39	19.04 ± 4.29	27.52 ± 9.54

▲Significant trend ($p \leq 0.05$) by Jonckheere's test.

▲▲ $p \leq 0.01$.

*Significantly different ($p \leq 0.05$) from the respective control group by Shirley's or Dunn's test; ** $p \leq 0.01$.

^aAll values are presented as mean ± standard error.

Appendix D. Genetic Toxicology

Tables

Table D-1. Frequency of Micronucleated Erythrocytes in Peripheral Blood of Rats Following Treatment with Fullerene Micro-C ₆₀ (1 μm) by Nose-only Inhalation for Three Months.....	D-2
Table D-2. Frequency of Micronucleated Erythrocytes in Peripheral Blood of Rats Following Treatment with Fullerene Nano-C ₆₀ (50 nm) by Nose-only Inhalation for Three Months.....	D-3
Table D-3. Frequency of Micronucleated Erythrocytes in Peripheral Blood of Mice Following Treatment with Fullerene Micro-C ₆₀ (1 μm) by Nose-only Inhalation for Three Months.....	D-4
Table D-4. Frequency of Micronucleated Erythrocytes in Peripheral Blood of Mice Following Treatment with Fullerene Nano-C ₆₀ (50 nm) by Nose-only Inhalation for Three Months.....	D-5

Table D-1. Frequency of Micronucleated Erythrocytes in Peripheral Blood of Rats Following Treatment with Fullerene Micro-C₆₀ (1 µm) by Nose-only Inhalation for Three Months^a

	Concentration (mg/m ³)	Number of Rats with Erythrocytes Scored	Micronucleated PCEs/1,000 PCEs ^b	P Value ^c	Micronucleated NCEs/1,000 NCEs ^b	P Value ^c	PCEs ^b (%)	P Value ^c
Male								
Air ^d	0	5	0.74 ± 0.12		0.03 ± 0.01		0.989 ± 0.07	
Fullerene C ₆₀	2	5	0.62 ± 0.10	1.0000	0.05 ± 0.02	0.1780	1.050 ± 0.12	0.7245
	15	5	0.88 ± 0.18	0.8863	0.06 ± 0.01	0.1503	1.135 ± 0.06	0.3396
	30	5	0.60 ± 0.09	1.0000	0.04 ± 0.01	0.1599	1.124 ± 0.10	0.3616
			p = 0.607 ^e		p = 0.395 ^f		p = 0.252 ^f	
Female								
Air	0	5	0.62 ± 0.09		0.08 ± 0.02		1.243 ± 0.10	
Fullerene C ₆₀	2	5	0.79 ± 0.14	0.1737	0.04 ± 0.01	0.8514	1.272 ± 0.10	0.9531
	15	5	0.94 ± 0.17	0.1268	0.04 ± 0.01	0.9125	1.338 ± 0.25	0.9947
	30	5	0.76 ± 0.06	0.1342	0.07 ± 0.01	0.7281	1.225 ± 0.12	0.9908
			p = 0.266 ^f		p = 0.372 ^f		p = 0.845 ^f	

NCE = normochromatic erythrocyte; PCE = polychromatic erythrocyte.

^aStudy was performed at ILS, Inc. The detailed protocol is presented by Witt et al.⁸²

^bMean ± standard error.

^cPairwise comparison with the control group; significant if $p \leq 0.025$ by Dunn's or Williams' test.

^dControl.

^eSignificance tested by Jonckheere's trend test; significant if $p \leq 0.025$.

^fSignificance tested by a linear regression trend test; significant if $p \leq 0.025$.

Table D-2. Frequency of Micronucleated Erythrocytes in Peripheral Blood of Rats Following Treatment with Fullerene Nano-C₆₀ (50 nm) by Nose-only Inhalation for Three Months^a

	Concentration (mg/m ³)	Number of Rats with Erythrocytes Scored	Micronucleated PCEs/1,000 PCEs ^b	P Value ^c	Micronucleated NCEs/1,000 NCEs ^b	P Value ^c	PCEs ^b (%)	P Value ^c
Male								
Air ^d	0	5	0.84 ± 0.13		0.06 ± 0.01		0.930 ± 0.10	
Fullerene C ₆₀	0.5	5	0.73 ± 0.16	0.5925	0.06 ± 0.01	0.7256	0.867 ± 0.06	0.7408
	2	5	0.84 ± 0.19	0.5837	0.03 ± 0.00	0.8077	0.883 ± 0.11	0.8437
			p = 0.438 ^e		p = 0.983		p = 0.763	
Female								
Air	0	5	0.87 ± 0.07		0.13 ± 0.03		1.044 ± 0.08	
Fullerene C ₆₀	0.5	5	0.83 ± 0.10	0.6902	0.05 ± 0.01	0.9586	1.038 ± 0.07	0.9775
	2	5	0.74 ± 0.07	0.7746	0.05 ± 0.01	0.9824	1.026 ± 0.15	0.8548
			p = 0.883		p = 0.963		p = 0.701	

NCE = normochromatic erythrocyte; PCE = polychromatic erythrocyte.

^aStudy was performed at ILS, Inc. The detailed protocol is presented by Witt et al.⁸²

^bMean ± standard error.

^cPairwise comparison with the control group; significant if $p \leq 0.025$ by Williams' test.

^dControl group.

^eSignificance tested by a linear regression trend test; significant if $p \leq 0.025$.

Table D-3. Frequency of Micronucleated Erythrocytes in Peripheral Blood of Mice Following Treatment with Fullerene Micro-C₆₀ (1 µm) by Nose-only Inhalation for Three Months^a

	Concentration (mg/m ³)	Number of Mice with Erythrocytes Scored	Micronucleated PCEs/1,000 PCEs ^b	P Value ^c	Micronucleated NCEs/1,000 NCEs ^b	P Value ^c	PCEs ^b (%)	P Value ^c
Male								
Air ^d	0	5	2.72 ± 0.12		1.49 ± 0.05		1.494 ± 0.12	
Fullerene C ₆₀	2	5	2.67 ± 0.19	0.5642	1.38 ± 0.05	0.8838	1.786 ± 0.14	0.5306
	15	5	2.66 ± 0.20	0.6514	1.38 ± 0.03	0.9366	1.761 ± 0.10	0.6337
	30	5	2.98 ± 0.11	0.1776	1.39 ± 0.05	0.9527	1.372 ± 0.16	0.5467
				p = 0.100 ^e		p = 0.835 ^e		p = 0.204 ^e
Female								
Air	0	5	1.68 ± 0.09		1.00 ± 0.01		1.428 ± 0.09	
Fullerene C ₆₀	2	5	2.32 ± 0.18	0.0276	1.04 ± 0.03	0.5886	1.617 ± 0.09	0.4532
	15	5	1.85 ± 0.09	0.0328	0.97 ± 0.01	1.0000	1.642 ± 0.18	0.5448
	30	5	2.00 ± 0.13	0.0348	1.00 ± 0.02	1.0000	1.588 ± 0.20	0.5801
				p = 0.485 ^e		p = 0.770 ^f		p = 0.788 ^e

NCE = normochromatic erythrocyte; PCE = polychromatic erythrocyte.

^aStudy was performed at ILS, Inc. The detailed protocol is presented by Witt et al.⁸²

^bMean ± standard error.

^cPairwise comparison with the control group; significant if $p \leq 0.025$ by Dunn's or Williams' test.

^dControl group.

^eSignificance tested by a linear regression trend test; significant if $p \leq 0.025$.

^fSignificance tested by Jonckheere's trend test; significant if $p \leq 0.025$.

Table D-4. Frequency of Micronucleated Erythrocytes in Peripheral Blood of Mice Following Treatment with Fullerene Nano-C₆₀ (50 nm) by Nose-only Inhalation for Three Months^a

	Concentration (mg/m ³)	Number of Mice with Erythrocytes Scored	Micronucleated PCEs/1,000 PCEs ^b	P Value ^c	Micronucleated NCEs/1,000 NCEs ^b	P Value ^c	PCEs ^b (%)	P Value ^c
Male								
Air ^d	0	5	2.42 ± 0.22		1.54 ± 0.08		1.559 ± 0.06	
Fullerene C ₆₀	0.5	5	2.33 ± 0.09	0.5650	1.48 ± 0.02	0.7532	1.683 ± 0.07	0.3173
	2	5	2.50 ± 0.22	0.4558	1.44 ± 0.02	0.8323	1.615 ± 0.05	0.3814
			p = 0.327 ^e		p = 0.889 ^e		p = 0.765 ^e	
Female								
Air	0	5	2.03 ± 0.08		1.05 ± 0.03		1.583 ± 0.10	
Fullerene C ₆₀	0.5	5	1.92 ± 0.22	0.7029	1.02 ± 0.01	0.6615	1.741 ± 0.04	0.5777
	2	5	1.77 ± 0.14	0.7871	1.09 ± 0.03	0.1005	1.715 ± 0.21	1.0000
			p = 0.872 ^e		p = 0.043 ^e		p = 0.634 ^f	

NCE = normochromatic erythrocyte; PCE = polychromatic erythrocyte.

^aStudy was performed at ILS, Inc. The detailed protocol is presented by Witt et al.⁸²

^bMean ± standard error.

^cPairwise comparison with the control group; values are significant if $p \leq 0.025$ by Dunn's or Williams' test.

^dControl.

^eSignificance tested by a linear regression trend test; significant if $p \leq 0.025$.

^fSignificance tested by Jonckheere's trend test; significant if $p \leq 0.025$.

Appendix E. Chemical Characterization and Generation of Carousel Concentrations

Table of Contents

E.1. Procurement and Characterization of Bulk Fullerene C ₆₀	E-2
E.2. Aerosol Generation and Exposure System for the Micro-C ₆₀ Studies	E-3
E.3. Aerosol Generation and Exposure System for the Nano-C ₆₀ Studies	E-4
E.4. Aerosol Concentration Monitoring for the Micro-C ₆₀ and Nano-C ₆₀ Studies.....	E-4
E.5. Carousel Atmosphere Characterization or the Micro-C ₆₀ and Nano-C ₆₀ Studies	E-5

Tables

Table E-1. Summary of Carousel Concentrations in the Three-month Nose-only Inhalation Studies of Fullerene Micro-C ₆₀ (1 μm)	E-8
Table E-2. Summary of Carousel Concentrations in the Three-month Nose-only Inhalation Studies of Fullerene Nano-C ₆₀ (50 nm).....	E-8
Table E-3. Summary of Aerosol Size Measurements and Aerosol Surface-Area-to-Mass Ratios for the Rat and Mouse Exposure Carousels in the Three-month Nose-only Inhalation Studies of Fullerene Micro-C ₆₀ (1 μm)	E-9
Table E-4. Summary of Aerosol Size Measurements for the Rat and Mouse Exposure Carousels in the Three-month Nose-only Inhalation Studies of Fullerene Nano-C ₆₀ (50 nm)	E-9
Table E-5. Summary of Aerosol Surface-Area-to-Mass Ratios for the Rat and Mouse Exposure Carousels in the Three-month Nose-only Inhalation Studies of Fullerene Nano-C ₆₀ (50 nm)	E-10

Figures

Figure E-1. Infrared Absorption Spectrum of Bulk Fullerene C ₆₀	E-11
Figure E-2. Laser Raman Spectrum of Bulk Fullerene C ₆₀	E-11
Figure E-3. X-ray Diffraction Pattern of Bulk Fullerene C ₆₀	E-12
Figure E-4. Schematic of the Aerosol Generation and Delivery System in the Three-month Nose-only Inhalation Studies of Fullerene Micro-C ₆₀ (1 μm)	E-13
Figure E-5. Schematic of the Aerosol Generation and Delivery System in the Three-month Nose-only Inhalation Studies of Fullerene Nano-C ₆₀ (50 nm).....	E-14

E.1. Procurement and Characterization of Bulk Fullerene C₆₀

Fullerene C₆₀ was obtained from SES Research (Houston, TX) in one lot (BT-6947). The study laboratory milled the test chemical in a ball mill to reduce particle size. After milling, initial purity and exposure testing revealed an insoluble impurity that was not present in the original unmilled material. The milled fullerene C₆₀ was sent back to the manufacturer for repurification. The reprocessed fullerene C₆₀ with the impurity removed (99.5% pure) was received from SES Research in one lot (BT-6947-Reprocess) that was used during the 3-month studies. Identity, purity, and moisture analyses were performed by the study laboratory at Battelle Toxicology Northwest [Richland, WA; high-performance liquid chromatography (HPLC) and gas chromatography (GC) analyses] and by the analytical chemistry laboratories at Cyanta Analytical Services [Maryland Heights, MO; Fourier transform infrared (FTIR) spectroscopy, elemental analyses, and Karl Fisher titration]; H & M Analytical Services, Inc. [Allentown, NJ; X-ray diffraction (XRD) analysis]; and Pacific Northwest National Laboratory (Richland, WA; laser Raman analysis). Reports on analyses performed in support of the fullerene C₆₀ studies are on file at the National Institute of Environmental Health Sciences.

Lot BT-6947-Reprocess of the chemical, a black solid with no detectable odor, was identified as fullerene C₆₀ by FTIR and laser Raman spectroscopy and XRD analyses. The FTIR and laser Raman spectra of the test chemical were consistent with literature spectra (FTIR; Nakamoto and McKinney⁶⁵) and the structure and composition of fullerene C₆₀. XRD with Rietveld analysis showed only the face-centered cubic polymorph of fullerene C₆₀. Representative FTIR, laser Raman, and XRD spectra are presented in Figure E-1, Figure E-2, and Figure E-3, respectively.

Karl Fischer titration was used to determine the water content of lot BT-6947-Reprocess. The purity of the bulk chemical was determined by elemental analysis, GC by system A, and HPLC by system B.

- A) Agilent gas chromatograph (model 6890; Agilent Technologies, Inc., Palo Alto, CA), a DB-5 (30 m × 0.53 mm ID, 5.0 μm film thickness) column (J&W Scientific, Folsom, CA), flame ionization detection (FID), helium as the carrier gas at 6.0 psi head pressure, and an oven temperature program of 45°C for 10 minutes, then 20°C/minute to 270°C, then held for 10 minutes
- B) Agilent high-performance liquid chromatograph (model 1100; Agilent Technologies, Inc.), a Buckyprep (4.6 mm × 250 mm) column (Waters Corporation, Milford, MA), a mobile phase of A) *n*-hexane:toluene (70:30) and B) toluene:chlorobenzene (70:30) with a linear gradient program of 100% A to 100% B in 30 minutes, held for 30 minutes, to 100% A in 5 minutes, held for 5 minutes, with ultraviolet/visible detection at 330 nm, and a flow rate of 1.0 mL/minute

For lot BT-6947-Reprocess, Karl Fischer titration indicated a water content of less than 900 ppm. Elemental analyses showed a composition of 99.7% carbon, 0.24% nitrogen, less than 0.1% hydrogen, and less than 300 ppm sulfur. GC/FID by system A indicated one residual solvent, 1,2,4-trimethylbenzene (TMB) at 0.8% (predrying) and 0.6% (postdrying). HPLC by system B indicated an area percent purity of 98.5%. The overall purity of lot BT-6947-Reprocess was determined to be at least 98.5%.

To ensure stability, the bulk chemical was stored at room temperature in amber glass containers. Periodic reanalyses of the bulk chemical were performed during the 3-month studies by the study laboratory using HPLC by system B; no degradation of the bulk chemical was detected.

E.2. Aerosol Generation and Exposure System for the Micro-C₆₀ Studies

A diagram of the fullerene C₆₀ (1 μm) aerosol generation and delivery system used in the studies is shown in Figure E-4. The system used a linear feed powder-metering device, particle attrition chamber, dispersion jet, and cyclone separator all located within a glove box in the exposure room. The air-driven shuttle bar in the powder-metering device dispersed the bulk material at timed intervals into a nitrogen gas stream; the nitrogen gas was used to minimize oxidation of the test chemical during the vaporization phase. The material suspended in the gas stream was further reduced in size by passing through the particle attrition chamber, which used a pressurized nitrogen stream to promote particle-to-particle impaction, breaking apart the particles. A high-pressure dispersion jet at the output of the particle attrition chamber added dispersion energy to drive the aerosol into the cyclone separator, which removed unwanted large particles from the aerosol stream. The aerosol stream from the glove box was directed to a residence chamber to allow for additional separation of larger particles by gravitational settling. The residence chamber was monitored to maintain generator output consistency using a real-time aerosol monitor (RAM) (Micro Dust *pro*, Casella USA, Amherst, NH), and material in excess of that required to maintain the exposure units at target concentrations was withdrawn through high-efficiency particulate air (HEPA) filters prior to delivery to the residence chamber. Aerosol was delivered from the residence chamber to each exposure carousel through a metering element that fixed the flow to each carousel. Humidified air was added to the aerosol-laden air downstream from the metering element to provide dilution and humidify the airstream. Concentration was controlled by siphoning excess delivery flow from a point following the metering element but before the introduction of dilution air. Past the dilution air input, aerosol-laden air was directed to a computer-controlled pneumatic slide valve that served as the on/off control valve for the flow through a dedicated distribution system branch line to each exposure carousel.

The rodent exposure carousel was developed by the study laboratory and consisted of stackable tiers with 16 nose-only exposure ports per tier. Each carousel consisted of five tiers thus providing 80 ports for animal exposure. One end of the tube that served to restrain the individual was tapered to approximately fit the shape of the animal's head and the diameter of the remaining cylindrical portion of the tube made it difficult for the animal to turn in the tube. The back portion of the tube was covered with a plastic cap, and tubes containing animals were fastened to the inhalation carousel by means of a bracket, ensuring the nose portion of the tube protruded through a gasket and into the carousel.

The test aerosol entered the carousel through the top and then flowed out radially to each of the 16 evenly spaced exposure ports per tier. Each port received approximately 500 mL/minute of exposure atmosphere, which equated to a total exposure unit inlet flow of 40 L/minute. Ports not used for animal exposure or sampling were closed. This design provided uniform concentration and fresh test chemical to each animal connected to the exposure system and minimized any effect of the animals on the atmosphere because no exhaled air from one animal could reach the

breathing zone of another. Each exposure carousel was surrounded by a temperature-controlled ventilated enclosure that minimized the release of aerosol from the carousel to the room and provided a means of cooling the animals confined to the nose tubes.

E.3. Aerosol Generation and Exposure System for the Nano-C₆₀ Studies

A diagram of the fullerene C₆₀ (50 nm) aerosol generation and delivery system used in the studies is shown in Figure E-5. The aerosol generation and delivery system used the same glove box and residence chamber components as described for the micro-C₆₀ studies; but for the nano-C₆₀ studies, the aerosol-laden airstream from the residence chamber was directed into four identically configured delta tubes designed to provide a metered flow in relation to the pressure drop maintained in the residence chamber. Downstream from each delta tube, a flowmeter-controlled siphon allowed for regulation of the flow into quartz tube furnaces present at a target of approximately 520°C for flash vaporization of the test article. Near the exit of each furnace tube, additional nitrogen gas was introduced into the flow to rapidly cool the vaporized test material, condensing it into nanometer-sized particles. The additional nitrogen also increased the velocity of the carrier stream, diluted the concentration of the particles, and reduced the opportunity for particle agglomeration. Humidified air was added to the aerosol-laden nitrogen gas stream that exited each furnace tube to provide additional dilution, cooling, humidification, and oxygenation to the exposure atmosphere.

Subsequent aerosol flow through the computer-controlled pneumatic slide valves and exposure carousels was as described for the micro-C₆₀ studies except that a second siphon and dilution air assembly was located just prior to the slide valves to further reduce aerosol concentrations in the test atmosphere. Exposure carousels for the nano-C₆₀ studies provided a total of 40 ports for animal exposure via 8 ports on each of the 5 tiers.

E.4. Aerosol Concentration Monitoring for the Micro-C₆₀ and Nano-C₆₀ Studies

Summaries of the carousel aerosol concentrations are presented in Table E-1 and Table E-2. For the micro-C₆₀ studies, micrometer-sized fullerene C₆₀ aerosol was monitored for concentration using an online RAM (MicroDust *pro*; Casella USA). For the nano-C₆₀ studies, nanometer-sized fullerene C₆₀ was similarly monitored using a RAM-1 instrument (MIE, Inc., Bedford, MA). The analog output voltage from each RAM was recorded by the Battelle Exposure Data Acquisition and Control (BEDAC) software system and converted to mg/m³ exposure concentration by the application of a calibration curve. During the studies, if a measured concentration exceeded its allowed limits, the BEDAC program triggered an audible alarm or, in extreme cases, terminated the exposure.

RAM calibrations were performed by constructing response curves using RAM voltage recorded each day at the time duplicate atmosphere samples were collected from each exposure carousel on 25 mm Teflon[®]-coated glass-fiber filters (Pallflex[®] Emfab[™] TX40HI20WW filters; Pall Corporation, Ann Arbor, MI); RAM voltages were corrected for zero-offset voltage measured in a HEPA-filtered airstream. Fullerene C₆₀ collected on the filters from each exposure carousel was dissolved in a 50:50 mixture of TMB:toluene containing a known amount of internal

standard (fullerene-C70; MER Corporation, Tucson, AZ) and quantified using HPLC by system C on an off-line chromatograph.

- C) Agilent high-performance liquid chromatograph (model 1100; Agilent Technologies, Inc.), a Buckyprep (4.6 mm × 250 mm) column (Waters Corporation), an isocratic mobile phase of 100% toluene, ultraviolet/visible detection at 330 nm, and a flow rate of 1.0 mL/minute

The off-line chromatograph was calibrated using gravimetrically prepared standard solutions of the test article and the internal standard in 50:50 TMB:toluene. These methods were demonstrated by the study laboratory to have adequate precision, accuracy, linear working range, day-to-day repeatability, and detection limits for measuring 1 µm and 50 nm fullerene C₆₀ concentrations in the exposure carousels.

E.5. Carousel Atmosphere Characterization or the Micro-C₆₀ and Nano-C₆₀ Studies

Aerosol particle size distribution was determined once prior to and approximately monthly during the micro-C₆₀ studies by collecting aerosol samples from each exposure carousel (except the 0 mg/m³ carousels) using a Mercer style cascade impactor. Fullerene C₆₀ was collected on stages one through seven within the impactor on 22 mm diameter stainless steel slides (In-Tox Products, Moriarty, NM) coated with silicone spray. The final, stage eight sample was collected on a 25 mm diameter Pallflex[®] Emfab[™] glass-fiber filter (Pall Corporation). Collected aerosol was dissolved in a 50:50 mixture of TMB:toluene and assayed for mass of test material using HPLC by system C. The relative mass collected on each stage was analyzed by the probit-based CASPACT impactor analysis program developed at the study laboratory⁶⁶ to yield estimates of the mass median aerodynamic diameter (MMAD) of the particles.

The surface-area-to-mass ratio of micrometer-sized particles was estimated using data derived from the Mercer cascade impactor data and carousel mass concentrations. Mass median diameter (MMD) was calculated from MMAD using the Hatch-Choate relationships for log-normal distributions. Count median diameter (CMD) was calculated from MMD. The average surface area particle diameter (d_s) and the average mass particle diameter (d_m) were calculated from CMD, assuming a spherical particle shape. The surface area per particle was calculated from d_s . The total number of particles per volume of air was calculated from d_m and the aerosol concentration determined from the RAM data. Once the total number of particles per volume of air was determined, the surface area per particle was multiplied by this value to obtain total surface area per volume of air. Total surface area per volume of air was divided by total mass per volume of air to obtain total surface area to total mass. Estimates of particle sizes and surface-area-to-mass ratios during the micro-C₆₀ studies are presented in Table E-3; MMAD values fell well below the 3.0 µm upper limit criterion required by the design of the studies.

For the nano-C₆₀ studies, aerosol particle size distribution was initially measured without animals in the exposure carousels during prestart studies using a Model 125B NanoMOUDI[™] Low Pressure Cascade Impactor (MSP Corporation, Shoreview, MN). The NanoMOUDI[™] classified particles according to aerodynamic size by inertial impaction in several multinozzle stages stacked in series; the chemically analyzed relative mass collected on each impactor stage was analyzed from a validated spreadsheet using the manufacturer's values for impactor stage

effective cutoff diameter. Data from this impactor resulted in a true measurement of MMAD for the aerosolized test article in each exposure carousel, but the device could not be used with animals in the exposure carousels because diversion of approximately half the aerosol flow to each carousel was required for proper functioning of the impactor. Accordingly, size distribution of the nano-C₆₀ particles was also measured using a Scanning Mobility Particle Sizer (SMPSTM; TSI[®], Inc., Shoreview, MN) that combined particle sizing by electrical mobility with condensation particle counting. The primary measurement output of the SMPSTM was particle CMD. MMD was calculated from measured CMD and the associated geometric standard deviation (GSD) using Hatch-Choate relationships assuming log-normal aerosol size distribution and then converted to MMAD assuming a particle density of 1.72 g/cc. By these means, a correlation was established between the results of NanoMOUDITM impactor and SMPSTM analyses enabling the use of the SMPSTM during the animal exposures to provide estimates of particle size distribution.

Measurements of particle size during animal exposures were conducted daily during the nano-C₆₀ studies using the SMPSTM. Monthly averaged results for these measurements in each exposure carousel during the 3-month nano-C₆₀ studies are presented in Table E-4 and demonstrate that the particles delivered to each exposure unit were nanometer sized.

The surface-area-to-mass ratios of nanometer-sized particles in the nano-C₆₀ studies were estimated using data derived from the SMPSTM CMD and carousel exposure concentration using the same calculations as described for the micrometer-sized particles. The results are presented in Table E-5.

Buildup and decay rates for carousel aerosol concentrations were not determined. For nose-only carousels, the time for the concentration to reach 90% of its stable final concentration after start of exposure (T₉₀) is less than the resolving ability of the measurement instrumentation and is calculated at <2 seconds. For this reason, no measurements of T₉₀ or the time for the concentration to reach 10% of the concentration determined immediately before termination of the exposure (T₁₀) were performed.

Uniformity of the aerosol concentration in the inhalation exposure carousels without animals present was evaluated before the 3-month micro-C₆₀ and nano-C₆₀ studies began. The aerosol concentration was measured using the online monitor with continuous monitoring from the input line. Measurements were taken from carousel exposure ports located on the top, middle, and bottom tiers of the carousel. For the micro-C₆₀ studies, total port variability (TPV) for the three carousels ranged from 4.0% to 4.7% relative standard deviation (RSD), and for the nano-C₆₀ studies, TPV for the four carousels ranged from 4.3% to 4.8% RSD.

Uniformity of aerosol concentration in the inhalation exposure carousels during the animal studies was not evaluated.

Fullerene C₆₀ was determined to be stable under the generation and exposure conditions used during the 3-month studies by analyses conducted before and during the 3-month studies by the study laboratory and the analytical chemistry laboratories. Samples were collected and analyzed from all exposure carousels and from the generator reservoir; during the 3-month studies, bulk fullerene C₆₀ in the generator reservoir was refilled as needed, and the analysis sample was collected from the reservoir at the end of the day after it was placed in service. Analyses included HPLC by system B for area percent purity, GC with mass spectrometry (MS) detection by

system D for determination of residual TMB (not performed on reservoir samples before the 3-month studies), inductively coupled plasma/atomic emission spectroscopy (ICP/AES) by system E for elemental analysis, and XRD and laser Raman spectroscopy for characterization of the form of the test material.

- D) Agilent gas chromatograph/mass spectrometer (model 6890/5973; Agilent Technologies, Inc.), a DB-5 (30 m × 0.25 mm ID, 0.25 μm film thickness) column (J&W Scientific), MS detection using electron impact ionization with selected ion monitoring, helium as the carrier gas flowing at 0.9 mL/minute, and an oven temperature program of 45°C for 10 minutes, then 20°C/minute to 270°C, then held for 10 minutes, or 45°C for 1 minute, then 20°C to 150°C, then held for 1 minute
- E) Thermo Elemented IRIS Intrepid inductively coupled plasma/atomic emission spectrometer (Thermo Fisher Scientific, Waltham, MA), a nebulizer operated at 0 to 200 rpm and 15 to 45 psi, and a radio-frequency generator powered at 750 to 1,750 watts. This system was calibrated with traceable reference standards obtained from the National Institute of Standards and Technology

Exposure atmosphere samples were collected from all rat and mouse carousels on 25 mm glass-fiber Teflon[®]-coated filters (PallFlex[®] Emfab[™], Pall Corporation) for HPLC and ICP/AES analyses, and on A/E glass-fiber filters (Pall Corporation) for XRD and laser Raman analyses. Atmosphere samples for GC/MS analyses were collected on activated coconut charcoal sorbent tubes (ORBO[™] 32s; Supelco, Inc., Bellefonte, PA).

For area percent purity assessments, filters and generator reservoir samples were extracted with TMB:toluene (50:50). For determination of TMB as a residue of repurification of the bulk test material, the sorbent tubes and generator reservoir samples were extracted with carbon disulfide. For elemental analysis, samples were microwave-digested in concentrated HCl:HNO₃ (2:1) containing indium as an internal standard, filtered through Teflon[®]-coated syringe filters (Acrodisc[®] CR, 25 mm, 0.45 μm; Pall Corporation), and analyzed for the concentration of 15 elements.

XRD with Rietveld analysis indicated that the principal crystalline phase in samples from the generator reservoir and exposure atmosphere samples from all carousels both before and during the 3-month micro- and nano-C₆₀ studies in rats and mice was the disordered face-centered cubic form of fullerene C₆₀. The XRD-determined purity of all generator reservoir and atmosphere samples exceeded 99.7% and 98%, respectively. Laser Raman assays concluded that all elemental carbon in the samples was in the form of C₆₀ fullerene. Using HPLC by system B, average area percent purity for the generator reservoir samples exceeded 98% prior to and during all studies. Area percent purity for the atmosphere samples collected from all carousels prior to and during the micro-C₆₀ studies exceeded 98%; similar measurements prior to and during the nano-C₆₀ studies indicated an exposure atmosphere purity of 99% or greater. GC/MS by system D detected 0.6% TMB in all reservoir samples collected during the 3-month studies. TMB concentrations in atmosphere samples ranged from 0.4% to 0.6% prior to and during the micro-C₆₀ studies and from 0.6% to 2.5% prior to and during the nano-C₆₀ studies. ICP/AES analyses by system E showed no elemental contamination in either the generator reservoir or exposure atmosphere samples collected before or during each study.

Table E-1. Summary of Carousel Concentrations in the Three-month Nose-only Inhalation Studies of Fullerene Micro-C₆₀ (1 µm)

	Target Concentration (mg/m ³)	Total Number of Readings	Average Concentration ^a (mg/m ³)
Rat Carousels			
	2	3,350	2.0 ± 0.2
	15	3,368	14.7 ± 1.2
	30	3,360	30.7 ± 1.8
Mouse Carousels			
	2	3,327	2.1 ± 0.2
	15	3,341	14.6 ± 1.1
	30	3,328	30.2 ± 1.8

^aMean ± standard deviation.**Table E-2. Summary of Carousel Concentrations in the Three-month Nose-only Inhalation Studies of Fullerene Nano-C₆₀ (50 nm)**

	Target Concentration (mg/m ³)	Total Number of Readings	Average Concentration ^a (mg/m ³)
Rat Carousels			
Male			
	0.5	3,280	0.50 ± 0.07
	2.0	3,287	2.00 ± 0.23
Female			
	0.5	3,278	0.50 ± 0.07
	2.0	3,282	2.01 ± 0.24
Mouse Carousels			
Male			
	0.5	3,318	0.50 ± 0.07
	2.0	3,327	2.01 ± 0.23
Female			
	0.5	3,317	0.50 ± 0.07
	2.0	3,332	2.00 ± 0.23

^aMean ± standard deviation.

Table E-3. Summary of Aerosol Size Measurements and Aerosol Surface-Area-to-Mass Ratios for the Rat and Mouse Exposure Carousels in the Three-month Nose-only Inhalation Studies of Fullerene Micro-C₆₀ (1 µm)^a

Target Concentration (mg/m ³)	November 12–13, 2007		December 10-11, 2007		January 8–9, 2008		Surface-Area-to-Mass Ratio ^b (m ² /g)
	MMAD (µm)	GSD	MMAD (µm)	GSD	MMAD (µm)	GSD	
Rat Carousels							
2	1.19	2.26	1.15	2.21	1.11	2.15	5.4
15	1.18	2.41	1.04	2.28	1.20	2.34	5.8
30	1.19	2.42	1.17	2.30	1.20	2.32	5.5
Mouse Carousels							
2	1.43	2.43	1.25	2.28	1.11	2.18	5.1
15	1.28	2.52	1.21	2.42	1.27	2.36	5.4
30	1.25	2.54	1.19	2.34	1.16	2.36	5.6

MMAD = mass median aerodynamic diameter; GSD = geometric standard deviation.

^aAerosol samples were collected three times during the studies with animals present in the carousels.

^bSurface areas were calculated from averaged monthly cascade impactor data.

Table E-4. Summary of Aerosol Size Measurements for the Rat and Mouse Exposure Carousels in the Three-month Nose-only Inhalation Studies of Fullerene Nano-C₆₀ (50 nm)^a

Target Concentration (mg/m ³)/Carousel Number	CMD (nm)	GSD	MMAD (nm)	CMD (nm)	GSD	MMAD (nm)	CMD (nm)	GSD	MMAD (nm)
Rat Carousels									
	November 14, 2007			December 14, 2007			January 10, 2008		
0.5/1	36	1.6	85	38	1.6	93	35	1.5	69
0.5/2	36	1.4	70	33	1.5	69	35	1.4	67
2.0/1	46	1.5	91	43	1.5	85	45	1.5	91
2.0/2	45	1.5	94	41	1.5	81	43	1.5	86
Mouse Carousels									
	November 13, 2007			December 13, 2007			January 9, 2008		
0.5/1	31	1.6	79	37	1.5	86	34	1.5	72
0.5/2	35	1.5	72	35	1.5	79	33	1.4	64
2.0/1	45	1.5	93	45	1.5	93	44	1.5	87
2.0/2	39	1.5	80	44	1.5	89	42	1.5	85

CMD = count median diameter; GSD = geometric standard deviation; MMAD = mass median aerodynamic diameter.

^aAerosol samples were collected daily during the studies (monthly averages are presented here) with animals present in the carousels.

Table E-5. Summary of Aerosol Surface-Area-to-Mass Ratios for the Rat and Mouse Exposure Carousels in the Three-month Nose-only Inhalation Studies of Fullerene Nano-C₆₀ (50 nm)^a

Target Concentration (mg/m ³)/Carousel Number	Surface-Area-to-Mass Ratio (m ² /g)		
	November 14, 2007	December 14, 2007	January 10, 2008
Rat Carousels			
0.5/1	59	55	71
0.5/2	70	72	73
2.0/1	54	58	54
2.0/2	53	60	57
Mouse Carousels			
0.5/1	65	59	69
0.5/2	68	63	76
2.0/1	53	53	56
2.0/2	62	56	58

^aAerosol samples were collected daily during the studies (monthly averages are presented here) with animals present in the carousels.

Fullerene C₆₀, TOX 87

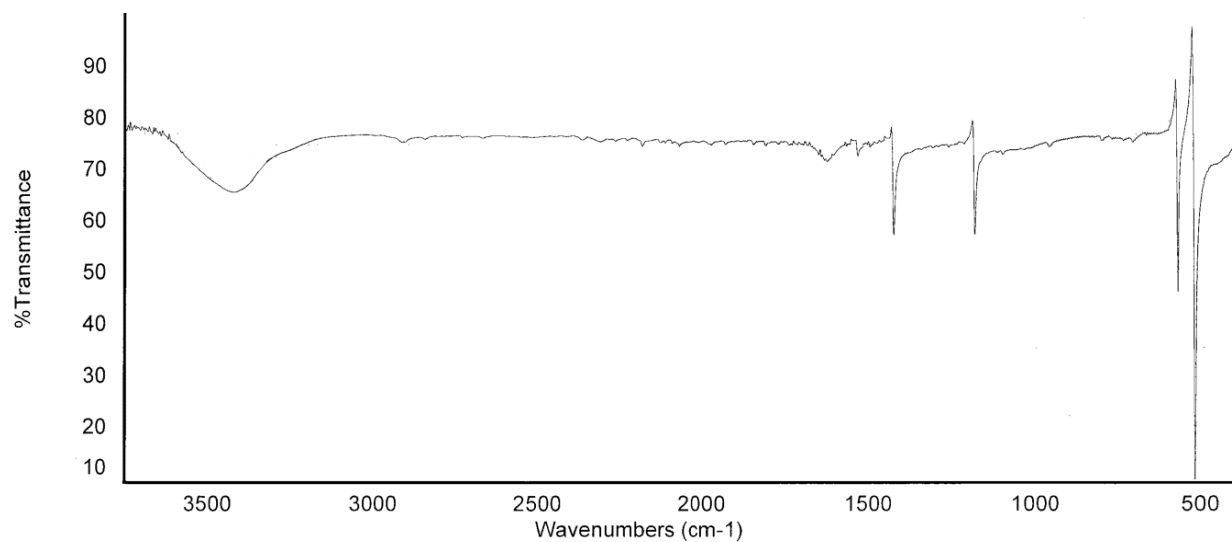


Figure E-1. Infrared Absorption Spectrum of Bulk Fullerene C₆₀

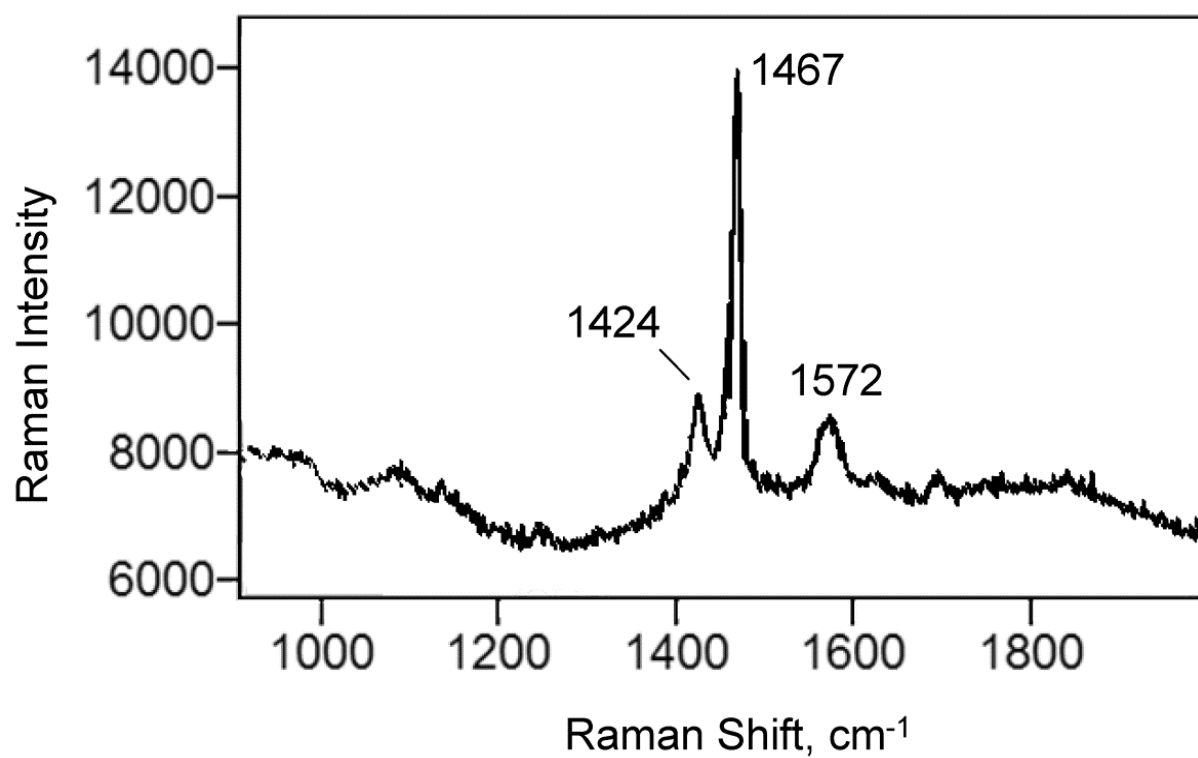


Figure E-2. Laser Raman Spectrum of Bulk Fullerene C₆₀

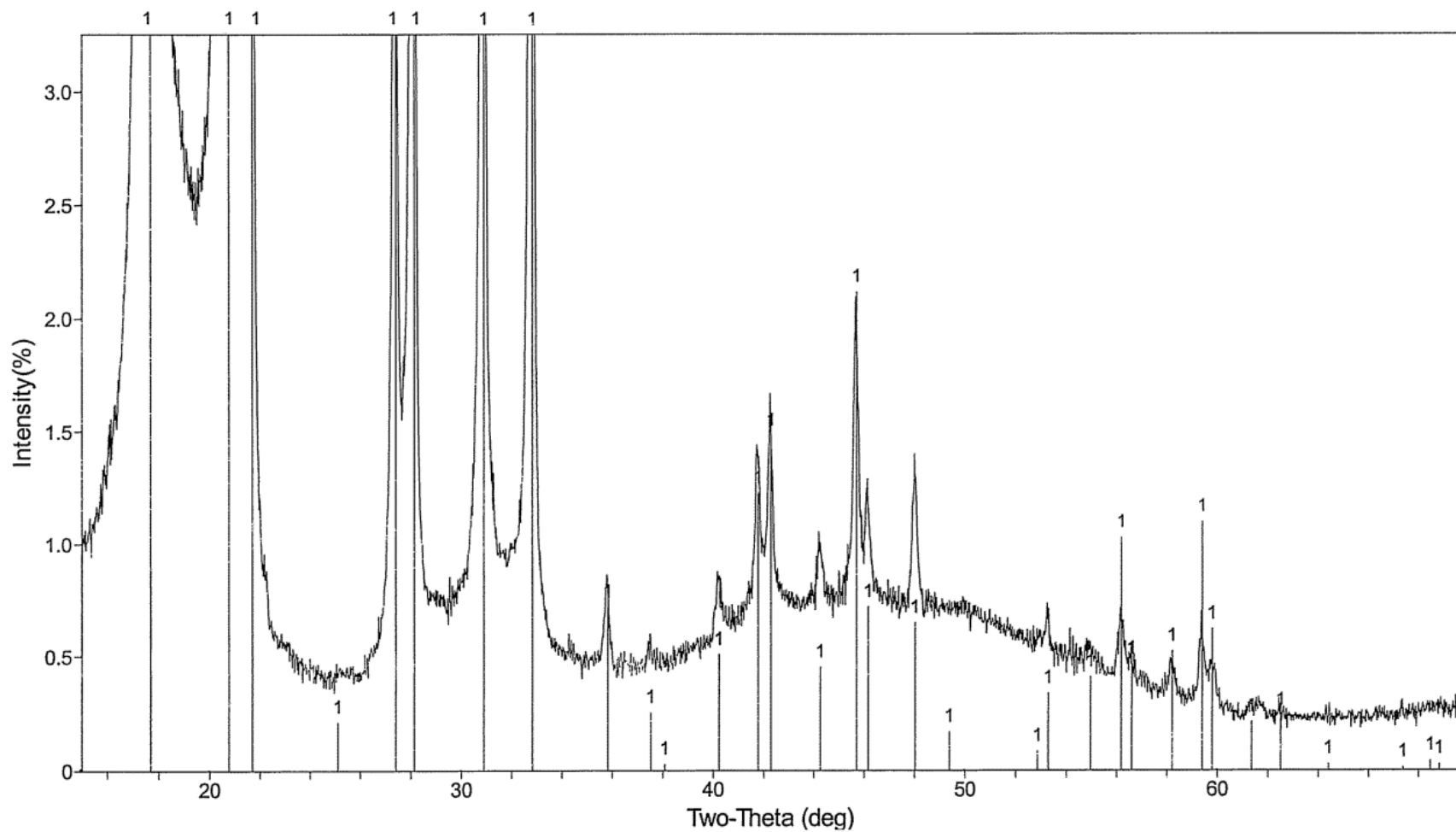


Figure E-3. X-ray Diffraction Pattern of Bulk Fullerene C₆₀

The stick pattern shown under the spectral peaks of this expanded view are the theoretical diffraction patterns of fullerene C₆₀.

Fullerene C₆₀, TOX 87

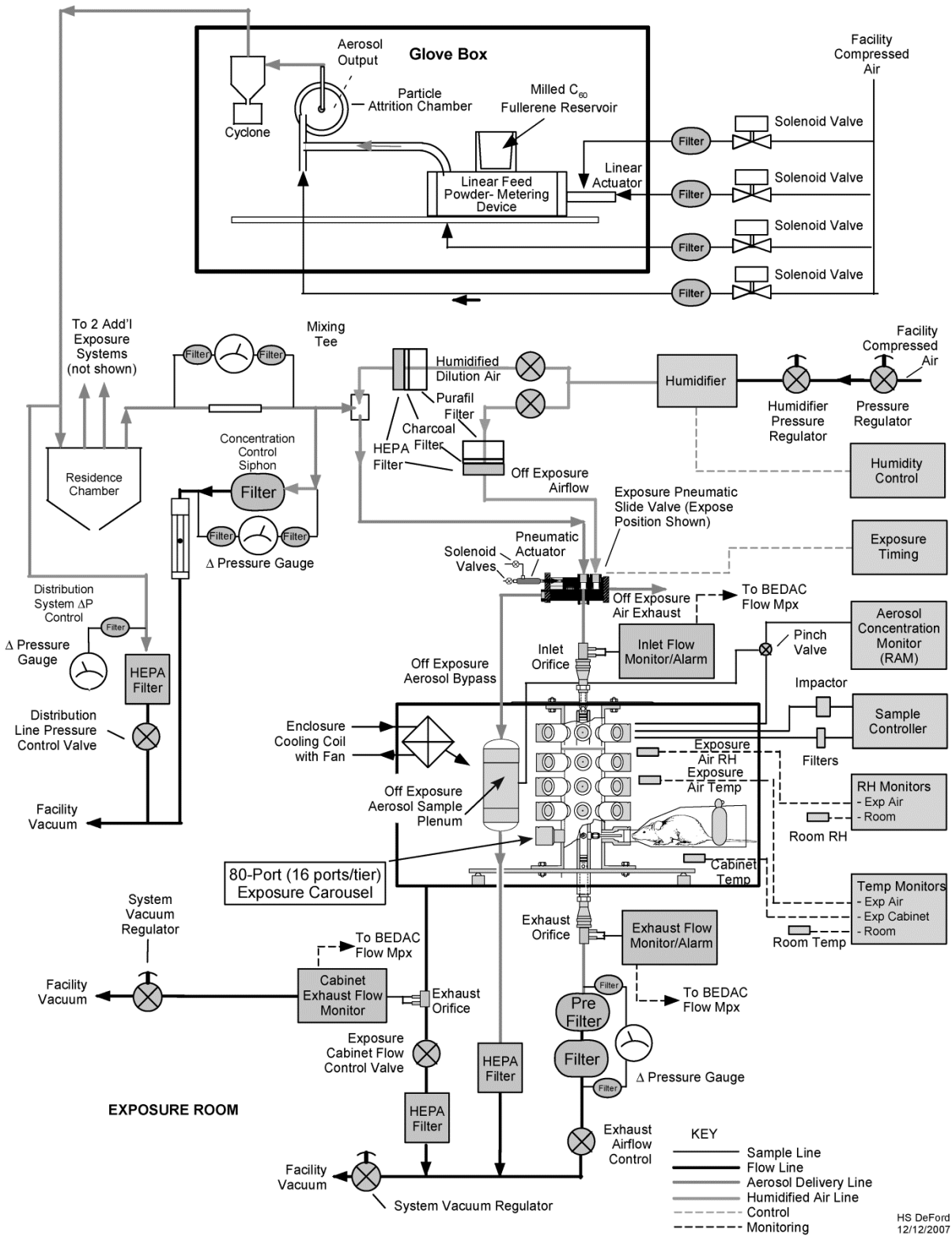


Figure E-4. Schematic of the Aerosol Generation and Delivery System in the Three-month Nose-only Inhalation Studies of Fullerene Micro-C₆₀ (1 μm)

Fullerene C₆₀, TOX 87

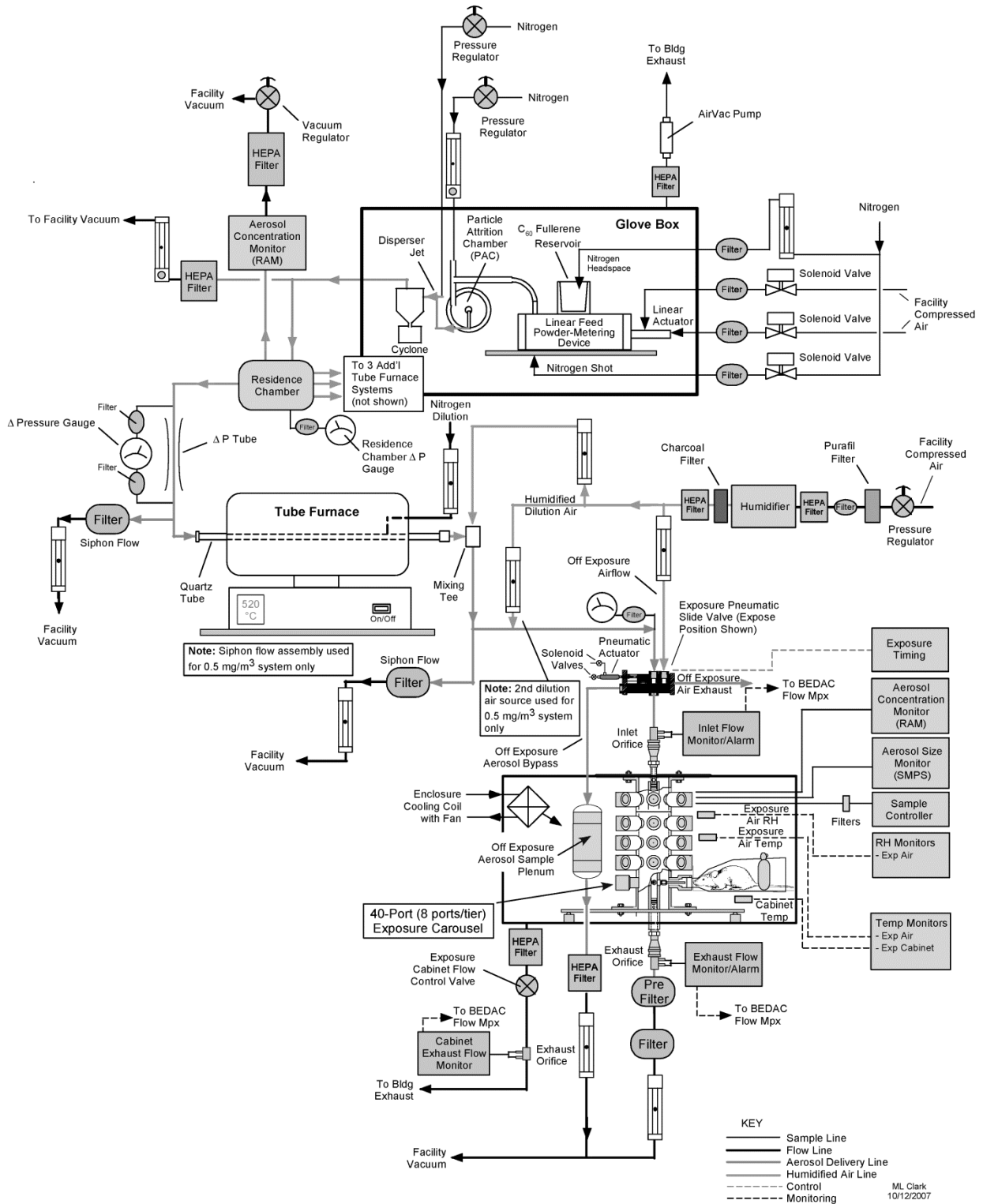


Figure E-5. Schematic of the Aerosol Generation and Delivery System in the Three-month Nose-only Inhalation Studies of Fullerene Nano-C₆₀ (50 nm)

Appendix F. Ingredients, Nutrient Composition, and Contaminant Levels in NTP-2000 Rat and Mouse Ration

Tables

Table F-1. Ingredients of NTP-2000 Rat and Mouse Ration.....	F-2
Table F-2. Vitamins and Minerals in NTP-2000 Rat and Mouse Ration	F-3
Table F-3. Nutrient Composition of NTP-2000 Rat and Mouse Ration.....	F-4
Table F-4. Contaminant Levels in NTP-2000 Rat and Mouse Ration.....	F-6

Table F-1. Ingredients of NTP-2000 Rat and Mouse Ration

Ingredients	Percent by Weight
Ground Hard Winter Wheat	22.26
Ground #2 Yellow Shelled Corn	22.18
Wheat Middlings	15.0
Oat Hulls	8.5
Alfalfa Meal (Dehydrated, 17% Protein)	7.5
Purified Cellulose	5.5
Soybean Meal (49% Protein)	5.0
Fish Meal (60% Protein)	4.0
Corn Oil (without Preservatives)	3.0
Soy Oil (without Preservatives)	3.0
Dried Brewer's Yeast	1.0
Calcium Carbonate (USP)	0.9
Vitamin Premix ^a	0.5
Mineral Premix ^b	0.5
Calcium Phosphate, Dibasic (USP)	0.4
Sodium Chloride	0.3
Choline Chloride (70% Choline)	0.26
Methionine	0.2

USP = United States Pharmacopeia.

^aWheat middlings as carrier.

^bCalcium carbonate as carrier.

Table F-2. Vitamins and Minerals in NTP-2000 Rat and Mouse Ration^a

	Amount	Source
Vitamins		
A	4,000 IU	Stabilized vitamin A palmitate or acetate
D	1,000 IU	D-activated animal sterol
K	1.0 mg	Menadione sodium bisulfite complex
α -Tocopheryl Acetate	100 IU	–
Niacin	23 mg	–
Folic Acid	1.1 mg	–
<i>d</i> -Pantothenic Acid	10 mg	<i>d</i> -Calcium pantothenate
Riboflavin	3.3 mg	–
Thiamine	4 mg	Thiamine mononitrate
B ₁₂	52 μ g	–
Pyridoxine	6.3 mg	Pyridoxine hydrochloride
Biotin	0.2 mg	<i>d</i> -Biotin
Minerals		
Magnesium	514 mg	Magnesium oxide
Iron	35 mg	Iron sulfate
Zinc	12 mg	Zinc oxide
Manganese	10 mg	Manganese oxide
Copper	2.0 mg	Copper sulfate
Iodine	0.2 mg	Calcium iodate
Chromium	0.2 mg	Chromium acetate

^aPer kg of finished product.

Table F-3. Nutrient Composition of NTP-2000 Rat and Mouse Ration

Nutrient	Mean ± Standard Deviation	Range	Number of Samples
Protein (% by Weight)	14.76 ± 0.727	13.8–15.4	5
Crude Fat (% by Weight)	8.4 ± 0.439	7.7–8.8	5
Crude Fiber (% by Weight)	8.88 ± 0.661	8.2–9.7	5
Ash (% by Weight)	5.12 ± 0.045	5.1–5.2	5
Amino Acids (% of Total Diet)			
Arginine	0.794 ± 0.070	0.67–0.97	26
Cystine	0.220 ± 0.022	0.15–0.25	26
Glycine	0.700 ± 0.038	0.62–0.80	26
Histidine	0.344 ± 0.074	0.27–0.68	26
Isoleucine	0.546 ± 0.041	0.43–0.66	26
Leucine	1.092 ± 0.063	0.96–1.24	26
Lysine	0.700 ± 0.110	0.31–0.86	26
Methionine	0.408 ± 0.043	0.26–0.49	26
Phenylalanine	0.621 ± 0.048	0.47–0.72	26
Threonine	0.508 ± 0.040	0.43–0.61	26
Tryptophan	0.153 ± 0.027	0.11–0.20	26
Tyrosine	0.413 ± 0.063	0.28–0.54	26
Valine	0.663 ± 0.040	0.55–0.73	26
Essential Fatty Acids (% of Total Diet)			
Linoleic	3.95 ± 0.242	3.49–4.55	26
Linolenic	0.31 ± 0.030	0.21–0.35	26
Vitamins			
Vitamin A (IU/kg)	3,398 ± 46	2,790 – 4,020	5
Vitamin D (IU/kg)	1,000 ^a	–	–
α-Tocopherol (ppm)	80 ± 20.42	27–124	26
Thiamine (ppm) ^b	6.62 ± 1.44	5.1–8.7	5
Riboflavin (ppm)	8.1 ± 2.91	4.20–17.50	26
Niacin (ppm)	78.9 ± 8.52	66.4–98.2	26
Pantothenic Acid (ppm)	26.7 ± 11.63	17.4–81.0	26
Pyridoxine (ppm) ^b	9.7 ± 2.09	6.44–14.3	26
Folic Acid (ppm)	1.59 ± 0.45	1.15–3.27	26
Biotin (ppm)	0.32 ± 0.10	0.20–0.704	26
Vitamin B ₁₂ (ppb)	51.8 ± 36.6	18.3–174.	26
Choline (ppm) ^b	2,665 ± 631	1,160–3,790	26

Fullerene C₆₀, TOX 87

Nutrient	Mean ± Standard Deviation	Range	Number of Samples
Minerals			
Calcium (%)	0.952 ± 0.051	0.875–1.02	5
Phosphorus (%)	0.551 ± 0.023	0.526–0.585	5
Potassium (%)	0.669 ± 0.030	0.626–0.733	26
Chloride (%)	0.386 ± 0.037	0.300–0.474	26
Sodium (%)	0.193 ± 0.024	0.160–0.283	26
Magnesium (%)	0.216 ± 0.057	0.185–0.490	26
Sulfur (%)	0.170 ± 0.029	0.116–0.209	14
Iron (ppm)	190.5 ± 38.0	135–311	26
Manganese (ppm)	50.7 ± 9.72	21.0–73.1	26
Zinc (ppm)	58.2 ± 26.89	43.3–184.0	26
Copper (ppm)	7.44 ± 2.60	3.21–16.3	26
Iodine (ppm)	0.514 ± 0.195	0.158–0.972	26
Chromium (ppm)	0.674 ± 0.265	0.330–1.380	25
Cobalt (ppm)	0.235 ± 0.157	0.094–0.864	24

^aFrom formulation.

^bAs hydrochloride (thiamine and pyridoxine) or chloride (choline).

Table F-4. Contaminant Levels in NTP-2000 Rat and Mouse Ration^a

	Mean ± Standard Deviation ^b	Range	Number of Samples
Contaminants			
Arsenic (ppm)	0.217 ± 0.023	0.184–0.248	5
Cadmium (ppm)	0.063 ± 0.007	0.051–0.069	5
Lead (ppm)	0.101 ± 0.033	0.077–0.156	5
Mercury (ppm)	<0.02	–	5
Selenium (ppm)	0.345 ± 0.377	0.158–1.02	5
Aflatoxins (ppb)	<5.00	–	5
Nitrate Nitrogen (ppm) ^c	14.26 ± 6.62	10.0–25.8	5
Nitrite Nitrogen (ppm) ^c	0.61	2.81–5.81	5
BHA (ppm) ^d	<1.0	–	5
BHT (ppm) ^d	<1.0	–	5
Aerobic Plate Count (CFU/g)	<10	–	5
Coliform (MPN/g)	3.0 ± 0.0	3.0	5
<i>Escherichia coli</i> (MPN/g)	<10	–	5
<i>Salmonella</i> (MPN/g)	Negative	–	5
Total Nitrosoamines (ppb) ^e	13.64 ± 10.38	2.4–28	5
<i>N</i> -Nitrosodimethylamine (ppb) ^e	3.42 ± 3.97	1.1–10.3	5
<i>N</i> -Nitrosopyrrolidine (ppb) ^e	10.22 ± 7.23	1.2–17.7	5
Pesticides (ppm)			
α-BHC	<0.01	–	5
β-BHC	<0.02	–	5
γ-BHC	<0.01	–	5
δ-BHC	<0.01	–	5
Heptachlor	<0.01	–	5
Aldrin	<0.01	–	5
Heptachlor Epoxide	<0.01	–	5
DDE	<0.01	–	5
DDD	<0.01	–	5
DDT	<0.01	–	5
HCB	<0.01	–	5
Mirex	<0.01	–	5
Methoxychlor	<0.05	–	5
Dieldrin	<0.01	–	5
Endrin	<0.01	–	5
Telodrin	<0.01	–	5

Fullerene C₆₀, TOX 87

	Mean ± Standard Deviation ^b	Range	Number of Samples
Chlordane	<0.05	–	5
Toxaphene	<0.10	–	5
Estimated PCBs	<0.20	–	5
Ronnel	<0.01	–	5
Ethion	<0.02	–	5
Trithion	<0.05	–	5
Diazinon	<0.10	–	5
Methyl Chlorpyrifos	0.062 ± 0.040	0.02–0.109	5
Methyl Parathion	<0.02	–	5
Ethyl Parathion	<0.02	–	5
Malathion	0.065 ± 0.055	0.02–0.15	5
Endosulfan I	<0.01	–	5
Endosulfan II	<0.01	–	5
Endosulfan Sulfate	<0.03	–	5

CFU = colony-forming units; MPN = most probable number; BHC = hexachlorocyclohexane or benzene hexachloride.

^aAll samples were irradiated.

^bFor values less than the limit of detection, the detection limit is given as the mean.

^cSources of contamination: alfalfa, grains, and fish meal.

^dSources of contamination: soy oil and fish meal.

^eAll values were corrected for percent recovery.

Appendix G. Sentinel Animal Program

Table of Contents

G.1. Methods.....	G-2
G.2. Results.....	G-3

Table

Table G-1. Laboratory Methods and Agents Tested for in the Sentinel Animal Program	G-2
--	-----

G.1. Methods

Rodents used in the National Toxicology Program are produced in optimally clean facilities to eliminate potential pathogens that might affect study results. The Sentinel Animal Program is part of the periodic monitoring of animal health that occurs during the toxicological evaluation of test compounds. Under this program, the disease state of the rodents is monitored via sera or feces from extra (sentinel) or dosed animals in the study rooms. The sentinel animals and the study animals are subject to identical environmental conditions. Furthermore, the sentinel animals are from the same production source and weanling groups as the animals used for the studies of test compounds.

In these toxicity studies of fullerene C₆₀ administered by nose-only inhalation for 3 months to Wistar Han [CrI:WI (Han)] rats and B6C3F1/N mice, blood samples were collected from the sentinel animals and allowed to clot and the serum was separated. All samples were processed appropriately with serology testing performed in house or sent to IDEXX BioResearch (formerly Research Animal Diagnostic Laboratory [RADIL], University of Missouri), Columbia, MO for determination of the presence of pathogens. The laboratory methods and agents for which testing was performed are tabulated below; the times at which samples were collected during the studies are also listed.

Blood was collected from five animals per sex per time point.

Table G-1. Laboratory Methods and Agents Tested for in the Sentinel Animal Program

Method and Test	Time of Collection
Rats	
ELISA (in house)	
<i>Mycoplasma pulmonis</i>	3 weeks postarrival
Pneumonia virus of mice (PVM)	3 weeks postarrival
Rat coronavirus/sialodacryoadenitis virus (RCV/SDA)	3 weeks postarrival
Rat parvovirus (RPV)	3 weeks postarrival
Sendai	3 weeks postarrival
Multiplex Fluorescent Immunoassay (RADIL)	
Kilham rat virus (KRV)	Study termination
<i>M. pulmonis</i>	Study termination
Parvo NS-1	Study termination
PVM	Study termination
RCV/SDA	Study termination
Rat minute virus (RMV)	Study termination
RPV	Study termination
Rat theilovirus (RTV)	Study termination
Sendai	Study termination
Theiler's murine encephalomyelitis virus (TMEV GDVII)	Study termination
Toolan's H-1 virus	Study termination

Method and Test	Time of Collection
Mice	
ELISA (in house)	3 weeks postarrival
Mouse hepatitis virus (MHV)	3 weeks postarrival
Mouse parvovirus (MPV)	3 weeks postarrival
<i>M. pulmonis</i>	3 weeks postarrival
PVM	3 weeks postarrival
Sendai	3 weeks postarrival
TMEV	3 weeks postarrival
Multiplex Fluorescent Immunoassay (RADIL)	
Ectromelia virus	Study termination
Episodic diarrhea of infant mice (EDIM)	Study termination
Lymphocytic choriomeningitis virus (LCMV)	Study termination
<i>M. pulmonis</i>	Study termination
MHV	Study termination
Mouse norovirus (MNV)	Study termination
Parvo NS-1	Study termination
MPV	Study termination
Minute virus of mice (MVM)	Study termination
PVM	Study termination
Reovirus	Study termination
TMEV GDVII	Study termination
Sendai	Study termination

G.2. Results

All test results were negative.

Appendix H. Supplemental Data

Tables with supplemental data can be found here: <https://doi.org/10.22427/NTP-DATA-TOX-87>.

H.1. Three-month 50 Nanometers Study Tables in Rats

E03 – Growth Curves

E04 – Mean Body Weights and Survival Table

E05 – Clinical Observations Summary

P03 – Incidence Rates of Non-Neoplastic Lesions by Anatomic Site

P04 – Neoplasms by Individual Animal

P05 – Incidence Rates of Neoplasms by Anatomic Sites (Systemic Lesions Abridged)

P09 – Non-Neoplastic Lesions by Individual Animal

P10 – Statistical Analysis of Non-Neoplastic Lesions

P14 – Individual Animal Pathology Data

P18 – Incidence Rates of Non-Neoplastic Lesions by Anatomic Site with Average Severity Grades

P40 – Survival Curves

H.2. Three-month 50 Nanometers Individual Animal Data in Rats

Female Individual Animal Body Weight Data

Female Individual Animal Clinical Observations

Female Individual Animal Non-Neoplastic Pathology Data

Female Individual Animal Organ Weight Data

Female Individual Animal Survival Data

Male Individual Animal Body Weight Data

Male Individual Animal Clinical Observations

Male Individual Animal Non-Neoplastic Pathology Data

Male Individual Animal Organ Weight Data

Male Individual Animal Survival Data

H.3. Three-month 50 Nanometers Study Tables in Mice

E03 – Growth Curves

E04 – Mean Body Weights and Survival Table

E05 – Clinical Observations Summary

P03 – Incidence Rates of Non-Neoplastic Lesions by Anatomic Site

P04 – Neoplasms by Individual Animal

P05 – Incidence Rates of Neoplasms by Anatomic Sites (Systemic Lesions Abridged)

P09 – Non-Neoplastic Lesions by Individual Animal

P10 – Statistical Analysis of Non-Neoplastic Lesions

P14 – Individual Animal Pathology Data

P18 – Incidence Rates of Non-Neoplastic Lesions by Anatomic Site with Average Severity Grades

P40 – Survival Curves

H.4. Three-month 50 Nanometers Individual Animal Data in Mice

Female Individual Animal Body Weight Data

Female Individual Animal Non-Neoplastic Pathology Data

Female Individual Animal Organ Weight Data

Female Individual Animal Survival Data

Male Individual Animal Body Weight Data

Male Individual Animal Clinical Observations

Male Individual Animal Non-Neoplastic Pathology Data

Male Individual Animal Organ Weight Data

Male Individual Animal Survival Data

H.5. Three-month 1.0 Micron Study Tables in Rats

E03 – Growth Curves

E04 – Mean Body Weights and Survival Table

E05 – Clinical Observations Summary

P03 – Incidence Rates of Non-Neoplastic Lesions by Anatomic Site

P04 – Neoplasms by Individual Animal

P05 – Incidence Rates of Neoplasms by Anatomic Sites (Systemic Lesions Abridged)

P09 – Non-Neoplastic Lesions by Individual Animal

P10 – Statistical Analysis of Non-Neoplastic Lesions

P14 – Individual Animal Pathology Data

P18 – Incidence Rates of Non-Neoplastic Lesions by Anatomic Site with Average Severity Grades

P40 – Survival Curves

H.6. Three-month 1.0 Individual Animal Data in Rats

Female Individual Animal Body Weight Data

Female Individual Animal Clinical Observations

Female Individual Animal Non-Neoplastic Pathology Data

Female Individual Animal Organ Weight Data

Female Individual Animal Survival Data

Male Individual Animal Body Weight Data

Male Individual Animal Non-Neoplastic Pathology Data

Male Individual Animal Organ Weight Data

Male Individual Animal Survival Data

H.7. Three-month 1.0 Micron Study Tables in Mice

E03 – Growth Curves

E04 – Mean Body Weights and Survival Table

E05 – Clinical Observations Summary

P03 – Incidence Rates of Non-Neoplastic Lesions by Anatomic Site

P04 – Neoplasms by Individual Animal

P05 – Incidence Rates of Neoplasms by Anatomic Sites (Systemic Lesions Abridged)

P09 – Non-Neoplastic Lesions by Individual Animal

P10 – Statistical Analysis of Non-Neoplastic Lesions

P14 – Individual Animal Pathology Data

P18 – Incidence Rates of Non-Neoplastic Lesions by Anatomic Site with Average Severity Grades

P40 – Survival Curves

H.8. Three-month 1.0 Micron Individual Animal Data in Mice

Female Individual Animal Body Weight Data

Female Individual Animal Non-Neoplastic Pathology Data

Female Individual Animal Organ Weight Data

Female Individual Animal Survival Data

Male Individual Animal Body Weight Data

Male Individual Animal Clinical Observations

Male Individual Animal Neoplastic Pathology Data

Male Individual Animal Non-Neoplastic Pathology Data

Male Individual Animal Organ Weight Data

Male Individual Animal Survival Data



National Toxicology Program

NTP Central Data Management, MD EC-03
National Institute of Environmental Health Sciences
P.O. Box 12233
Research Triangle Park, NC 27709

<http://ntp.niehs.nih.gov>

ISSN 2378-8992